On the Origin of the Elliptic Flow and its Dependence on the Equation of State in Heavy Ion Reactions at Intermediate Energies

On print in Phys. Rev. C (2018)

by A. Le Fèvre[1] , Y. Leifels[1] , C. Hartnack[2] and J. Aichelin[2,3]
[1]GSI Helmholtzzentrum für Schwerionenforschung GmbH, Darmstadt, Germany
[2]SUBATECH, UMR 6457, Ecole des Mines de Nantes - IN2P3/CNRS - Université de Nantes, France
[3]FIAS, Frankfurt University, Germany

On the Origin of the Elliptic Flow and its Dependence on the Equation of State in Heavy Ion Reactions at Intermediate Energies

On print in Phys. Rev. C (2018)

by A. Le Fèvre[1] , Y. Leifels[1] , C. Hartnack[2] and J. Aichelin[2,3]

[1]GSI Helmholtzzentrum für Schwerionenforschung GmbH, Darmstadt, Germany

[2]SUBATECH, UMR 6457, Ecole des Mines de Nantes - IN2P3/CNRS - Université de Nantes, France

[3]FIAS, Frankfurt University, Germany

- Introduction
- The Quantum Molecular Dynamics approach
- Elliptic flow at mid-rapidity: the strongest sensitivity to the Nuclear Equation of State
- Survey of the reaction
- Collisions versus mean field
- Incident energy dependance
- Summary

GSI HELMHOLTZ ASSOCIATION

Introduction

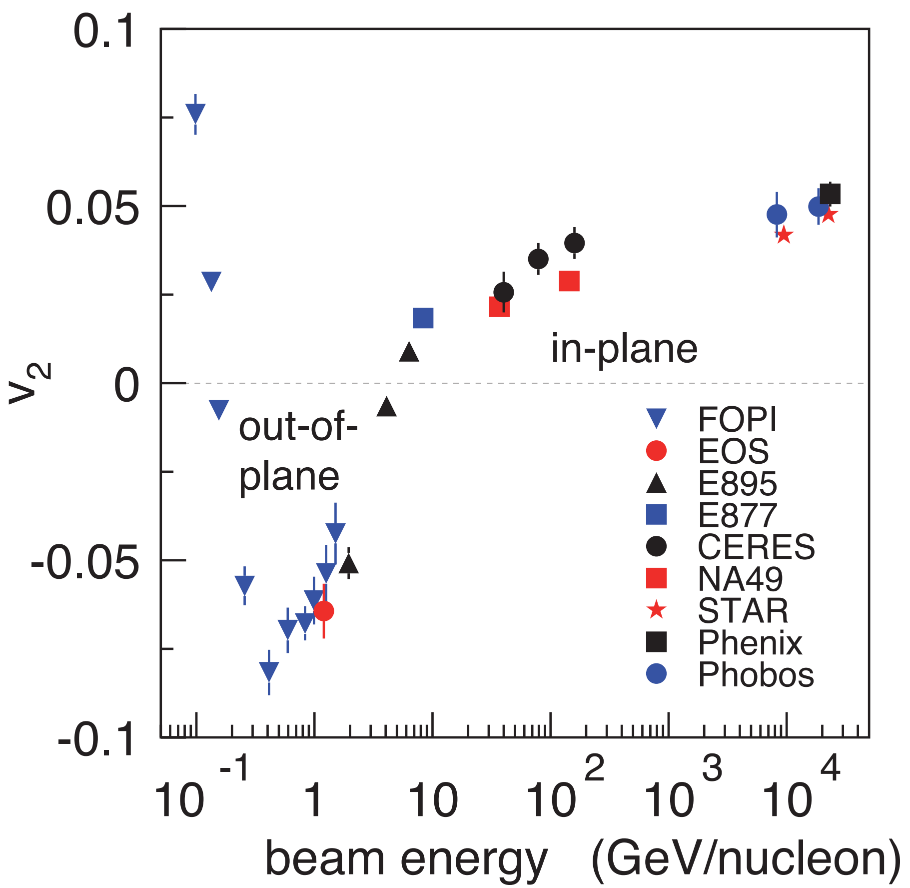

Introduction

The elliptic flow (v_2) at midrapidity, originally called out-of-plane emission or squeeze-out, has attracted a lot of attention during the last years.

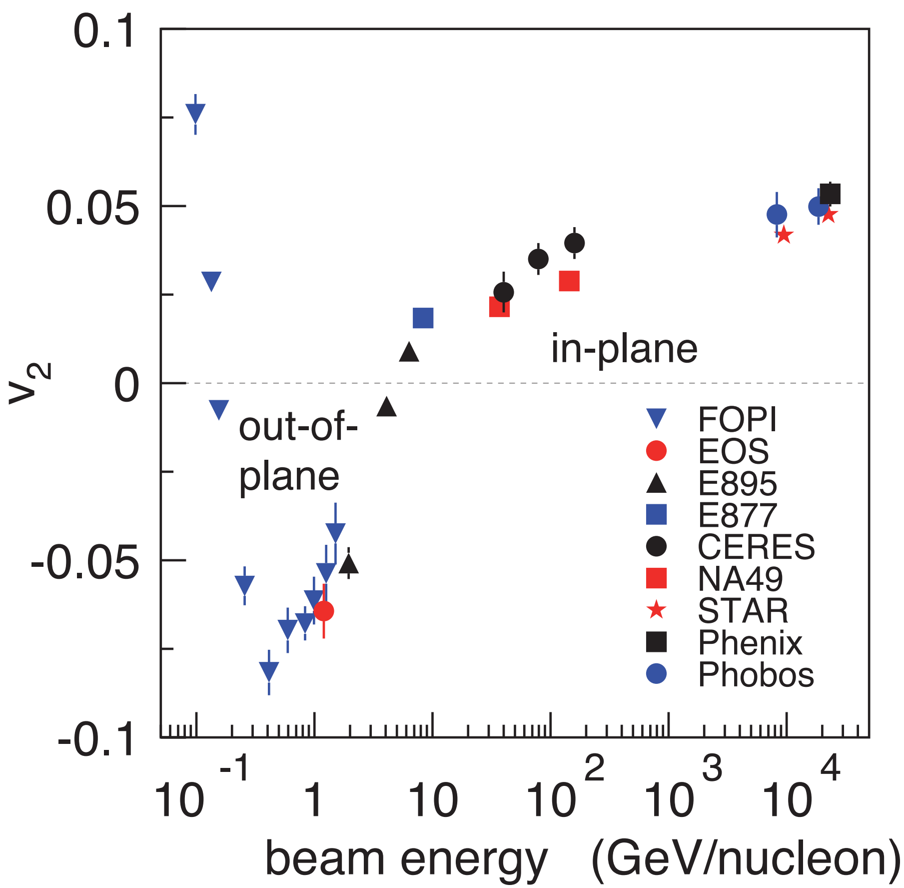

Introduction

The elliptic flow (v_2) at midrapidity, originally called out-of-plane emission or squeeze-out, has attracted a lot of attention during the last years.
It has been predicted in hydrodynamical simulations of heavy ion reactions

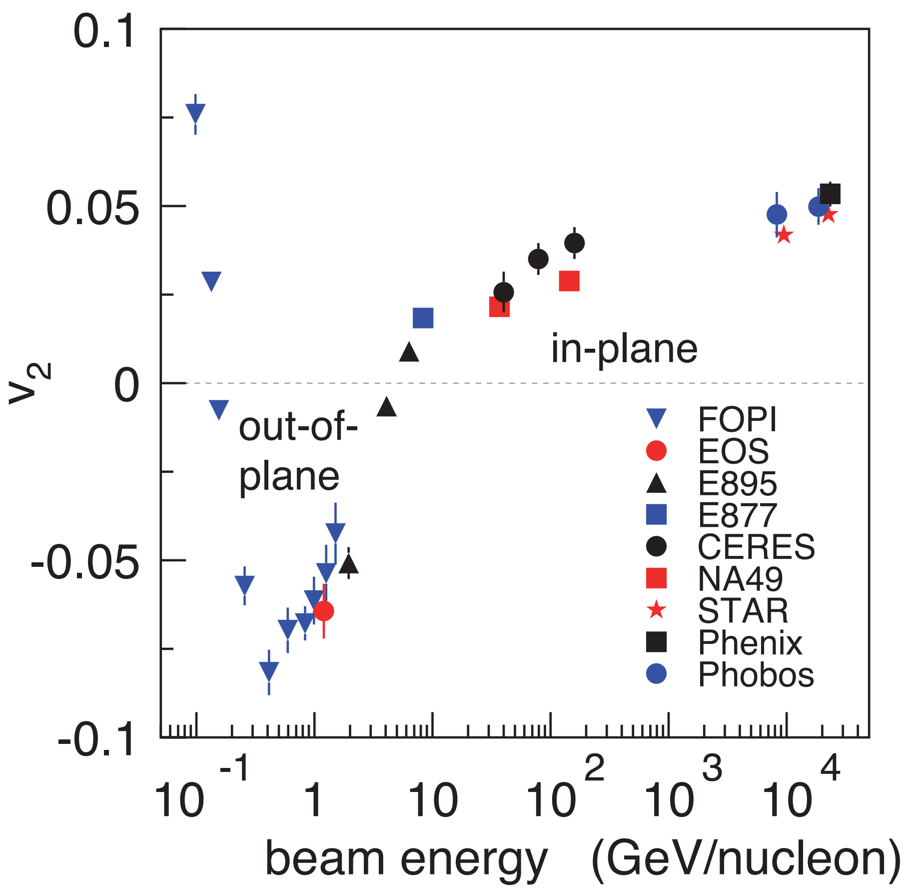

Introduction

The elliptic flow (v_2) at midrapidity, originally called out-of-plane emission or squeeze-out, has attracted a lot of attention during the last years.
It has been predicted in hydrodynamical simulations of heavy ion reactions

– H. Stoecker et al., Phys. Rev. C 25 (1982) 1873.

– G. Buchwald et al., Phys. Rev. C 28 (1983) 2349.

– H. Stoecker and W. Greiner, Phys. Rept. 137 (1986) 277.

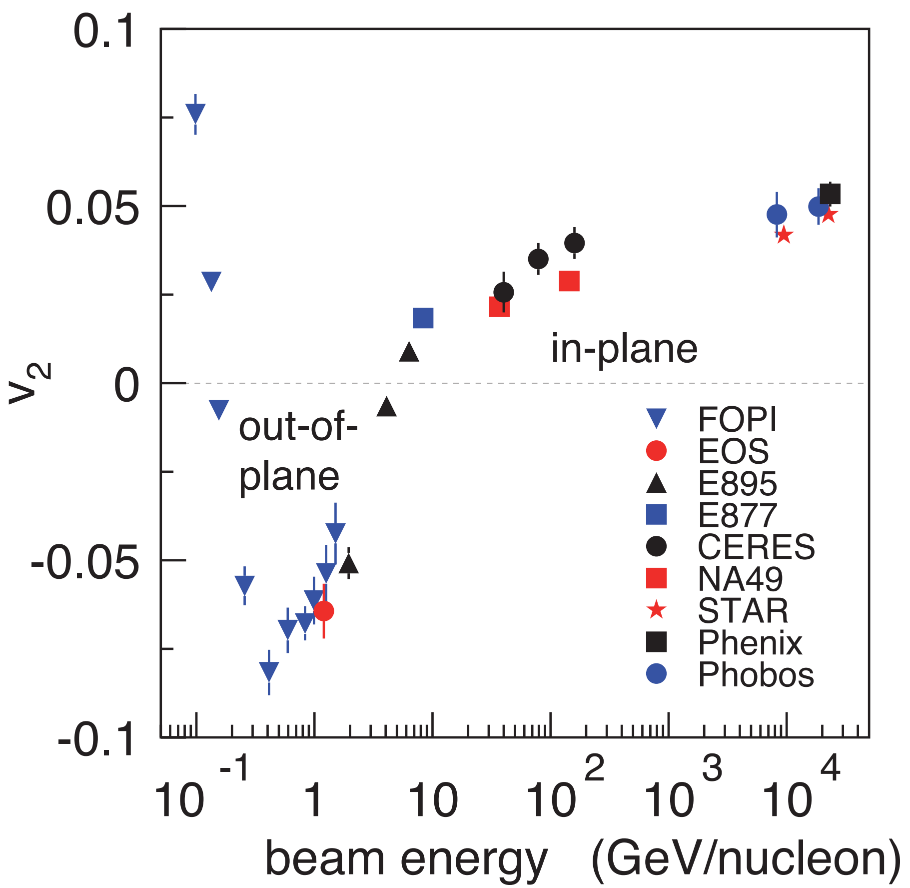

Introduction

The elliptic flow (v_2) at midrapidity, originally called out-of-plane emission or squeeze-out, has attracted a lot of attention during the last years.
It has been predicted in hydrodynamical simulations of heavy ion reactions

– H. Stoecker et al., Phys. Rev. C 25 (1982) 1873.

– G. Buchwald et al., Phys. Rev. C 28 (1983) 2349.

– H. Stoecker and W. Greiner, Phys. Rept. 137 (1986) 277.

and has later been found experimentally by the Plastic Ball collaboration

– H.H. Gutbrod et al., Phys. Rev. C 42 (1990) 640.

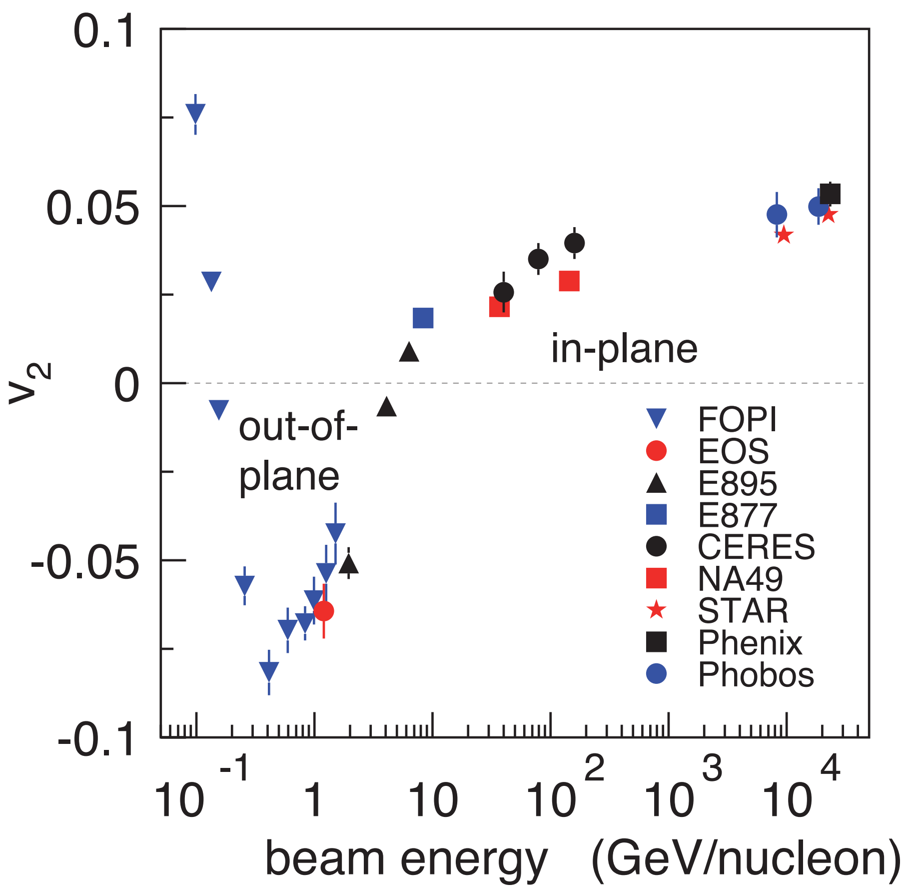

Introduction

The elliptic flow (v_2) at midrapidity, originally called out-of-plane emission or squeeze-out, has attracted a lot of attention during the last years.
It has been predicted in hydrodynamical simulations of heavy ion reactions

– H. Stoecker et al., Phys. Rev. C 25 (1982) 1873.

– G. Buchwald et al., Phys. Rev. C 28 (1983) 2349.

– H. Stoecker and W. Greiner, Phys. Rept. 137 (1986) 277.

and has later been found experimentally by the Plastic Ball collaboration

– H.H. Gutbrod et al., Phys. Rev. C 42 (1990) 640.

At ultra-relativiste energies: measured v_2 and centrality dependance ⇔ expansion of initially highly compressed almond shaped fireball ⇨ $v_2 > 0$ as predicted by hydrodynamics

– M. Luzum and P. Romatschke, Phys. Rev. Lett. 103 (2009) 262302

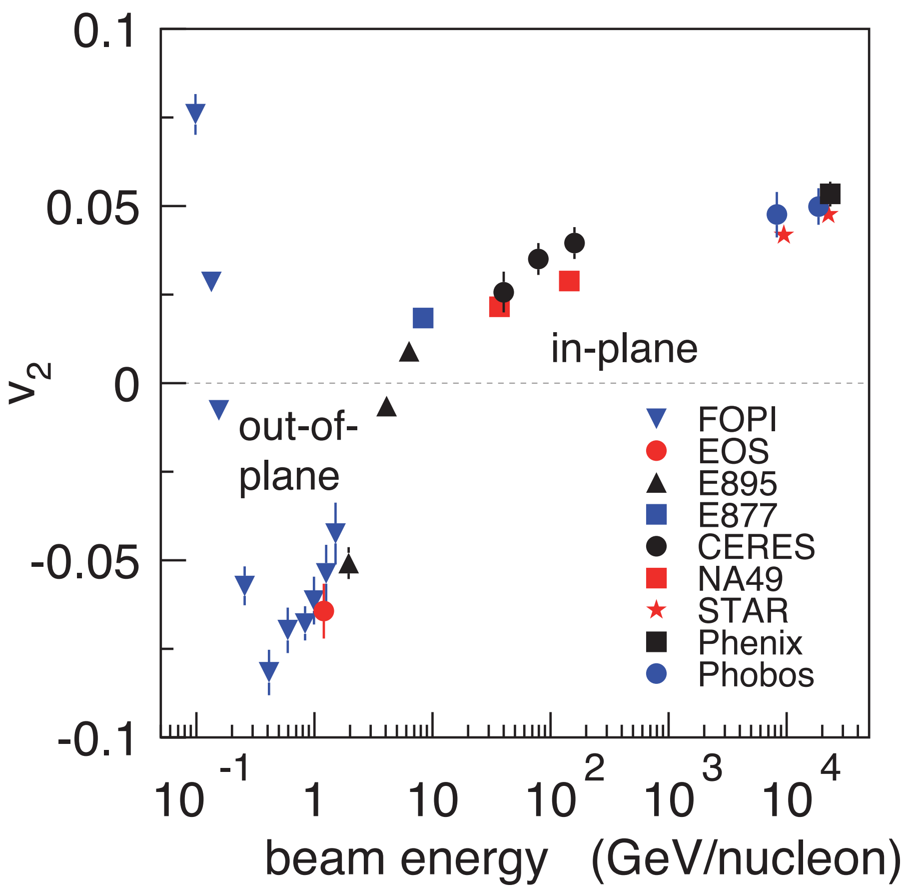

The elliptic flow (v_2) at midrapidity, originally called out-of-plane emission or squeeze-out, has attracted a
years.
It has been pre
simulations of h
– H. Stoecker et al., P
– G. Buchwald et al.,
– H. Stoecker and W.

and has later b
the Plastic Ball
– H.H. Gutbrod et al
At ultra-relativis
centrality depe
highly compres
v_2 > 0 as predic
– M. Luzum and P. Romatschke, Phys. Rev. Lett. 103 (2009) 262302

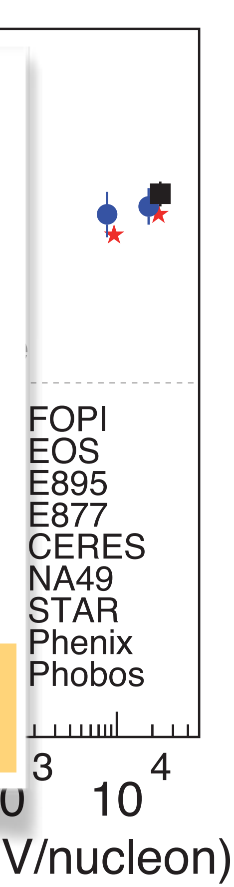

Flows at high density in heavy-ion collisions

$$\frac{dN}{d(\phi-\phi_R)}(y,p_t)=\frac{N_0}{2\pi}\left(1+2\sum_{n\geq1}v_n\cos n(\phi-\phi_R)\right)$$

Y = rapidity
p_t = transverse momentum
Φ_R = reaction plane azimuthal angle

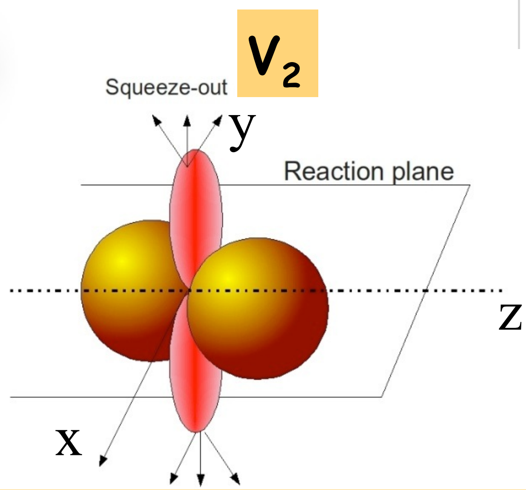

V_1 = 'side/directed flow', cos($\Phi-\Phi_R$) mode

$$V_2(y,p_t)=\left\langle\frac{p_x^2-p_y^2}{p_t^2}\right\rangle$$

'Elliptic flow': cos(2($\Phi-\Phi_R$)) mode, competition between 'in-plane' (V_2>0) and 'out-of-plane' ejection (V_2<0).

GSI HELMHOLTZ ASSOCIATION

Introduction

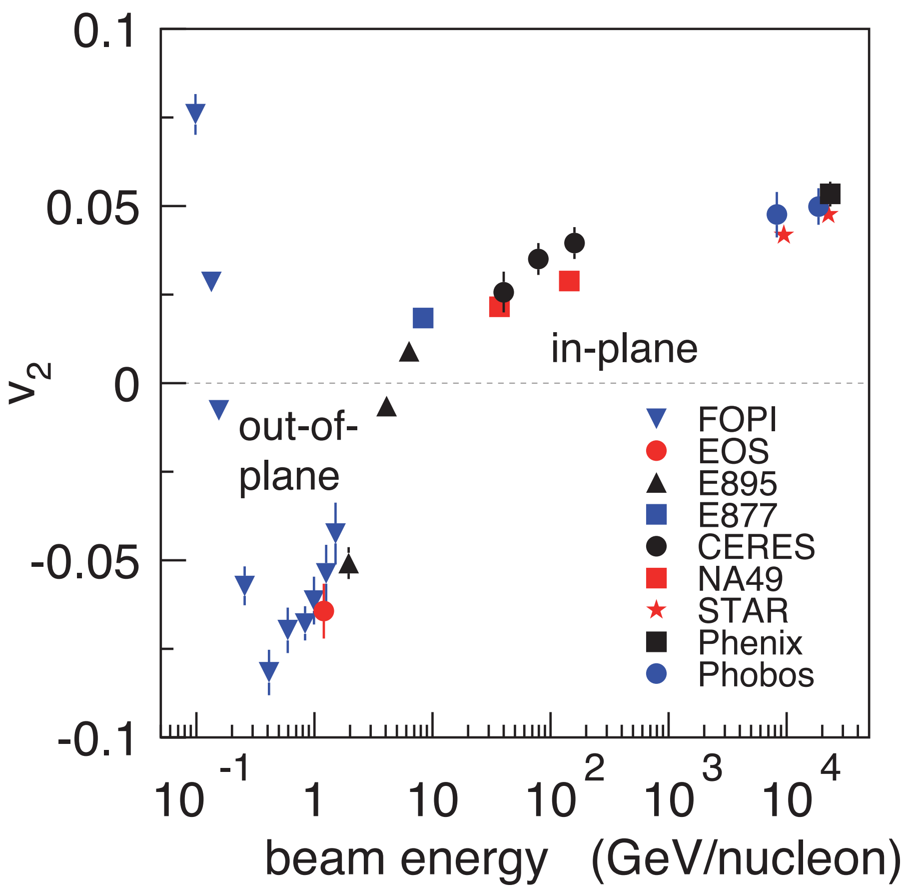

At lower energies: various experimental groups

– H. H. Gutbrod et al. Phys. Rev. C 42 (1990) 640.

– C. Pinkenburg et al. [E895 Collaboration], Phys. Rev. Lett. 83 (1999) 1295 [nucl-ex/9903010].

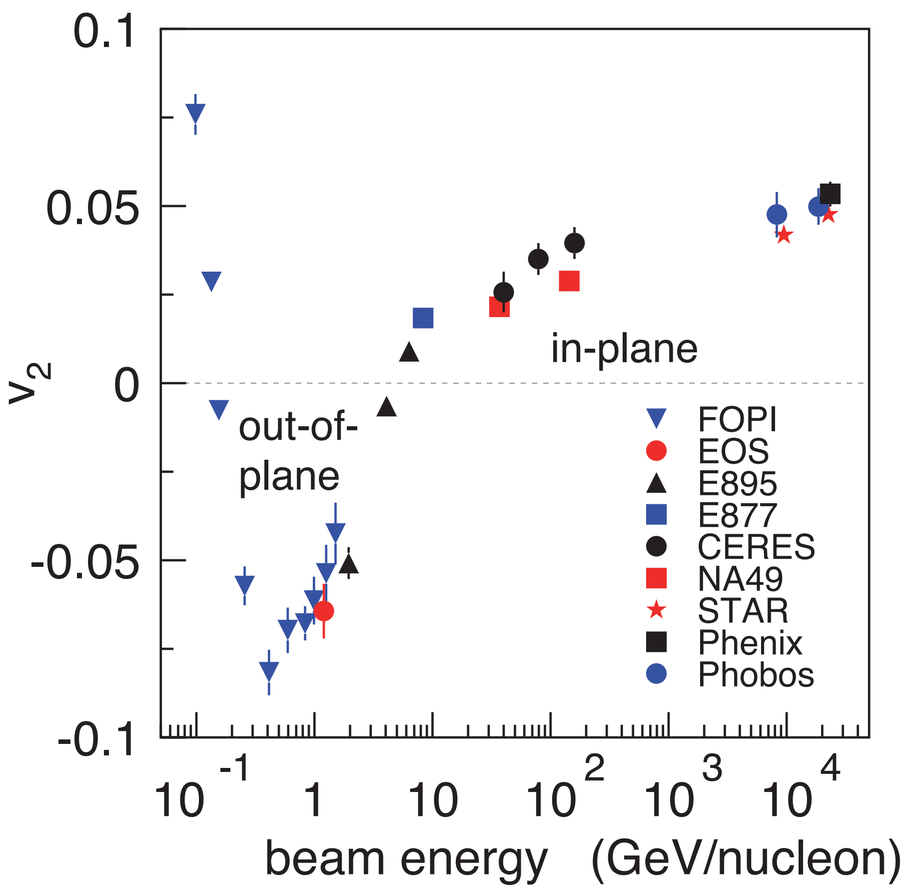

Introduction

At lower energies: various experimental groups

– H. H. Gutbrod et al. Phys. Rev. C 42 (1990) 640.

– C. Pinkenburg et al. [E895 Collaboration], Phys. Rev. Lett. 83 (1999) 1295 [nucl-ex/9903010].

and later the FOPI collaboration

– W. Reisdorf et al. [FOPI Collaboration], Nucl. Phys. A 876 (2012) 1

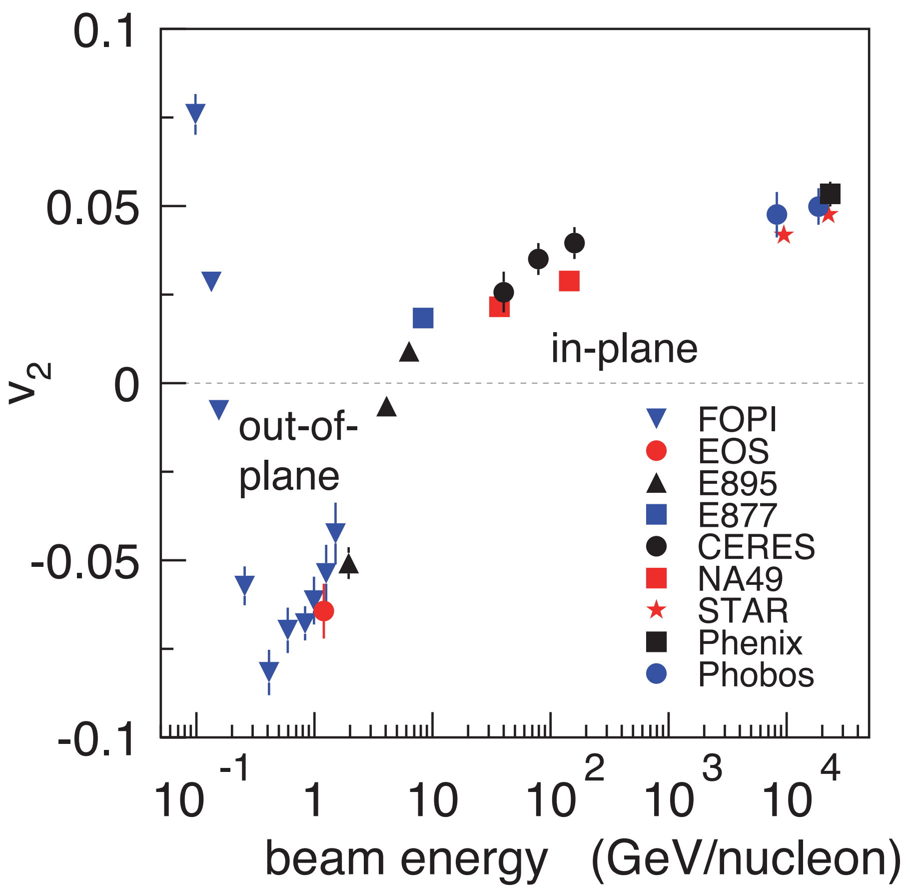

Introduction

At lower energies: various experimental groups

– H. H. Gutbrod et al. Phys. Rev. C 42 (1990) 640.

– C. Pinkenburg et al. [E895 Collaboration], Phys. Rev. Lett. 83 (1999) 1295 [nucl-ex/9903010].

and later the FOPI collaboration

– W. Reisdorf et al. [FOPI Collaboration], Nucl. Phys. A 876 (2012) 1

⇨ a negative v2 coefficient up to $E_{inc} \approx 6$ AGeV

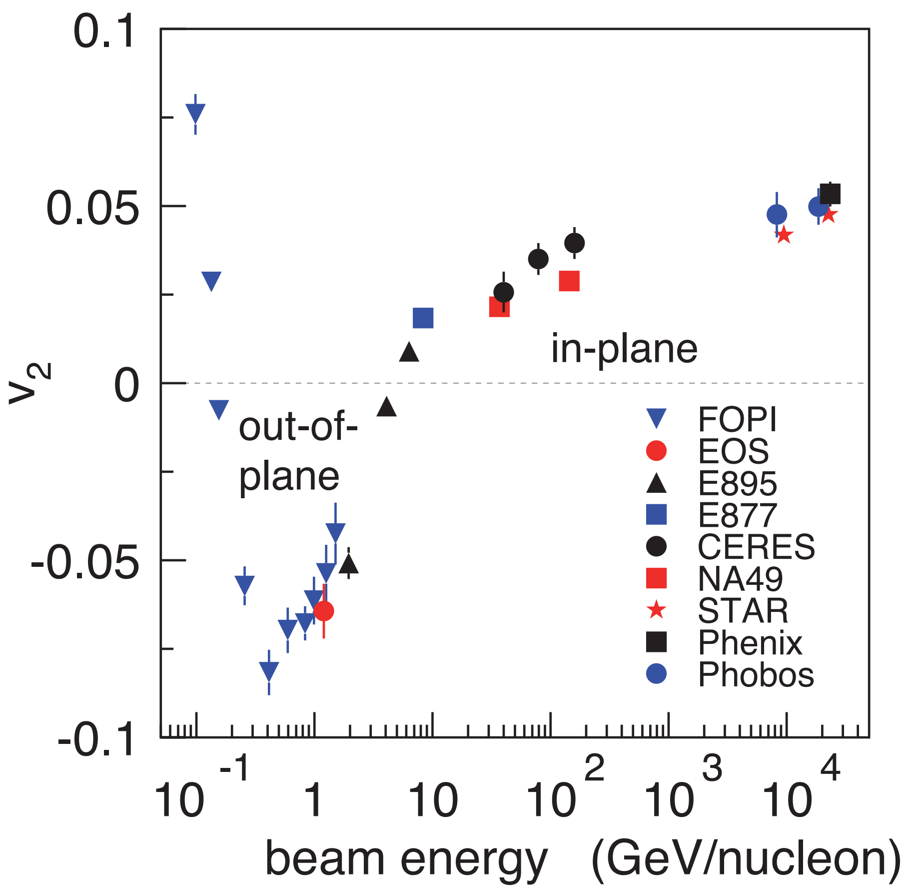

Introduction

At lower energies: various experimental groups

– H. H. Gutbrod et al. Phys. Rev. C 42 (1990) 640.

– C. Pinkenburg et al. [E895 Collaboration], Phys. Rev. Lett. 83 (1999) 1295 [nucl-ex/9903010].

and later the FOPI collaboration

– W. Reisdorf et al. [FOPI Collaboration], Nucl. Phys. A 876 (2012) 1

⇨ a negative v2 coefficient up to $E_{inc} \approx 6$ AGeV

⇨ with a minimum at around 0.4-0.6 AGeV

– A. Andronic et al. [FOPI Collaboration], Phys. Lett. B 612 (2005) 173.

– G. Stoicea et al. [FOPI Collaboration], Phys. Rev. Lett. 92 (2004) 072303

– A. Andronic, J. Lukasik, W. Reisdorf and W. Trautmann [FOPI and INDRA Collaborations], Eur. Phys. J. A 30 (2006) 31.

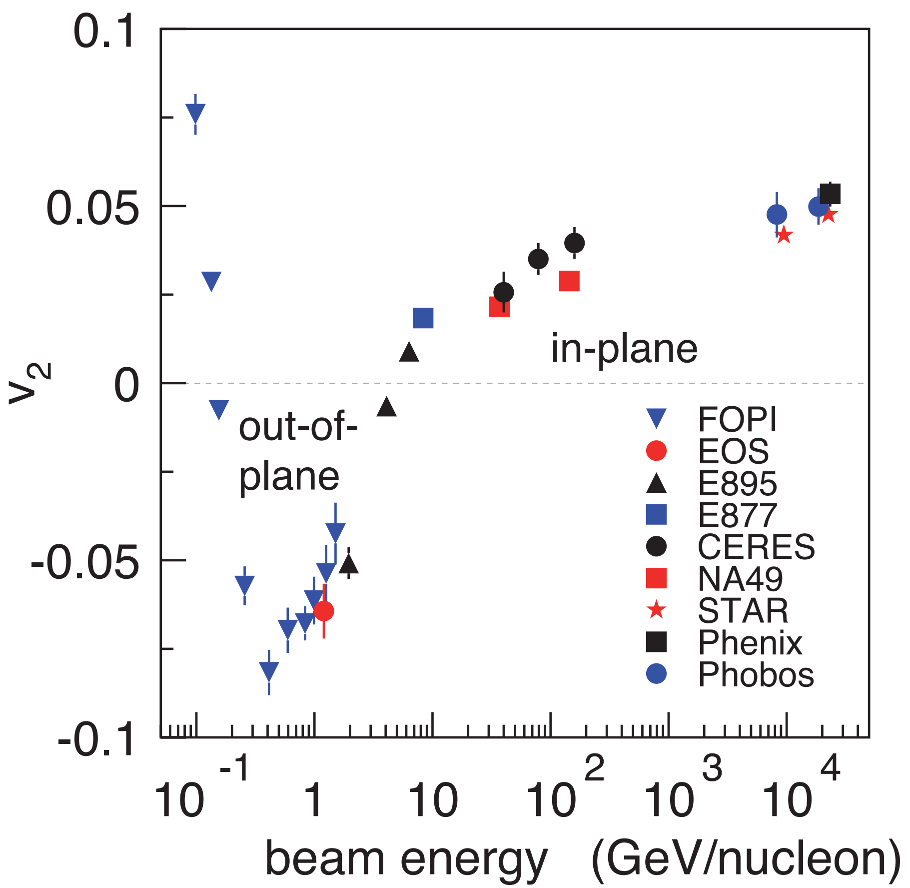

Introduction

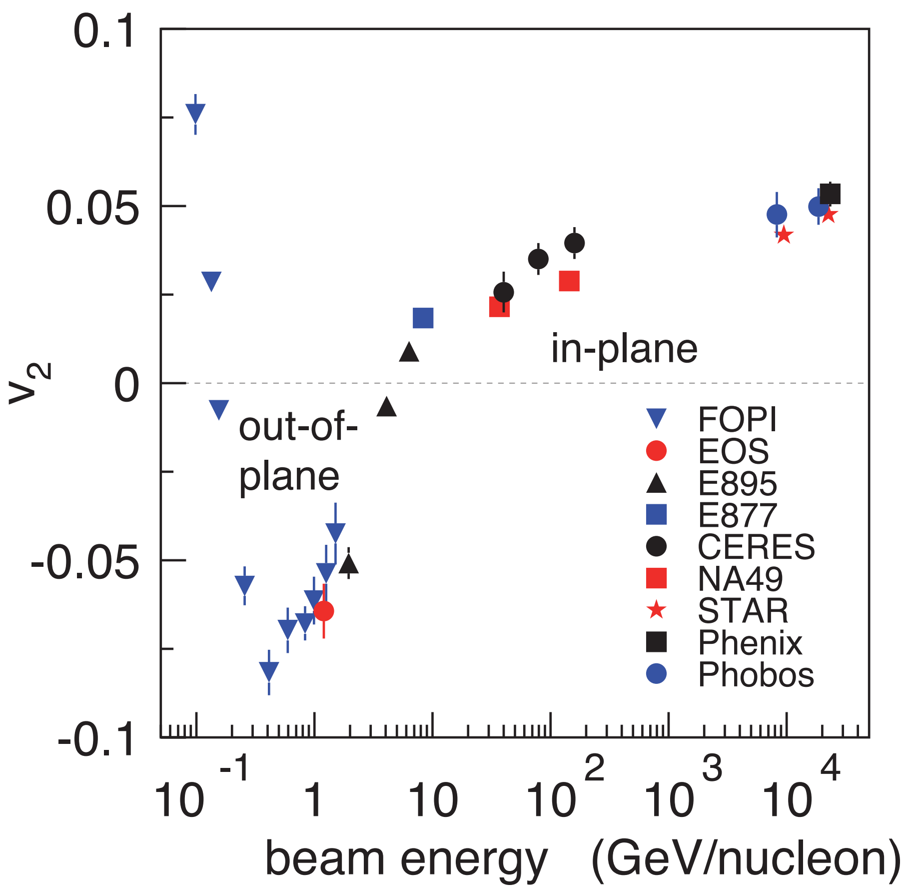

Introduction

⇨ The elliptic flow has to be of different origin at these energies.

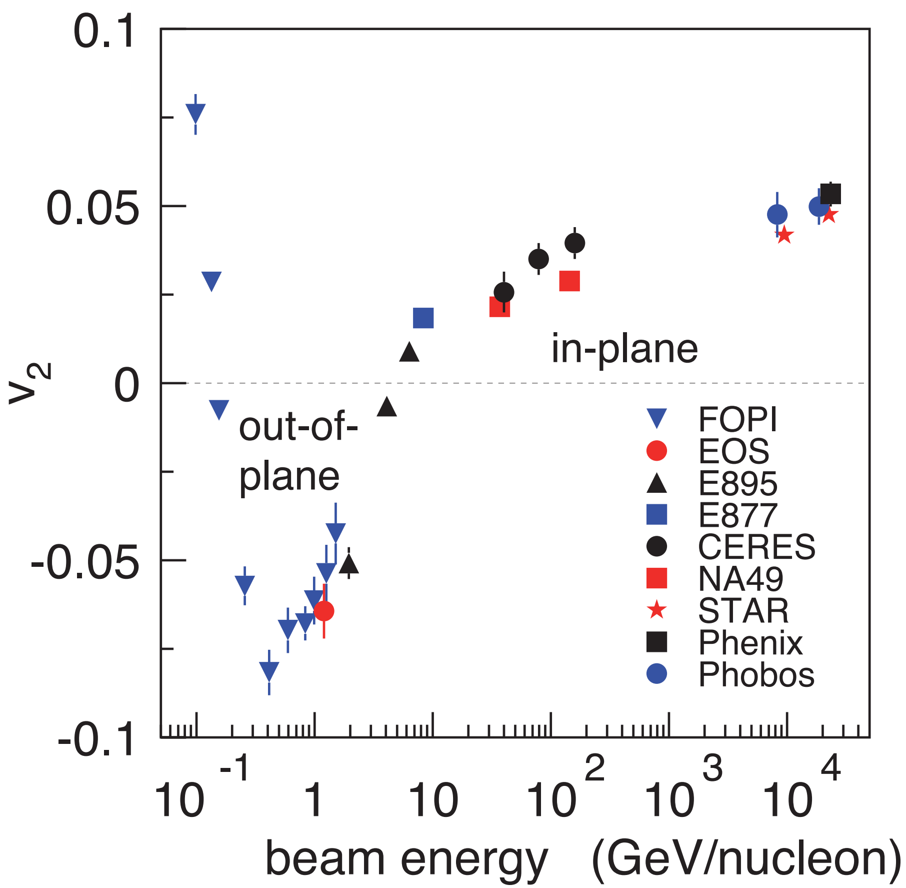

Introduction

⇨ The elliptic flow has to be of different origin at these energies.

It has been suggested in

P. Danielewicz, R. Lacey, and W. G. Lynch, Science 298 (2002) 1592

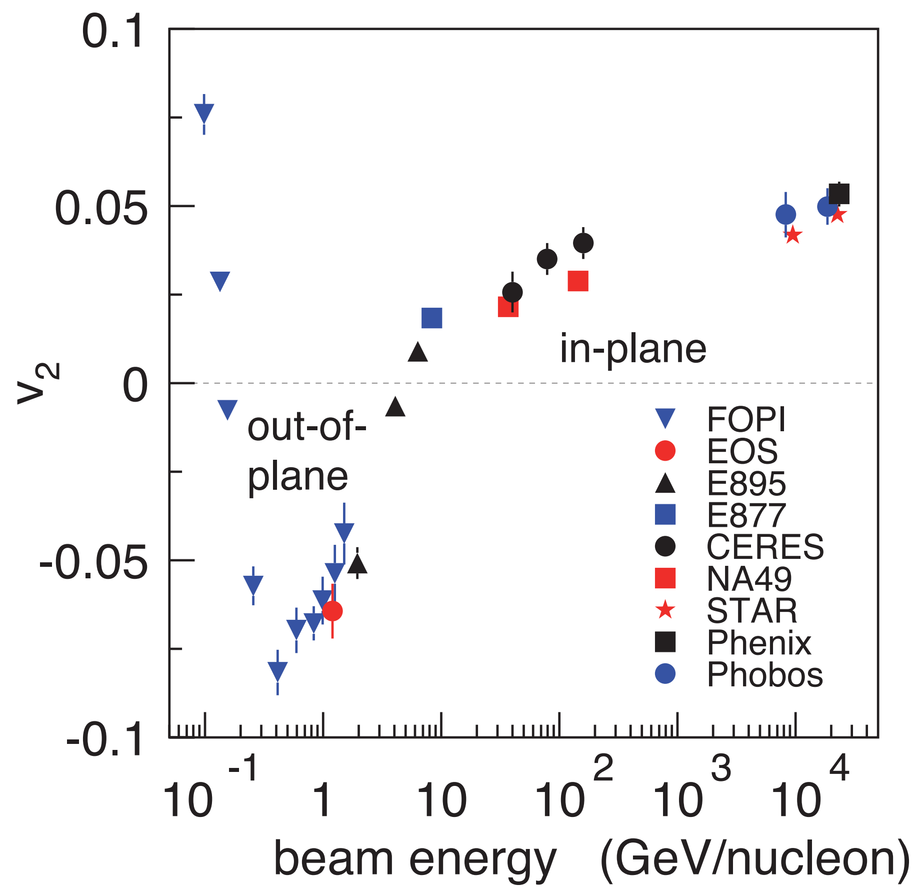

Introduction

⇨ The elliptic flow has to be of different origin at these energies.

It has been suggested in
P. Danielewicz, R. Lacey, and W. G. Lynch, Science 298 (2002) 1592
that the v_2 values are negative at low energies because the compressed matter expands while the spectator matter is still present and blocks the in-plane emission = « shadowing ».

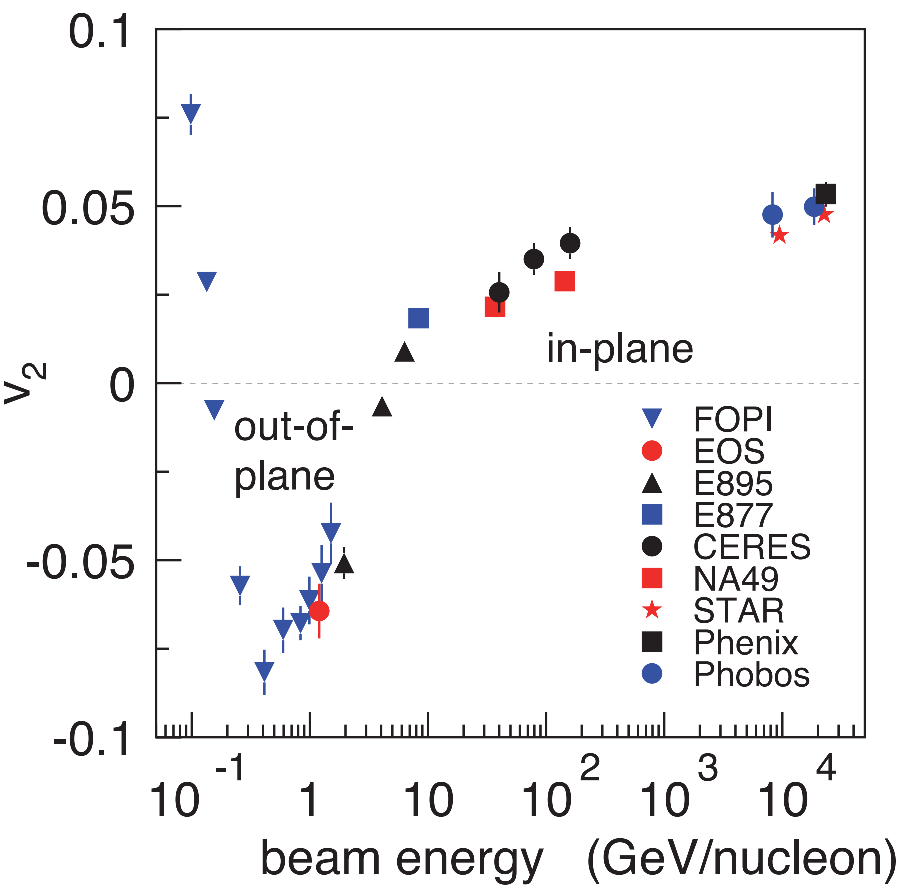

Introduction

⇨ The elliptic flow has to be of different origin at these energies.

It has been suggested in
P. Danielewicz, R. Lacey, and W. G. Lynch, Science 298 (2002) 1592
that the v_2 values are negative at low energies because the compressed matter expands while the spectator matter is still present and blocks the in-plane emission = « shadowing ».

At higher incident energies: the expansion takes place after the spectator matter has passed the compressed zone ⇨ v_2 is determined by the shape of the overlap region only ⇨ $\mathbf{v_2 > 0}$.

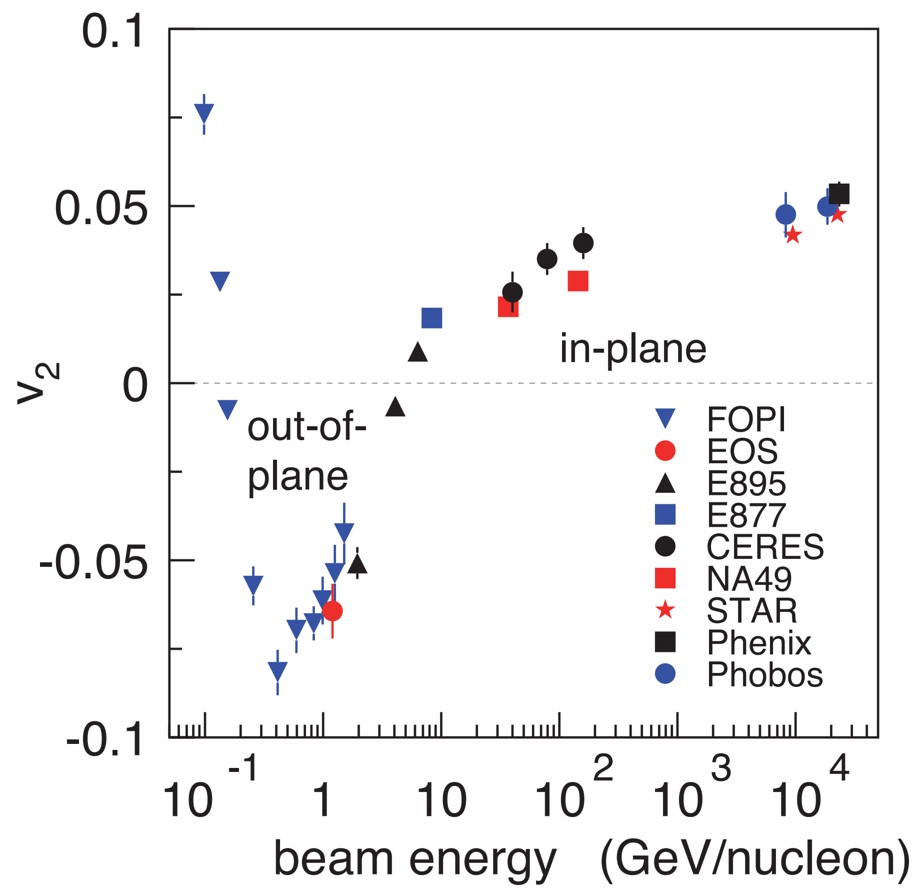

Introduction

⇨ The elliptic flow has to be of different origin at these energies.

It has been
P. Danielewicz,
1592
that the v_2 v
because th
while the s
blocks the

At higher i
takes place
passed the
determined
only ⇨ $v_2 > 0$.

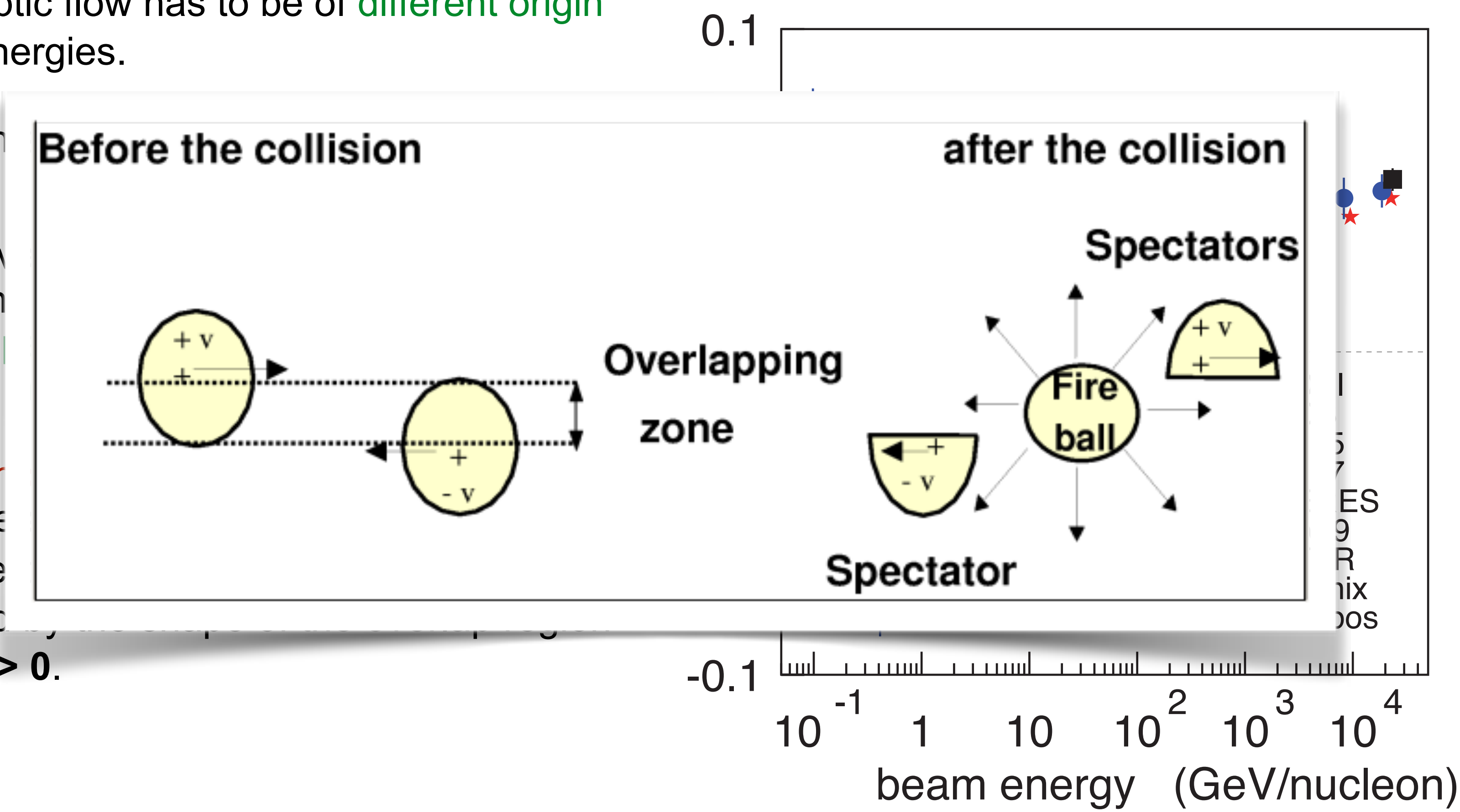

Introduction

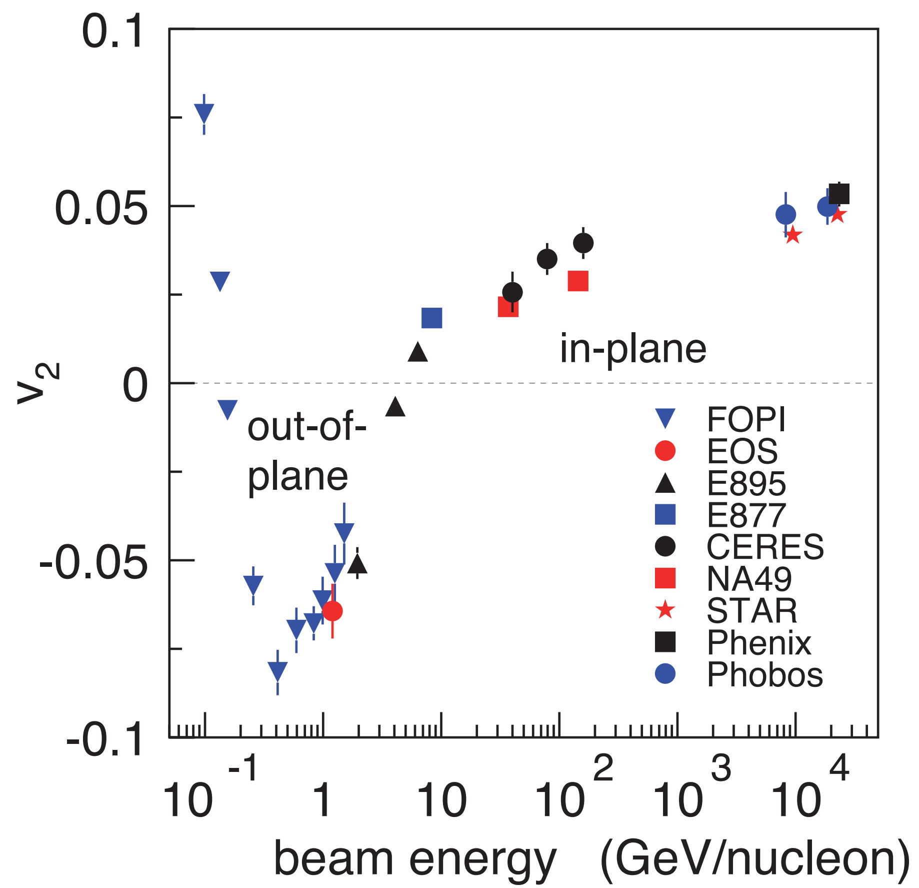

Introduction

Minimum of v_2 ⇔ maximum nuclear stopping
with high baryon densities reached.

– W. Reisdorf et al. [FOPI Collaboration], Phys. Rev. Lett. 92, 232301 (2004)

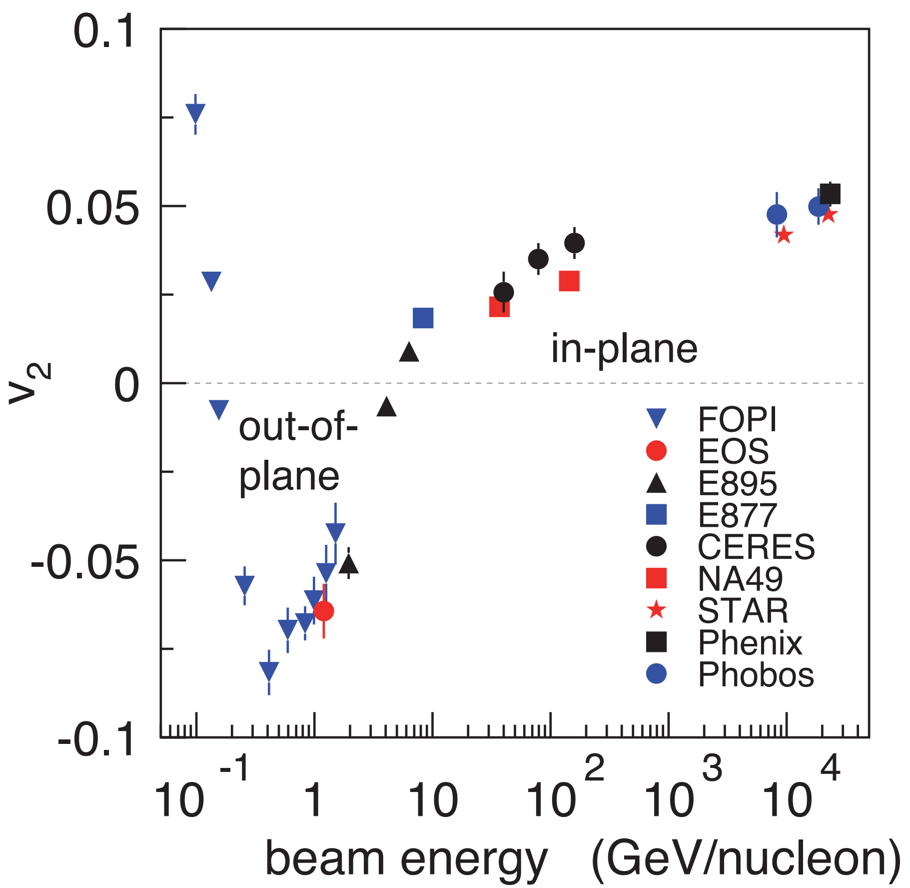

Introduction

Minimum of v_2 ⟺ maximum nuclear stopping with high baryon densities reached.

– W. Reisdorf et al. [FOPI Collaboration], Phys. Rev. Lett. 92, 232301 (2004)

Contrary to higher beam energies: no convincing experimental evidence that event-by-event fluctuations contribute to v_2 between 0.4 and 2 A GeV.

– N. Bastid et al. [FOPI Collaboration], Phys. Rev. C 72, 011901 (2005)

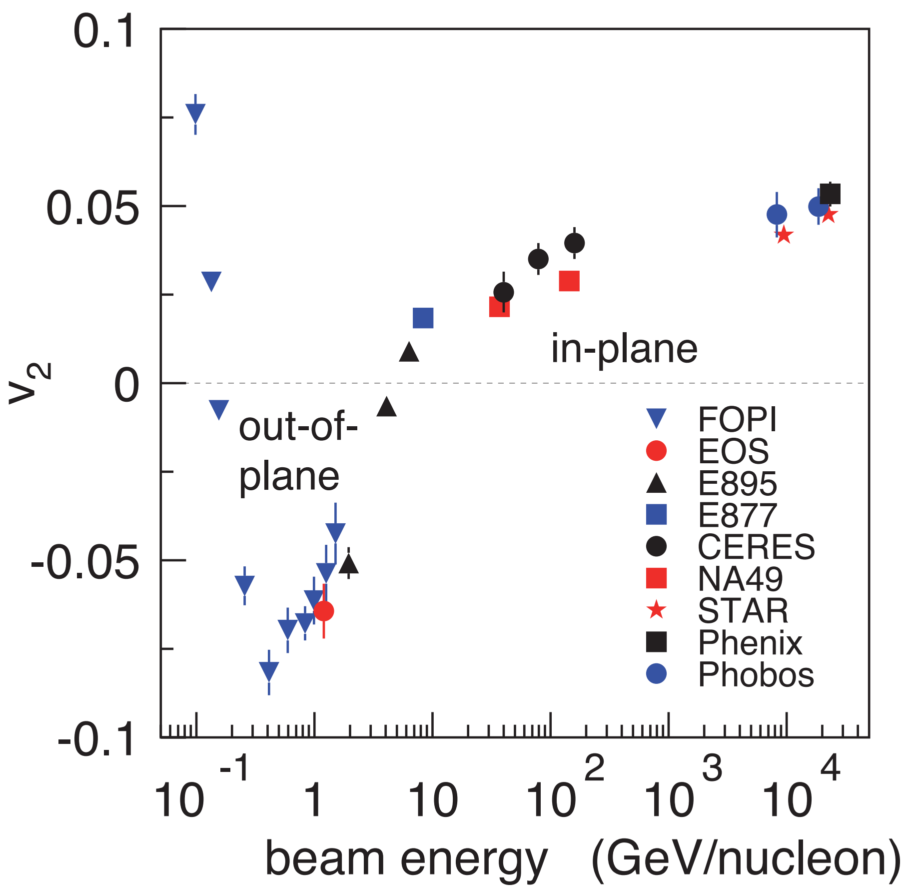

Introduction

Minimum of v_2 ⇔ maximum nuclear stopping with high baryon densities reached.

– W. Reisdorf et al. [FOPI Collaboration], Phys. Rev. Lett. 92, 232301 (2004)

Contrary to higher beam energies: no convincing experimental evidence that event-by-event fluctuations contribute to v_2 between 0.4 and 2 A GeV.

– N. Bastid et al. [FOPI Collaboration], Phys. Rev. C 72, 011901 (2005)

Most probable reasons:

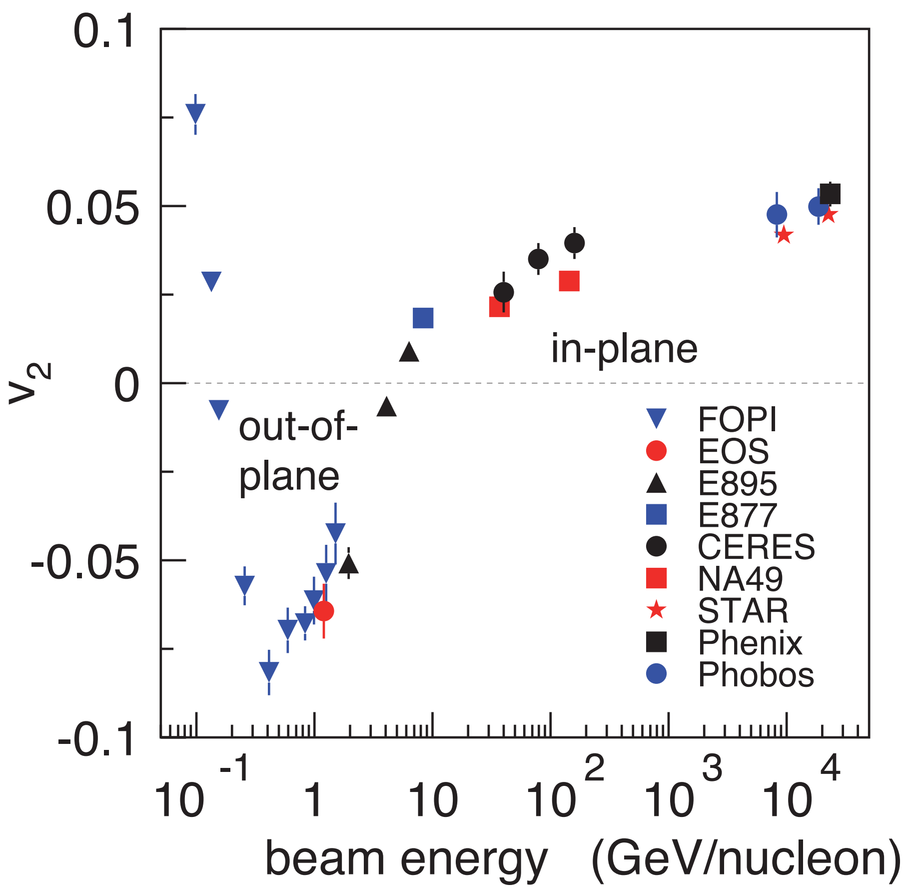

Introduction

Minimum of v_2 ⇔ maximum nuclear stopping with high baryon densities reached.

– W. Reisdorf et al. [FOPI Collaboration], Phys. Rev. Lett. 92, 232301 (2004)

Contrary to higher beam energies: no convincing experimental evidence that event-by-event fluctuations contribute to v_2 between 0.4 and 2 A GeV.

– N. Bastid et al. [FOPI Collaboration], Phys. Rev. C 72, 011901 (2005)

Most probable reasons:

- interactions with spectator matter

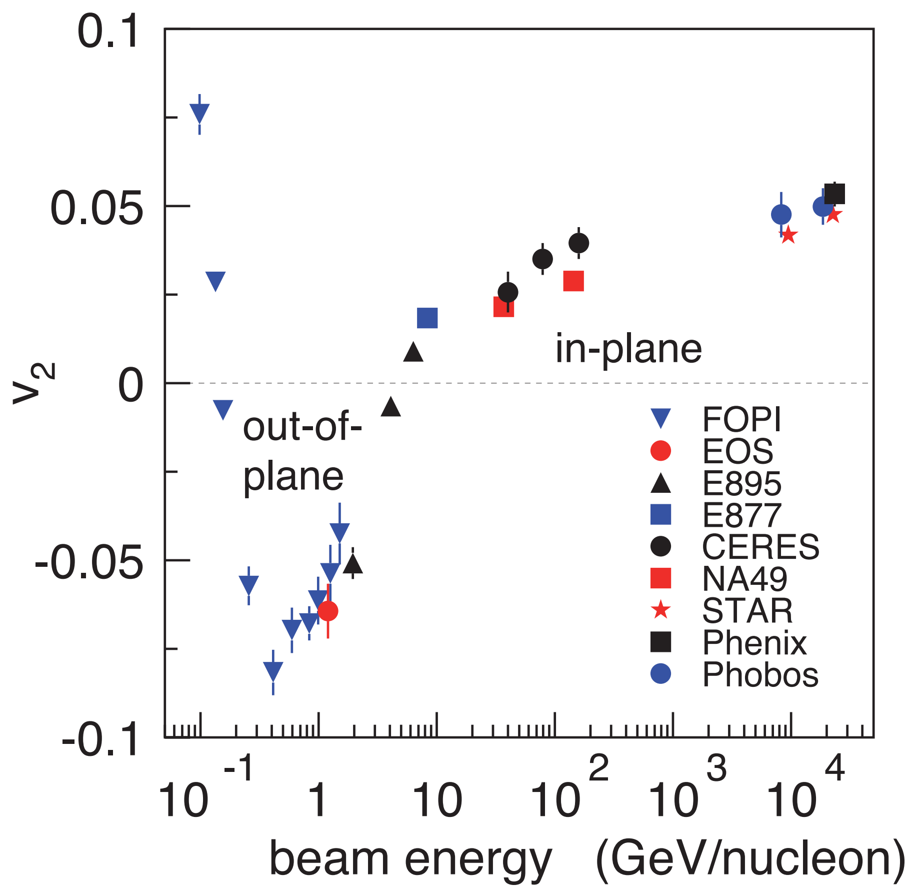

Introduction

Minimum of v_2 ⟺ maximum nuclear stopping with high baryon densities reached.

– W. Reisdorf et al. [FOPI Collaboration], Phys. Rev. Lett. 92, 232301 (2004)

Contrary to higher beam energies: no convincing experimental evidence that event-by-event fluctuations contribute to v_2 between 0.4 and 2 A GeV.

– N. Bastid et al. [FOPI Collaboration], Phys. Rev. C 72, 011901 (2005)

Most probable reasons:

- interactions with spectator matter
- much longer collision times.

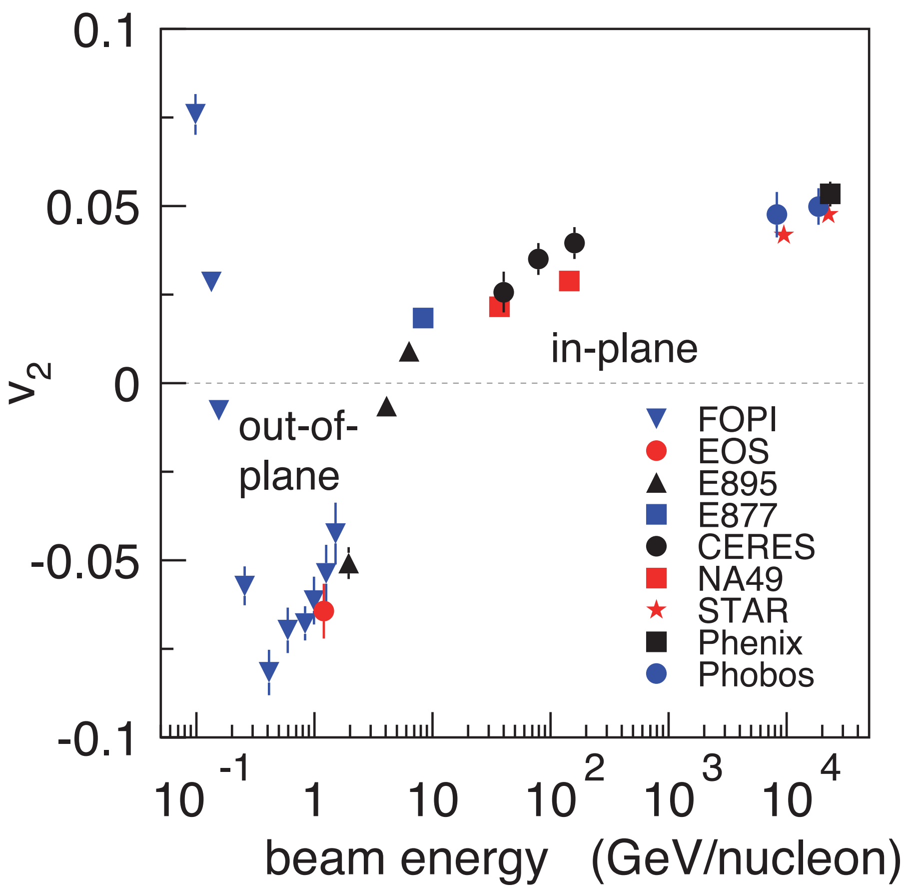

Introduction

Minimum of v_2 ⇔ maximum nuclear stopping with high baryon densities reached.

– W. Reisdorf et al. [FOPI Collaboration], Phys. Rev. Lett. 92, 232301 (2004)

Contrary to higher beam energies: no convincing experimental evidence that event-by-event fluctuations contribute to v_2 between 0.4 and 2 A GeV.

– N. Bastid et al. [FOPI Collaboration], Phys. Rev. C 72, 011901 (2005)

Most probable reasons:

- interactions with spectator matter
- much longer collision times.

At even lower incident energies: v_2 becomes positive again: attractive NN forces outweigh the repulsive NN collisions.

– J. Lukasik et al., Phys. Lett. B 608 (2005) 223.

– M. Zheng et al., Phys. Rev. Lett. 83 (1999)

– P. K. Sahu et al., Nucl. Phys. A 672 (2000) 376

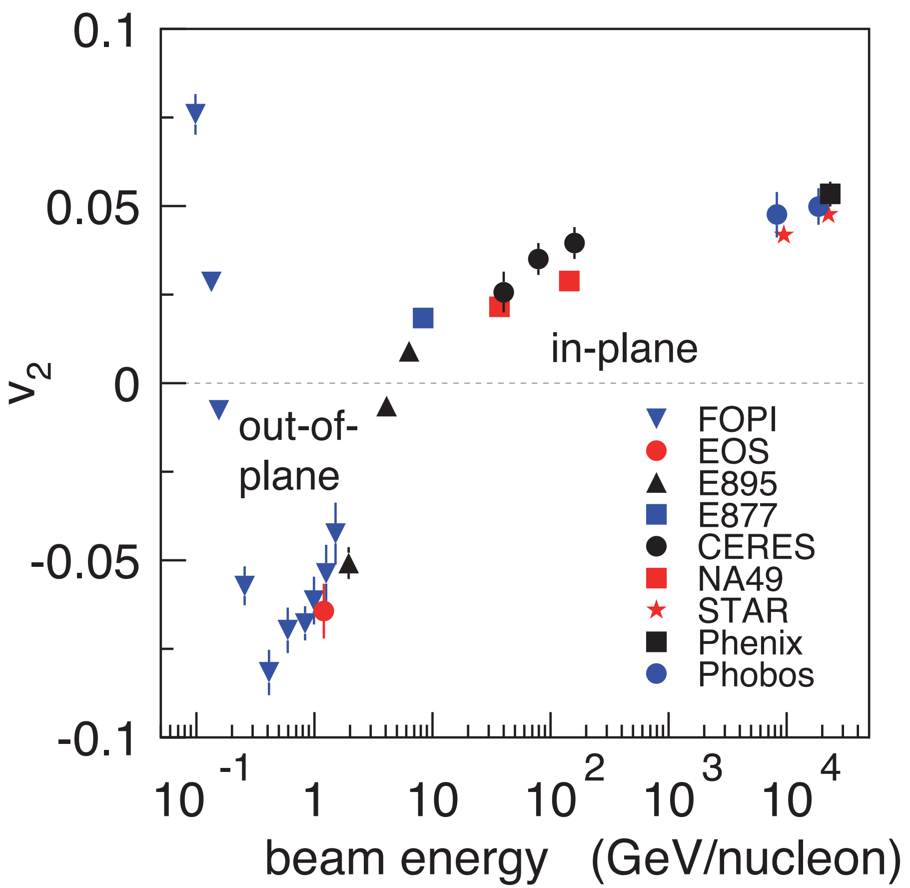

The Quantum Molecular Dynamics approach

The Quantum Molecular Dynamics approach

Details of the Quantum Molecular Dynamics (QMD) approach have been published in

– J. Aichelin, Phys. Rept. 202 (1991) 233.

– C. Hartnack et al., Phys. Rept. 510 (2012) 119

– C. Hartnack et al., Eur. Phys. J. A 1 (1998) 151

Comparisons to experimental bench-mark data measured in the incident energy region under consideration are published in

– W. Reisdorf et al. [FOPI Collaboration], Nucl. Phys. A 876 (2012) 1

Here, we quote only how this approach allows for an exploration of the nuclear EoS

Nucleons are represented as Gaussian wave functions -> single-particle Wigner density:

$$f_i(\mathbf{r},\mathbf{p},t) = \frac{1}{\pi^3 \hbar^3} \mathrm{e}^{-\frac{2}{L}(\mathbf{r}-\mathbf{r_i}(t))^2} \mathrm{e}^{-\frac{L}{2\hbar^2}(\mathbf{p}-\mathbf{p_i}(t))^2}$$

The total one-body Wigner density is the sum of the Wigner densities of all nucleons

The Quantum Molecular Dynamics approach

Details of the Quantum Molecular Dynamics (QMD) approach have been published in

– J. Aichelin, Phys. Rept. 202 (1991) 233.

– C. Hartnack et al., Phys. Rept. 510 (2012) 119

– C. Hartnack et al., Eur. Phys. J. A 1 (1998) 151

Comparisons to experimental bench-mark data measured in the incident energy region under consideration are published in

– W. Reisdorf et al. [FOPI Collaboration], Nucl. Phys. A 876 (2012) 1

Here, we quote only how this approach allows for an exploration of the nuclear EoS

Nucleons are represented as Gaussian wave functions single-particle Wigner density:

$$f_i(\mathbf{r},\mathbf{p},t) = \frac{1}{\pi^3\hbar^3} e^{-\frac{2}{L}(\mathbf{r}-\mathbf{r_i}(t))^2} e^{-\frac{L}{2\hbar^2}(\mathbf{p}-\mathbf{p_i}(t))^2}$$

The total one-body Wigner density is the sum of the Wigner densities of all nucleons

The potential consists of several terms:

$$\begin{aligned} V(\mathbf{r_i},\mathbf{r_j},\mathbf{p_i},\mathbf{p_j}) &= G + V_{\mathrm{Coul}} \\ &= V_{\mathrm{Skyrme}} + V_{\mathrm{Yuk}} + V_{\mathrm{mdi}} + +V_{sym} + V_{\mathrm{Coul}} \\ &= t_1\delta(\mathbf{r_i}-\mathbf{r_j}) + t_2\delta(\mathbf{r_i}-\mathbf{r_j})\rho^{\gamma-1}(\mathbf{r_i}) + \\ &\quad t_3\frac{\exp\{-|\mathbf{r_i}-\mathbf{r_j}|/\mu\}}{|\mathbf{r_i}-\mathbf{r_j}|/\mu} + \\ &\quad t_4 \ln^2(1+t_5(\mathbf{p_i}-\mathbf{p_j})^2)\delta(\mathbf{r_i}-\mathbf{r_j}) + \\ &\quad t_6\frac{1}{\varrho_0}T_3^i T_3^j\delta(\mathbf{r_i}-\mathbf{r_j}) + \frac{Z_i Z_j e^2}{|\mathbf{r_i}-\mathbf{r_j}|}. \end{aligned}$$

Convolution of the distribution functions f_i and f_j → single-particle potential (« mean-field ») = V_{Skyrme} + V_{mdi} (local interactions + momentum dependence)

$$U_i(\mathbf{r_i},t) = \alpha\left(\frac{\rho_{int}}{\rho_0}\right) + \beta\left(\frac{\rho_{int}}{\rho_0}\right)^{\gamma} + \delta \ln^2\left(\varepsilon\,(\Delta\mathbf{p})^2+1\right)\left(\frac{\rho_{int}}{\rho_0}\right)$$

In nuclear matter t_1, t_2, t_4, t_5 uniquely related α, β, δ, and ε

ε and δ : given by fits to the optical potential extracted from elastic scattering data in pA collisions.

α, β, γ : 2 are constrained by volume energy has a minimum of $E/A(\rho_0) = -16$ MeV at ρ_0.

	α (MeV)	β (MeV)	γ	δ (MeV)	$\varepsilon\left(\frac{c^2}{\mathrm{GeV}^2}\right)$	K (MeV)
SM	-390	320	1.14	1.57	500	200
HM	-130	59	2.09	1.57	500	376

The Quantum Molecular Dynamics approach

Details of the Quantum Molecular Dynamics (QMD) approach have been published in

– J. Aichelin, Phys. Rept. 202 (1991) 233.

– C. Hartnack et al., Phys. Rept. 510 (2012) 119

– C. Hartnack et al., Eur. Phys. J. A 1 (1998) 151

Comparisons to experimental bench-mark data measured in the incident energy region under consideration are published in

– W. Reisdorf et al. [FOPI Collaboration], Nucl. Phys. A 876 (2012) 1

Here, we quote only how this approach allows for an exploration of the nuclear EoS

Nucleons are represented as Gaussian wave functions single-particle Wigner density:

$$f_i(\mathbf{r},\mathbf{p},t) = \frac{1}{\pi^3\hbar^3} e^{-\frac{2}{L}(\mathbf{r}-\mathbf{r_i}(t))^2} e^{-\frac{L}{2\hbar^2}(\mathbf{p}-\mathbf{p_i}(t))^2}$$

The total one-body Wigner density is the sum of the Wigner densities of all nucleons

The potential consists of several terms:

$$\begin{aligned} V(\mathbf{r_i},\mathbf{r_j},\mathbf{p_i},\mathbf{p_j}) &= G + V_{\text{Coul}} \\ &= \boxed{V_{\text{Skyrme}}} + V_{\text{Yuk}} + V_{\text{mdi}} + +V_{sym} + V_{\text{Coul}} \\ &= \boxed{t_1\delta(\mathbf{r_i}-\mathbf{r_j}) + t_2\delta(\mathbf{r_i}-\mathbf{r_j})\rho^{\gamma-1}(\mathbf{r_i})} + \\ &\quad t_3\frac{\exp\{-|\mathbf{r_i}-\mathbf{r_j}|/\mu\}}{|\mathbf{r_i}-\mathbf{r_j}|/\mu} + \\ &\quad t_4\ln^2(1+t_5(\mathbf{p_i}-\mathbf{p_j})^2)\delta(\mathbf{r_i}-\mathbf{r_j}) + \\ &\quad t_6\frac{1}{\varrho_0}T_3^iT_3^j\delta(\mathbf{r_i}-\mathbf{r_j}) + \frac{Z_iZ_je^2}{|\mathbf{r_i}-\mathbf{r_j}|}. \end{aligned}$$

Convolution of the distribution functions f_i and f_j → single-particle potential (« mean-field ») = V_{Skyrme} + V_{mdi} (local interactions + momentum dependence)

$$U_i(\mathbf{r_i},t) = \alpha\left(\frac{\rho_{int}}{\rho_0}\right) + \beta\left(\frac{\rho_{int}}{\rho_0}\right)^\gamma + \delta\ln^2\left(\varepsilon\,(\Delta\mathbf{p})^2+1\right)\left(\frac{\rho_{int}}{\rho_0}\right)$$

In nuclear matter t_1, t_2, t_4, t_5 uniquely related α, β, δ, and ε

ε and δ : given by fits to the optical potential extracted from elastic scattering data in pA collisions.

α, β, γ : 2 are constrained by volume energy has a minimum of $E/A(\rho_0) = -16$ MeV at ρ_0.

	α (MeV)	β (MeV)	γ	δ (MeV)	$\varepsilon\left(\frac{c^2}{\text{GeV}^2}\right)$	K (MeV)
SM	-390	320	1.14	1.57	500	200
HM	-130	59	2.09	1.57	500	376

The Quantum Molecular Dynamics approach

Details of the Quantum Molecular Dynamics (QMD) approach have been published in

– J. Aichelin, Phys. Rept. 202 (1991) 233.

– C. Hartnack et al., Phys. Rept. 510 (2012) 119

– C. Hartnack et al., Eur. Phys. J. A 1 (1998) 151

Comparisons to experimental bench-mark data measured in the incident energy region under consideration are published in

– W. Reisdorf et al. [FOPI Collaboration], Nucl. Phys. A 876 (2012) 1

Here, we quote only how this approach allows for an exploration of the nuclear EoS

Nucleons are represented as Gaussian wave functions single-particle Wigner density:

$$f_i(\mathbf{r},\mathbf{p},t) = \frac{1}{\pi^3\hbar^3} e^{-\frac{2}{L}(\mathbf{r}-\mathbf{r_i}(t))^2} e^{-\frac{L}{2\hbar^2}(\mathbf{p}-\mathbf{p_i}(t))^2}$$

The total one-body Wigner density is the sum of the Wigner densities of all nucleons

The potential consists of several terms:

$$\begin{aligned}
V(\mathbf{r_i},\mathbf{r_j},\mathbf{p_i},\mathbf{p_j}) &= G + V_{\mathrm{Coul}} \\
&= V_{\mathrm{Skyrme}} \boxed{+ V_{\mathrm{Yuk}} +} V_{\mathrm{mdi}} + +V_{sym} + V_{\mathrm{Coul}} \\
&= t_1\delta(\mathbf{r_i}-\mathbf{r_j}) + t_2\delta(\mathbf{r_i}-\mathbf{r_j})\rho^{\gamma-1}(\mathbf{r_i}) + \\
&\quad \boxed{t_3\frac{\exp\{-|\mathbf{r_i}-\mathbf{r_j}|/\mu\}}{|\mathbf{r_i}-\mathbf{r_j}|/\mu}} + \\
&\quad t_4 \ln^2(1+t_5(\mathbf{p_i}-\mathbf{p_j})^2)\delta(\mathbf{r_i}-\mathbf{r_j}) + \\
&\quad t_6\frac{1}{\varrho_0}T_3^i T_3^j\delta(\mathbf{r_i}-\mathbf{r_j}) + \frac{Z_i Z_j e^2}{|\mathbf{r_i}-\mathbf{r_j}|}.
\end{aligned}$$

Convolution of the distribution functions f_i and f_j → single-particle potential (« mean-field ») = V_{Skyrme} + V_{mdi} (local interactions + momentum dependence)

$$U_i(\mathbf{r_i},t) = \alpha\left(\frac{\rho_{int}}{\rho_0}\right) + \beta\left(\frac{\rho_{int}}{\rho_0}\right)^{\gamma} + \delta \ln^2\left(\varepsilon\,(\Delta\mathbf{p})^2+1\right)\left(\frac{\rho_{int}}{\rho_0}\right)$$

In nuclear matter t_1, t_2, t_4, t_5 uniquely related α, β, δ, and ε
ε and δ : given by fits to the optical potential extracted from elastic scattering data in pA collisions.
α, β, γ : 2 are constrained by volume energy has a minimum of E/A(ρ_0) = −16 MeV at ρ_0.

	α (MeV)	β (MeV)	γ	δ (MeV)	ε $\left(\frac{c^2}{\mathrm{GeV}^2}\right)$	K (MeV)
SM	-390	320	1.14	1.57	500	200
HM	-130	59	2.09	1.57	500	376

GSI HELMHOLTZ ASSOCIATION

The Quantum Molecular Dynamics approach

Details of the Quantum Molecular Dynamics (QMD) approach have been published in

– J. Aichelin, Phys. Rept. 202 (1991) 233.

– C. Hartnack et al., Phys. Rept. 510 (2012) 119

– C. Hartnack et al., Eur. Phys. J. A 1 (1998) 151

Comparisons to experimental bench-mark data measured in the incident energy region under consideration are published in

– W. Reisdorf et al. [FOPI Collaboration], Nucl. Phys. A 876 (2012) 1

Here, we quote only how this approach allows for an exploration of the nuclear EoS

Nucleons are represented as Gaussian wave functions single-particle Wigner density:

$$f_i(\mathbf{r},\mathbf{p},t) = \frac{1}{\pi^3\hbar^3} e^{-\frac{2}{L}(\mathbf{r}-\mathbf{r_i}(t))^2} e^{-\frac{L}{2\hbar^2}(\mathbf{p}-\mathbf{p_i}(t))^2}$$

The total one-body Wigner density is the sum of the Wigner densities of all nucleons

The potential consists of several terms:

$$\begin{aligned} V(\mathbf{r_i},\mathbf{r_j},\mathbf{p_i},\mathbf{p_j}) &= G + V_{\mathrm{Coul}} \\ &= V_{\mathrm{Skyrme}} + V_{\mathrm{Yuk}} + \boxed{V_{\mathrm{mdi}}} + V_{sym} + V_{\mathrm{Coul}} \\ &= t_1\delta(\mathbf{r_i}-\mathbf{r_j}) + t_2\delta(\mathbf{r_i}-\mathbf{r_j})\rho^{\gamma-1}(\mathbf{r_i}) + \\ &\quad t_3\frac{\exp\{-|\mathbf{r_i}-\mathbf{r_j}|/\mu\}}{|\mathbf{r_i}-\mathbf{r_j}|/\mu} + \\ &\quad \boxed{t_4 \ln^2(1+t_5(\mathbf{p_i}-\mathbf{p_j})^2)\delta(\mathbf{r_i}-\mathbf{r_j})} + \\ &\quad t_6\frac{1}{\varrho_0}T_3^i T_3^j \delta(\mathbf{r_i}-\mathbf{r_j}) + \frac{Z_i Z_j e^2}{|\mathbf{r_i}-\mathbf{r_j}|}. \end{aligned}$$

Convolution of the distribution functions f_i and f_j → single-particle potential (« mean-field ») = V_{Skyrme} + V_{mdi} (local interactions + momentum dependence)

$$U_i(\mathbf{r_i},t) = \alpha\left(\frac{\rho_{int}}{\rho_0}\right) + \beta\left(\frac{\rho_{int}}{\rho_0}\right)^{\gamma} + \delta \ln^2\left(\varepsilon\,(\Delta\mathbf{p})^2+1\right)\left(\frac{\rho_{int}}{\rho_0}\right)$$

In nuclear matter t_1, t_2, t_4, t_5 uniquely related α, β, δ, and ε

ε and δ : given by fits to the optical potential extracted from elastic scattering data in pA collisions.

α, β, γ : 2 are constrained by volume energy has a minimum of $E/A(\rho_0) = -16$ MeV at ρ_0.

	α (MeV)	β (MeV)	γ	δ (MeV)	$\varepsilon\ \left(\frac{c^2}{\mathrm{GeV}^2}\right)$	K (MeV)
SM	-390	320	1.14	1.57	500	200
HM	-130	59	2.09	1.57	500	376

GSI HELMHOLTZ ASSOCIATION

The Quantum Molecular Dynamics approach

Details of the Quantum Molecular Dynamics (QMD) approach have been published in

- J. Aichelin, Phys. Rept. 202 (1991) 233.
- C. Hartnack et al., Phys. Rept. 510 (2012) 119
- C. Hartnack et al., Eur. Phys. J. A 1 (1998) 151

Comparisons to experimental bench-mark data measured in the incident energy region under consideration are published in

- W. Reisdorf et al. [FOPI Collaboration], Nucl. Phys. A 876 (2012) 1

Here, we quote only how this approach allows for an exploration of the nuclear EoS

Nucleons are represented as Gaussian wave functions single-particle Wigner density:

$$f_i(\mathbf{r},\mathbf{p},t) = \frac{1}{\pi^3\hbar^3} e^{-\frac{2}{L}(\mathbf{r}-\mathbf{r_i}(t))^2} e^{-\frac{L}{2\hbar^2}(\mathbf{p}-\mathbf{p_i}(t))^2}$$

The total one-body Wigner density is the sum of the Wigner densities of all nucleons

The potential consists of several terms:

$$\begin{aligned} V(\mathbf{r_i},\mathbf{r_j},\mathbf{p_i},\mathbf{p_j}) &= G + V_{\mathrm{Coul}} \\ &= V_{\mathrm{Skyrme}} + V_{\mathrm{Yuk}} + V_{\mathrm{mdi}} + \boxed{+V_{sym}+} V_{\mathrm{Coul}} \\ &= t_1\delta(\mathbf{r_i}-\mathbf{r_j}) + t_2\delta(\mathbf{r_i}-\mathbf{r_j})\rho^{\gamma-1}(\mathbf{r_i}) + \\ &\quad t_3\frac{\exp\{-|\mathbf{r_i}-\mathbf{r_j}|/\mu\}}{|\mathbf{r_i}-\mathbf{r_j}|/\mu} + \\ &\quad t_4\ln^2(1+t_5(\mathbf{p_i}-\mathbf{p_j})^2)\delta(\mathbf{r_i}-\mathbf{r_j}) + \\ &\quad \boxed{t_6\frac{1}{\varrho_0}T_3^iT_3^j\delta(\mathbf{r_i}-\mathbf{r_j})} + \frac{Z_iZ_je^2}{|\mathbf{r_i}-\mathbf{r_j}|}. \end{aligned}$$

Convolution of the distribution functions f_i and f_j → single-particle potential (« mean-field ») = V_{Skyrme} + V_{mdi} (local interactions + momentum dependence)

$$U_i(\mathbf{r_i},t) = \alpha\left(\frac{\rho_{int}}{\rho_0}\right) + \beta\left(\frac{\rho_{int}}{\rho_0}\right)^{\gamma} + \delta\ln^2\left(\varepsilon\left(\Delta\mathbf{p}\right)^2+1\right)\left(\frac{\rho_{int}}{\rho_0}\right)$$

In nuclear matter t_1, t_2, t_4, t_5 uniquely related α, β, δ, and ε

ε and δ : given by fits to the optical potential extracted from elastic scattering data in pA collisions.

α, β, γ : 2 are constrained by volume energy has a minimum of $E/A(\rho_0) = -16$ MeV at ρ_0.

	α (MeV)	β (MeV)	γ	δ (MeV)	$\varepsilon\ \left(\frac{c^2}{\mathrm{GeV}^2}\right)$	K (MeV)
SM	-390	320	1.14	1.57	500	200
HM	-130	59	2.09	1.57	500	376

The Quantum Molecular Dynamics approach

Details of the Quantum Molecular Dynamics (QMD) approach have been published in

– J. Aichelin, Phys. Rept. 202 (1991) 233.

– C. Hartnack et al., Phys. Rept. 510 (2012) 119

– C. Hartnack et al., Eur. Phys. J. A 1 (1998) 151

Comparisons to experimental bench-mark data measured in the incident energy region under consideration are published in

– W. Reisdorf et al. [FOPI Collaboration], Nucl. Phys. A 876 (2012) 1

Here, we quote only how this approach allows for an exploration of the nuclear EoS

Nucleons are represented as Gaussian wave functions single-particle Wigner density:

$$f_i(\mathbf{r},\mathbf{p},t) = \frac{1}{\pi^3\hbar^3} \mathrm{e}^{-\frac{2}{L}(\mathbf{r}-\mathbf{r_i}(t))^2} \mathrm{e}^{-\frac{L}{2\hbar^2}(\mathbf{p}-\mathbf{p_i}(t))^2}$$

The total one-body Wigner density is the sum of the Wigner densities of all nucleons

The potential consists of several terms:

$$\begin{aligned} V(\mathbf{r_i},\mathbf{r_j},\mathbf{p_i},\mathbf{p_j}) &= G + V_{\mathrm{Coul}} \\ &= V_{\mathrm{Skyrme}} + V_{\mathrm{Yuk}} + V_{\mathrm{mdi}} + +V_{sym} \boxed{+ V_{\mathrm{Coul}}} \\ &= t_1\delta(\mathbf{r_i}-\mathbf{r_j}) + t_2\delta(\mathbf{r_i}-\mathbf{r_j})\rho^{\gamma-1}(\mathbf{r_i}) + \\ &\quad t_3\frac{\exp\{-|\mathbf{r_i}-\mathbf{r_j}|/\mu\}}{|\mathbf{r_i}-\mathbf{r_j}|/\mu} + \\ &\quad t_4\ln^2(1+t_5(\mathbf{p_i}-\mathbf{p_j})^2)\delta(\mathbf{r_i}-\mathbf{r_j}) + \\ &\quad t_6\frac{1}{\varrho_0}T_3^iT_3^j\delta(\mathbf{r_i}-\mathbf{r_j}) \boxed{+\frac{Z_iZ_je^2}{|\mathbf{r_i}-\mathbf{r_j}|}}. \end{aligned}$$

Convolution of the distribution functions f_i and f_j → single-particle potential (« mean-field ») = V_{Skyrme} + V_{mdi} (local interactions + momentum dependence)

$$U_i(\mathbf{r_i},t) = \alpha\left(\frac{\rho_{int}}{\rho_0}\right) + \beta\left(\frac{\rho_{int}}{\rho_0}\right)^{\gamma} + \delta\ln^2\left(\varepsilon\left(\Delta\mathbf{p}\right)^2+1\right)\left(\frac{\rho_{int}}{\rho_0}\right)$$

In nuclear matter t_1, t_2, t_4, t_5 uniquely related α, β, δ, and ε

ε and δ : given by fits to the optical potential extracted from elastic scattering data in pA collisions.

α, β, γ : 2 are constrained by volume energy has a minimum of E/A(ρ_0) = −16 MeV at ρ_0.

	α (MeV)	β (MeV)	γ	δ (MeV)	ε $\left(\frac{c^2}{\mathrm{GeV}^2}\right)$	K (MeV)
SM	-390	320	1.14	1.57	500	200
HM	-130	59	2.09	1.57	500	376

The Quantum Molecular Dynamics approach

K
=
compression modulus of nuclear matter
=
curvature of the volume energy at ρ = ρ_0 (for T=0)

$$K = -V\frac{\partial p}{\partial V} = 9\rho^2 \frac{\partial^2 E/A(\rho)}{(\partial\rho)^2}\Big|_{\rho=\rho_0}$$

Details of the Q
approach have
– J. Aichelin, Phy

– C. Hartnack et a

– C. Hartnack et a

Comparisons to
in the incident e
published in

– W. Reisdorf et a
876 (2012) 1

l terms:

$+ V_{\text{mdi}} + +V_{sym} + V_{\text{Coul}}$

$t_2\delta(\mathbf{r_i} - \mathbf{r_j})\rho^{\gamma-1}(\mathbf{r_i}) +$

$\mathbf{r_j}|/\mu\} \; +$

μ

$- \mathbf{p_j})^2)\delta(\mathbf{r_i} - \mathbf{r_j}) +$

$- \mathbf{r_j}) + \frac{Z_iZ_je^2}{|\mathbf{r_i} - \mathbf{r_j}|}.$

inctions f_i and f_j → single-
) = V_{Skyrme} + V_{mdi} (local
interactions + momentum dependence)

Here, we quote
exploration of the nuclear EoS

$$U_i(\mathbf{r_i}, t) = \alpha\left(\frac{\rho_{int}}{\rho_0}\right) + \beta\left(\frac{\rho_{int}}{\rho_0}\right)^{\gamma} + \delta\ln^2\left(\varepsilon\,(\Delta\mathbf{p})^2 + 1\right)\left(\frac{\rho_{int}}{\rho_0}\right)$$

Nucleons are represented as Gaussian wave functions single-particle Wigner density:

$$f_i(\mathbf{r}, \mathbf{p}, t) = \frac{1}{\pi^3\hbar^3} e^{-\frac{2}{L}(\mathbf{r}-\mathbf{r_i}(t))^2} e^{-\frac{L}{2\hbar^2}(\mathbf{p}-\mathbf{p_i}(t))^2}$$

The total one-body Wigner density is the sum of the Wigner densities of all nucleons

In nuclear matter t_1, t_2, t_4, t_5 uniquely related α, β, δ, and ε
ε and δ : given by fits to the optical potential extracted from elastic scattering data in pA collisions.
α, β, γ : 2 are constrained by volume energy has a minimum of $E/A(\rho_0) = -16$ MeV at ρ_0.

	α (MeV)	β (MeV)	γ	δ (MeV)	ε $\left(\frac{c^2}{\text{GeV}^2}\right)$	K (MeV)
SM	-390	320	1.14	1.57	500	200
HM	-130	59	2.09	1.57	500	376

GSI HELMHOLTZ ASSOCIATION

Elliptic flow at mid-rapidity: the strongest sensitivity to the Nuclear Equation of State

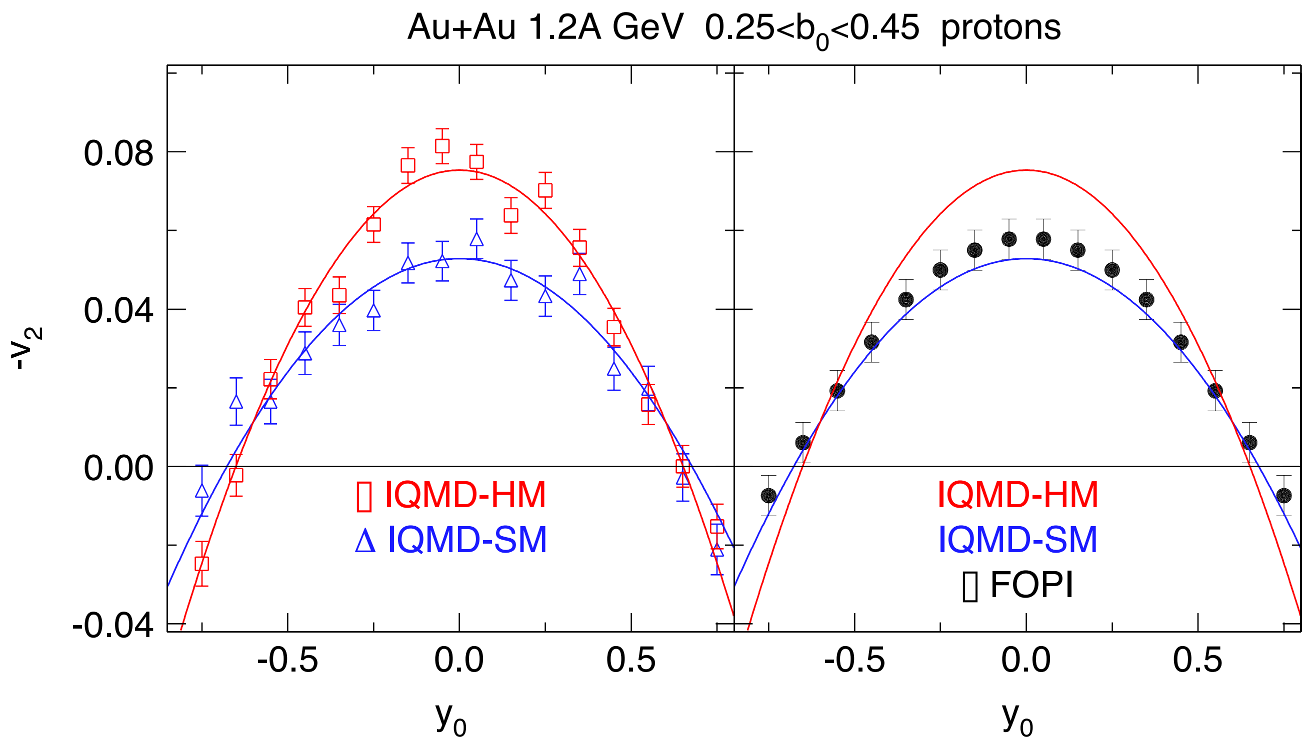

A. Le Fèvre et al., Nucl. Phys. A 945 (2016) 112.

Elliptic flow at mid-rapidity: the strongest sensitivity to the Nuclear Equation of State

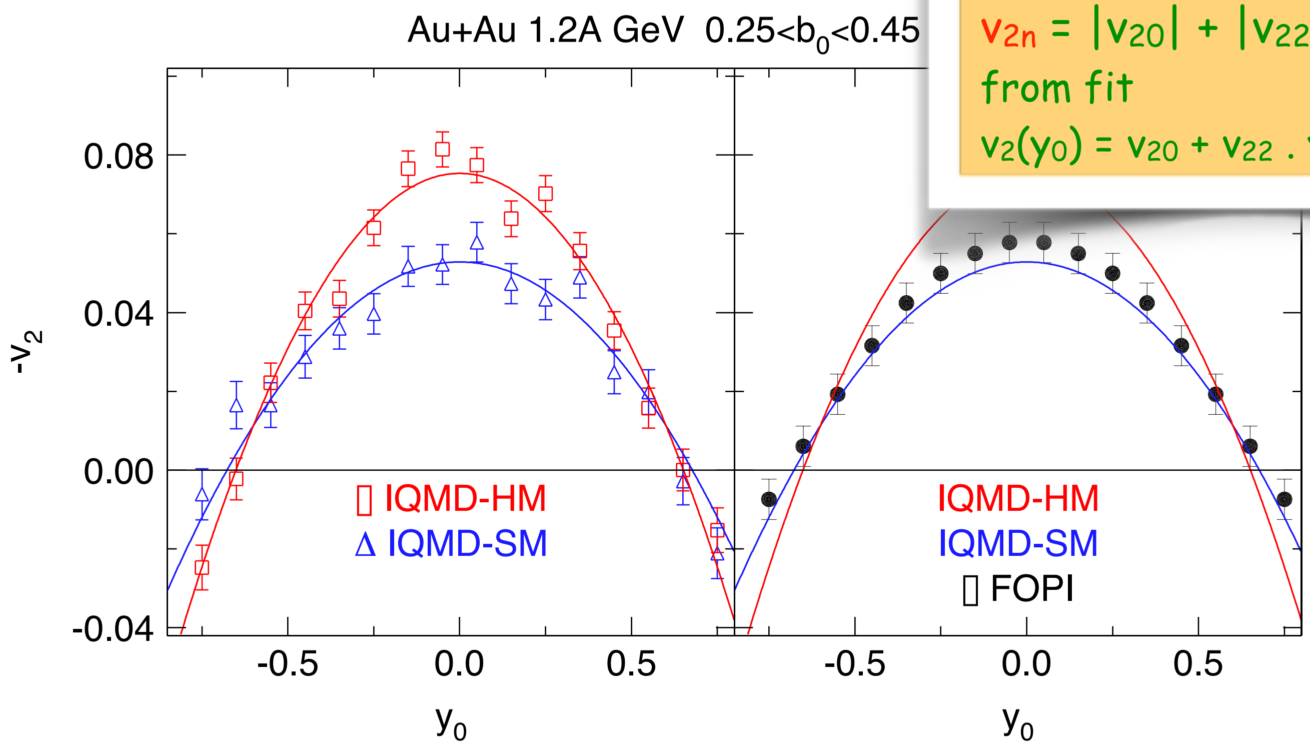

Complete shape of $v_2(y_0)$:
a new observable:
$v_{2n} = |v_{20}| + |v_{22}|$,
from fit
$v_2(y_0) = v_{20} + v_{22} \cdot y_0^2$

A. Le Fèvre et al., Nucl. Phys. A 945 (2016) 112.

Elliptic flow at mid-rapidity: the strongest sensitivity to the Nuclear Equation of State

Complete shape of $v_2(y_0)$:
a new observable:
$v_{2n} = |v_{20}| + |v_{22}|$,
from fit
$v_2(y_0) = v_{20} + v_{22} \cdot y_0^2$

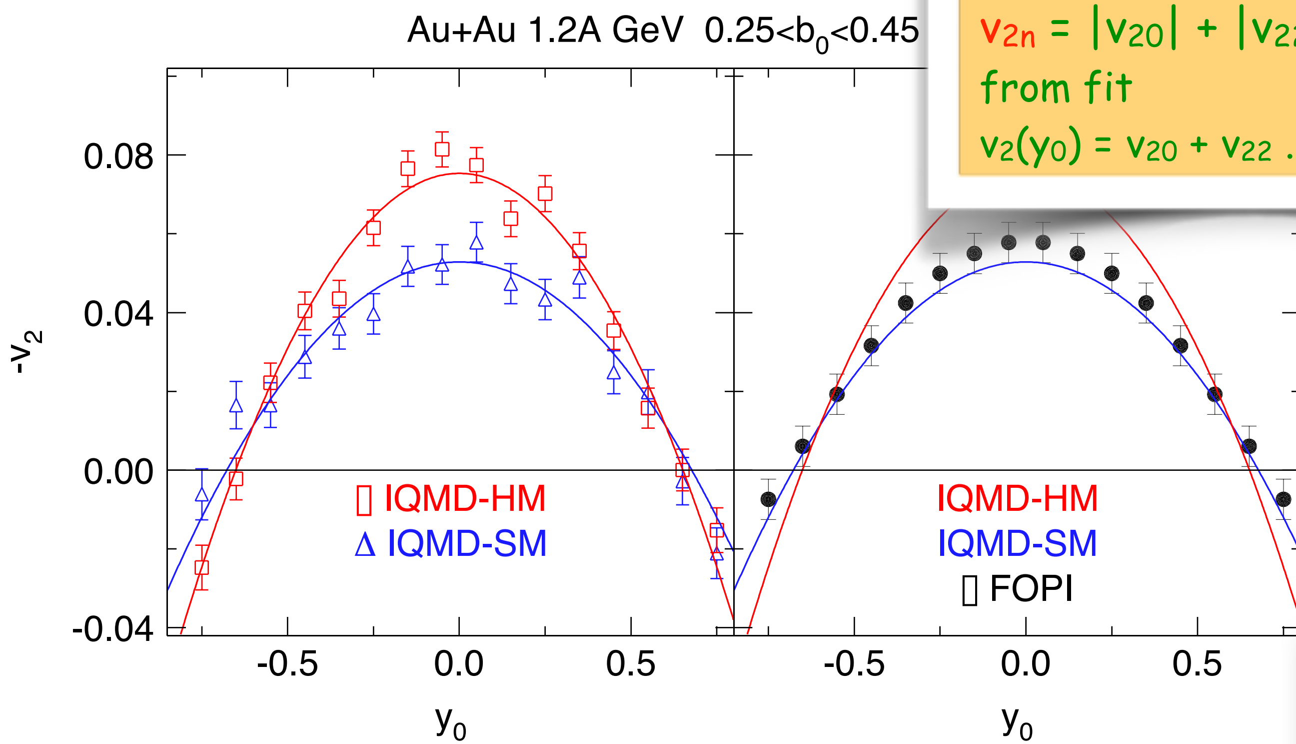

K =
380 MeV ('stiff')
200 MeV ('soft')

A. Le Fèvre et al., Nucl. Phys. A 945 (2016) 112.

Elliptic flow at mid-rapidity: the strongest sensitivity to the Nuclear Equation of State

➜ $v_{2n}(E_{beam})$ varies by a factor ≈1.6, >> measured uncertainty (≈1.1)

➜ clearly favors a 'soft' EOS.

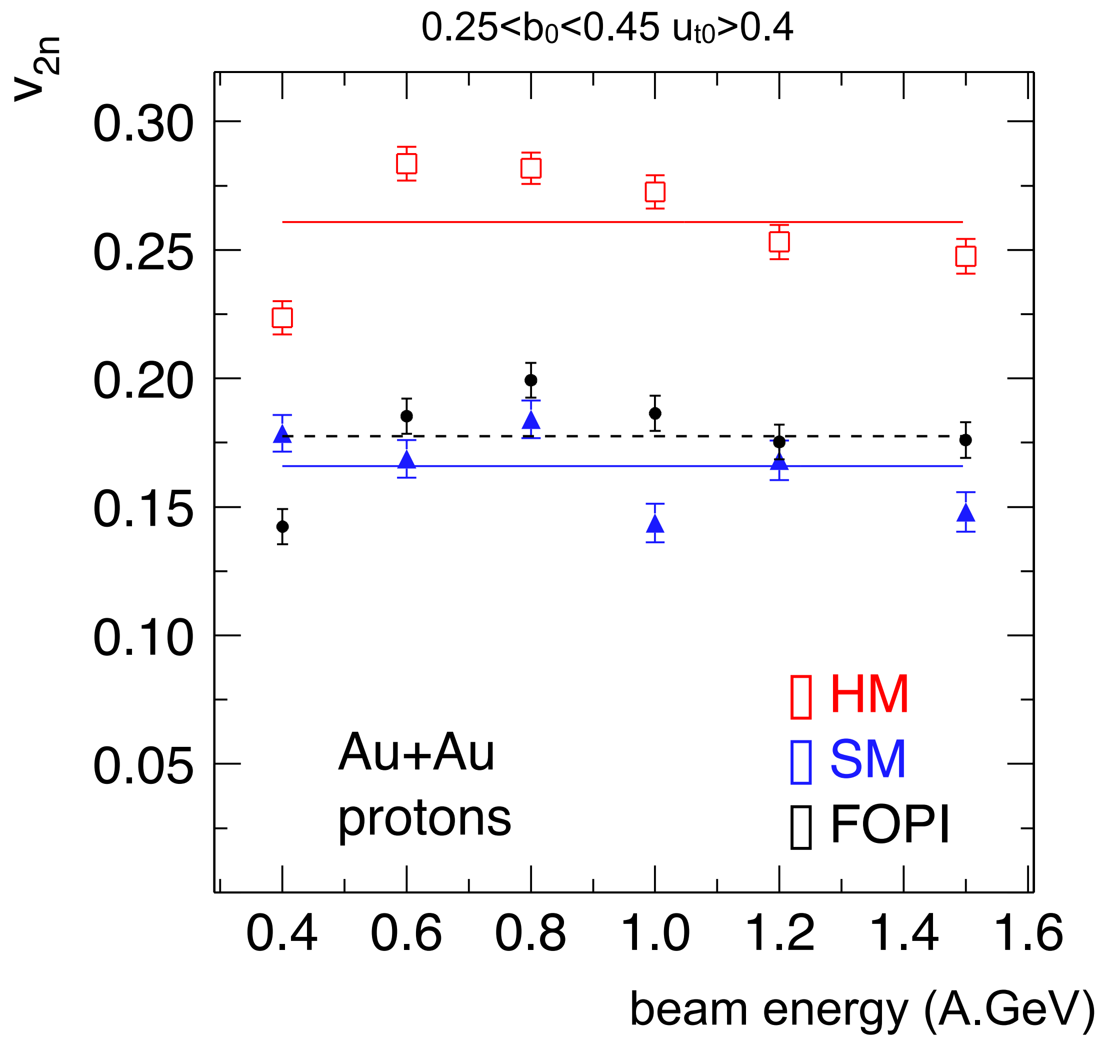

A. Le Fèvre et al., Nucl. Phys. A 945 (2016) 112.

Elliptic flow at mid-rapidity: the strongest sensitivity to the Nuclear Equation of State

➜ $v_{2n}(E_{beam})$ varies by a factor ≈1.6, >> measured uncertainty (≈1.1)

➜ clearly favors a 'soft' EOS.

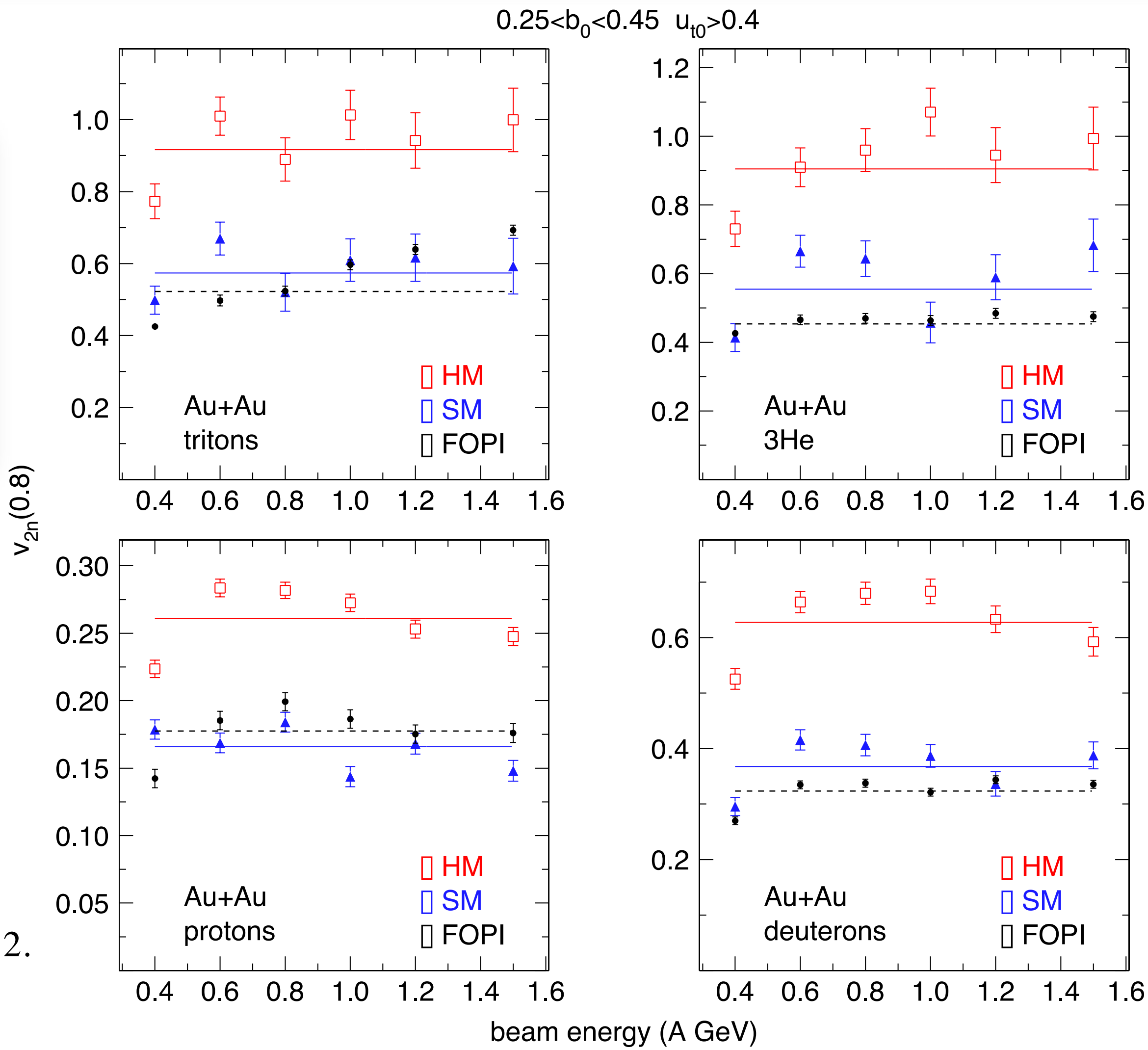

A. Le Fèvre et al., Nucl. Phys. A 945 (2016) 112.

Survey of the reaction

Only <u>protons</u> are considered in the following, Au+Au with b=6 fm as illustration

z: beam direction

x: impact parameter direction

y: perpendicular to reaction plane

t_{pass} = passing time

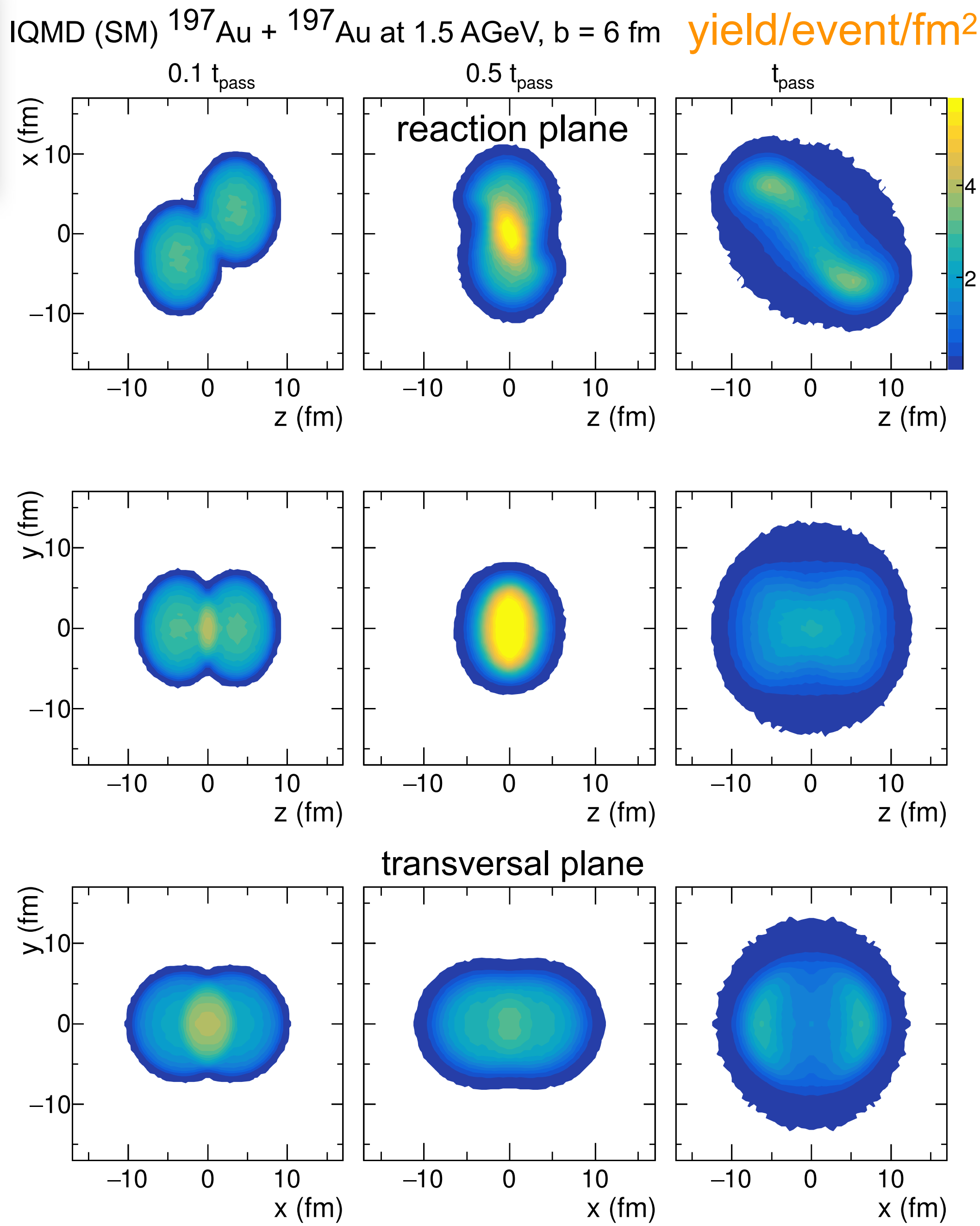

Survey of the reaction

Only <u>protons</u> are considered in the following, Au+Au with b=6 fm as illustration

z: beam direction

x: impact parameter direction

y: perpendicular to reaction plane

t_{pass} = passing time

Central (participant) matter is highly compressed at max. overlap ($t = 0.5t_{pass}$).

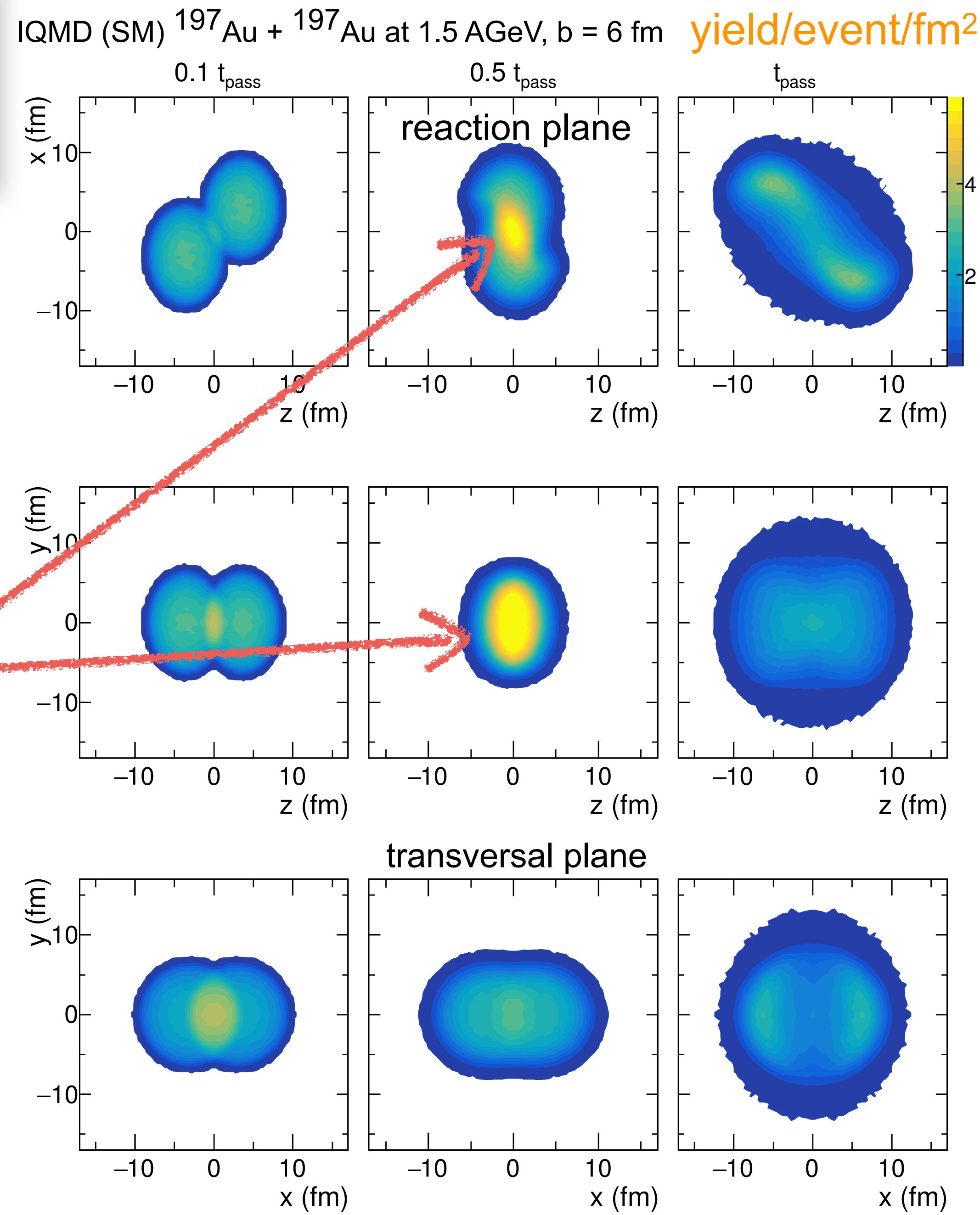

Survey of the reaction

Only protons are considered in the following, Au+Au with b=6 fm as illustration

z: beam direction

x: impact parameter direction

y: perpendicular to reaction plane

t_{pass} = passing time

Central (participant) matter is highly compressed at max. overlap ($t = 0.5t_{pass}$).

Projectile and target remnants stay connected for longer than t_{pass} by a ridge with a quite high particle density. This ridge will disintegrate when projectile and target remnants separate further.

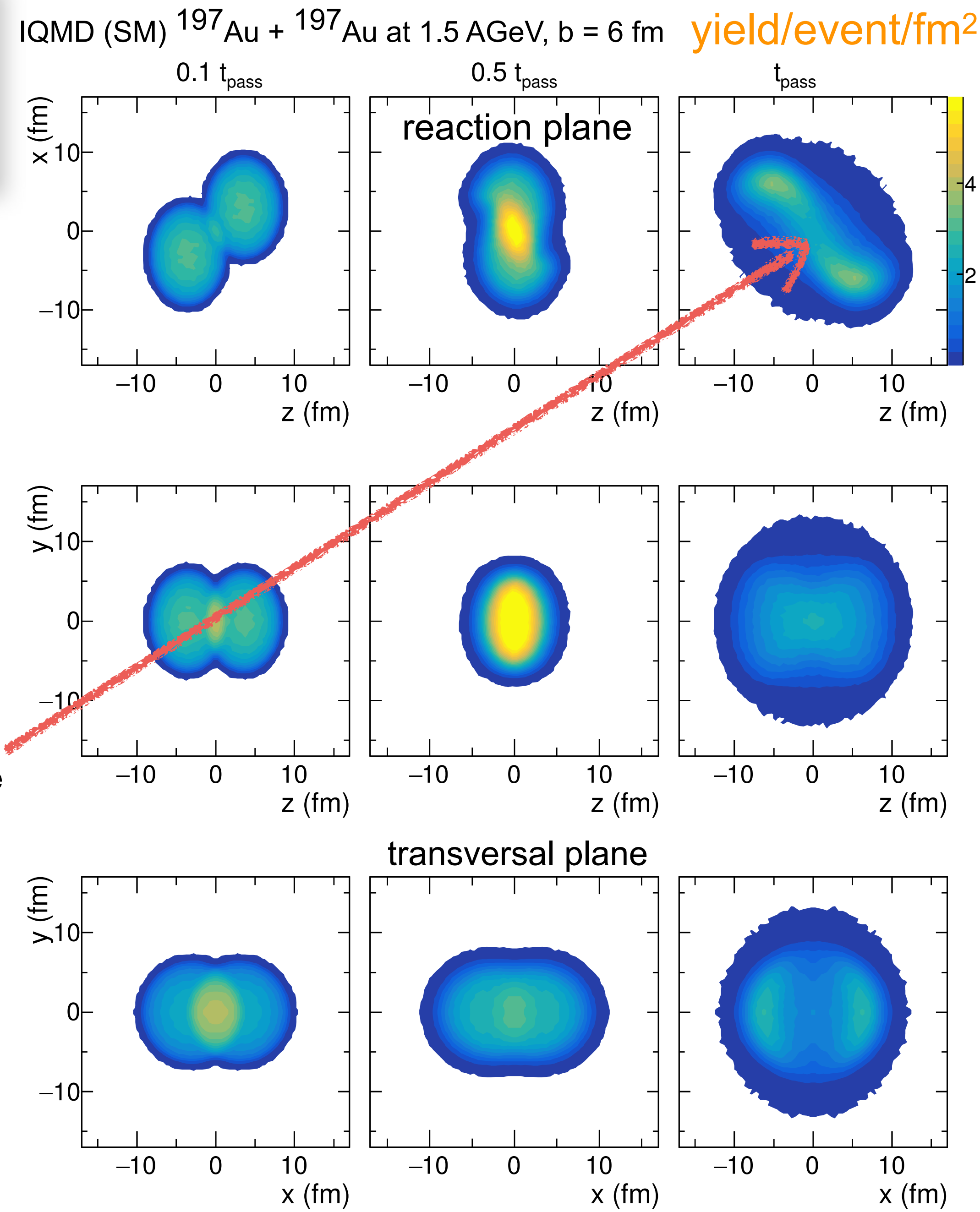

Survey of the reaction

Only protons are considered in the following, Au+Au with b=6 fm as illustration

z: beam direction

x: impact parameter direction

y: perpendicular to reaction plane

t_{pass} = passing time

Central (participant) matter is highly compressed at max. overlap ($t = 0.5t_{pass}$).

Projectile and target remnants stay connected for longer than t_{pass} by a ridge with a quite high particle density. This ridge will disintegrate when projectile and target remnants separate further.

The importance of this ridge can be seen in the zy plane at max. overlap → the highest density at z=0, in the ridge.

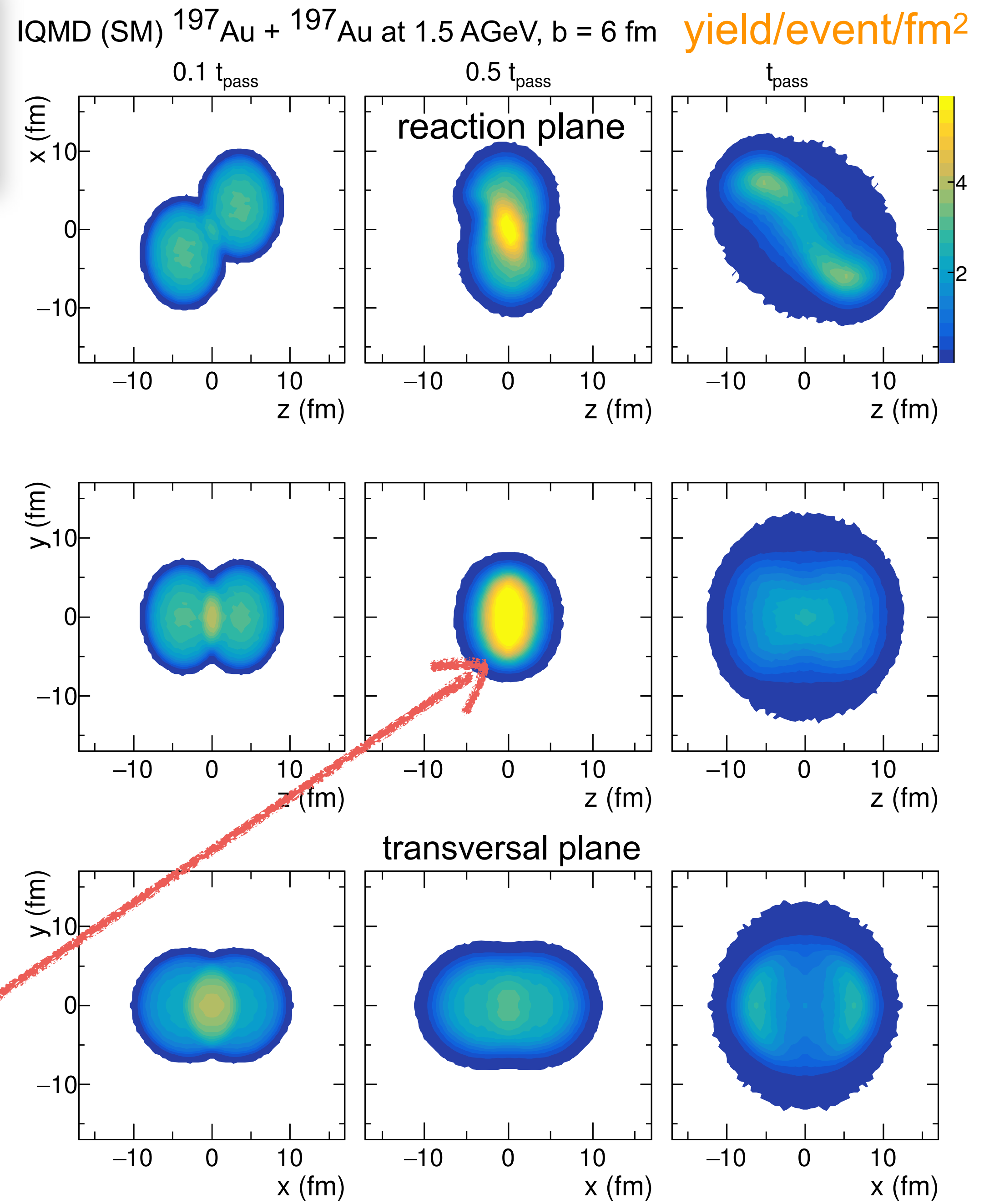

Survey of the reaction

$\Delta\rho_{SM-HM}$

at t_{pass}

The choice of the EoS influences the reaction scenario predicted by the model ⇨ reflected by the difference (SM-HM) of the proton densities projected onto the ij plane,

$$\Delta\rho_{ij} = \rho_{ij}^{SM} - \rho_{ij}^{HM} \ (\text{event}^{-1}\text{fm}^{-2})$$

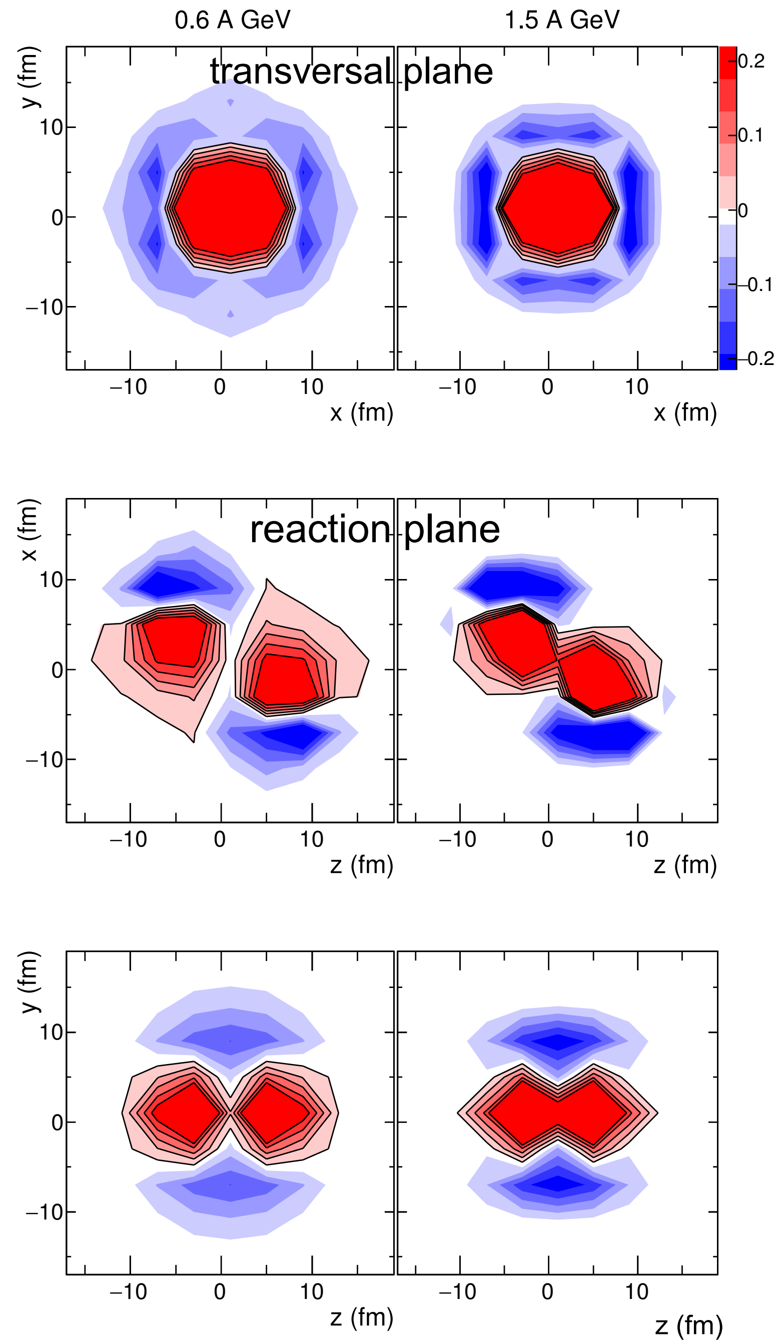

Survey of the reaction

$\Delta\varrho_{SM\text{-}HM}$

at t_{pass}

The choice of the EoS influences the reaction scenario predicted by the model ⇨ reflected by the difference (SM-HM) of the proton densities projected onto the ij plane,

$$\Delta\rho_{ij} = \rho_{ij}^{SM} - \rho_{ij}^{HM}\ (\text{event}^{-1}\text{fm}^{-2})$$

Density of protons in the geometrical overlap region of projectile and target: higher for a soft EoS.
At larger distances from the reaction center: higher density for a hard EoS

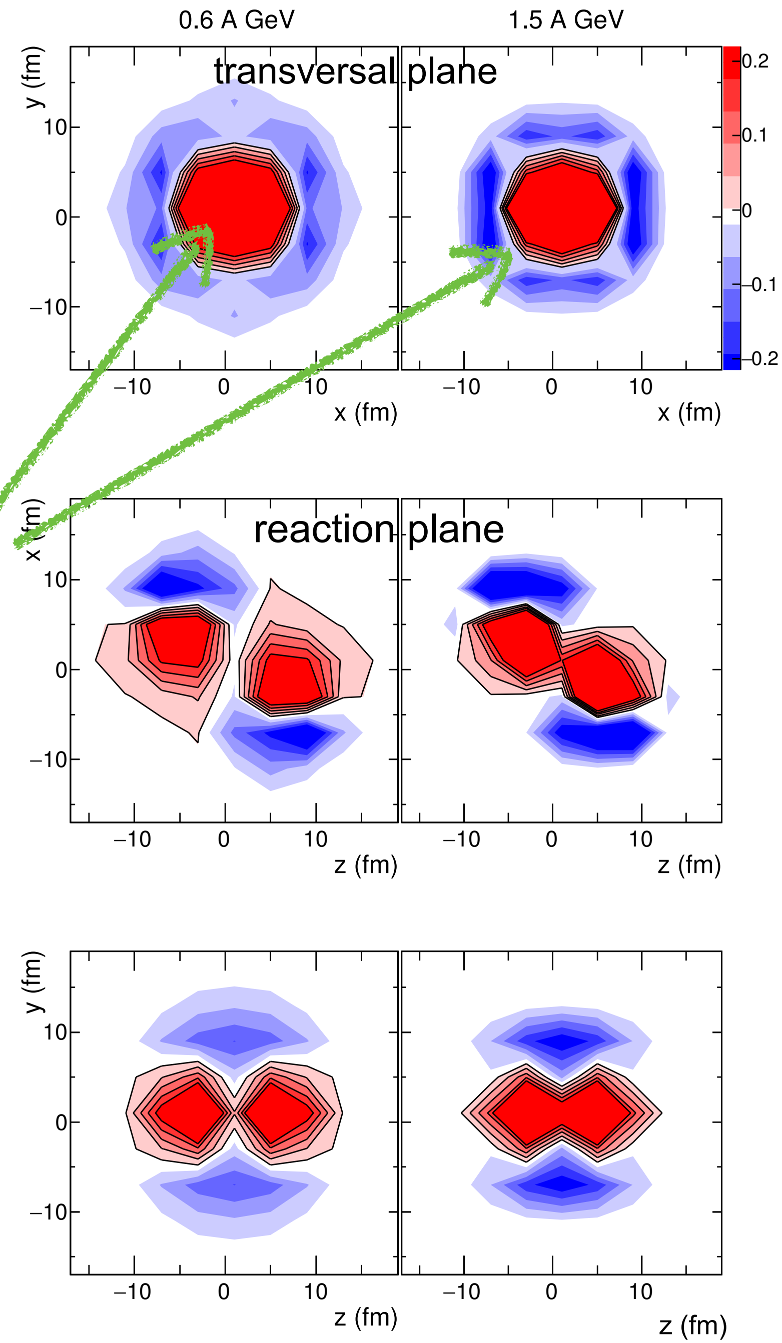

Survey of the reaction

$\Delta\rho_{SM\text{-}HM}$ at t_{pass}

The choice of the EoS influences the reaction scenario predicted by the model ⇨ reflected by the difference (SM-HM) of the proton densities projected onto the ij plane,

$$\Delta\rho_{ij} = \rho_{ij}^{SM} - \rho_{ij}^{HM} \ (\mathrm{event}^{-1}\mathrm{fm}^{-2})$$

Density of protons in the geometrical overlap region of projectile and target: higher for a soft EoS.
At larger distances from the reaction center: higher density for a hard EoS

At 0.6 AGeV: this surplus in the density for a hard EoS is larger in x-direction, but it becomes rather isotropic at 1.5 AGeV

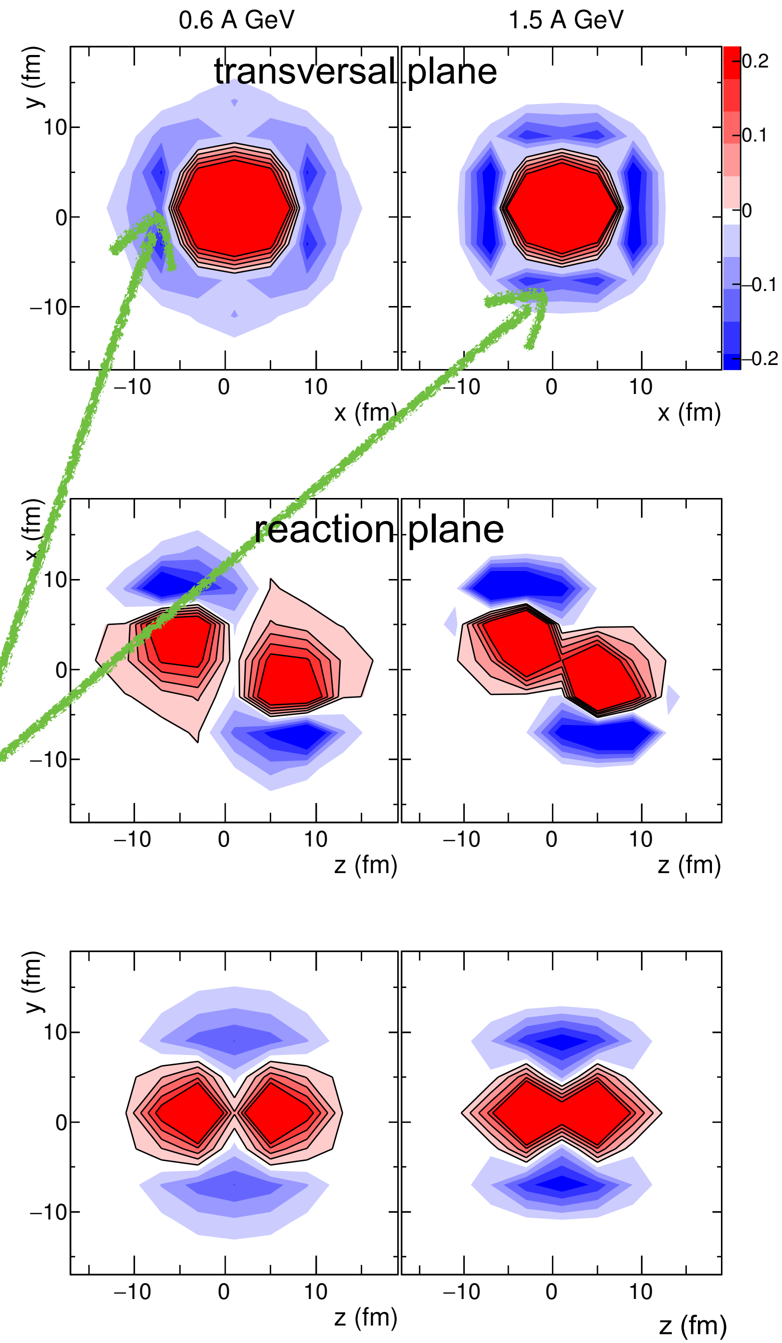

Survey of the reaction

$\Delta\rho_{SM\text{-}HM}$

at t_{pass}

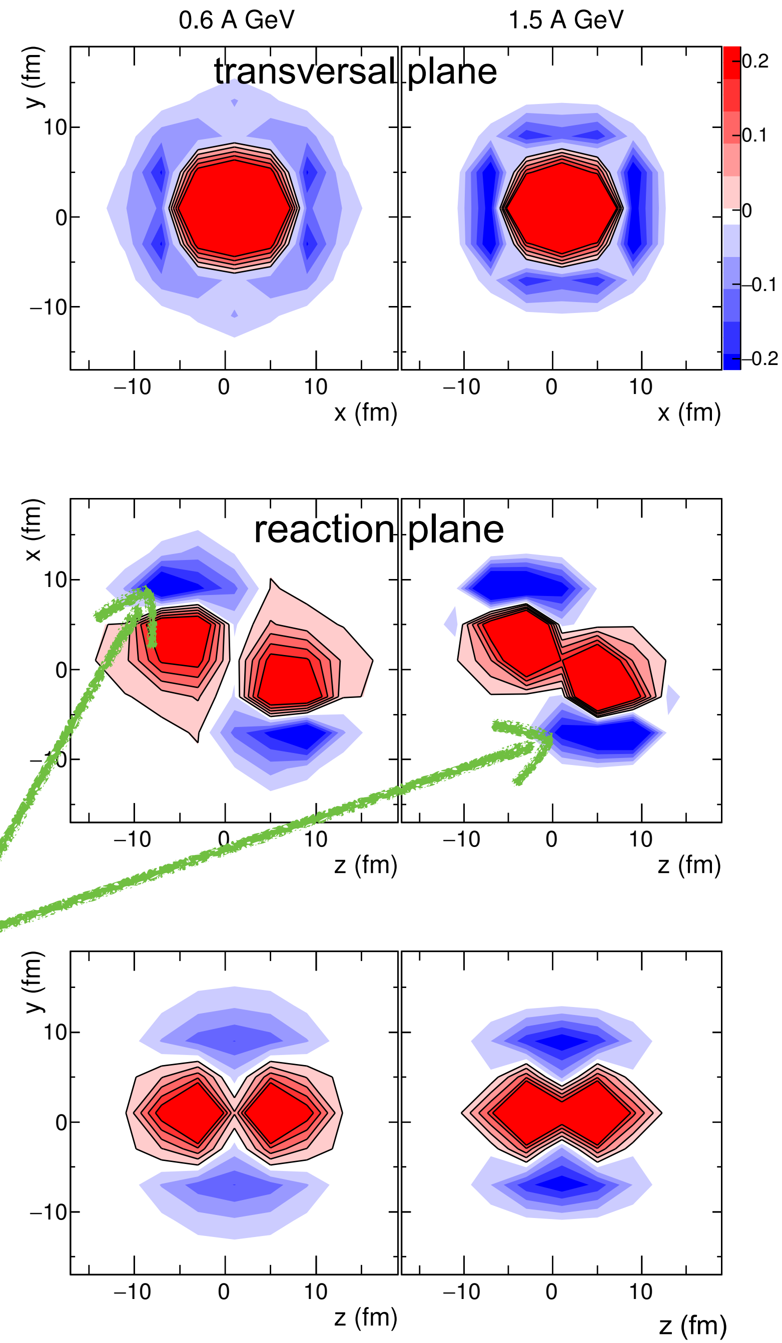

The choice of the EoS influences the reaction scenario predicted by the model ⇨ reflected by the difference (SM-HM) of the proton densities projected onto the ij plane,

$$\Delta\rho_{ij} = \rho_{ij}^{SM} - \rho_{ij}^{HM}\ (\text{event}^{-1}\text{fm}^{-2})$$

Density of protons in the geometrical overlap region of projectile and target: higher for a soft EoS.
At larger distances from the reaction center: higher density for a hard EoS

At 0.6 AGeV: this surplus in the density for a hard EoS is larger in x-direction, but it becomes rather isotropic at 1.5 AGeV

The excess in x-direction has its origin in the in-plane flow of the spectator matter expressed by a finite directed flow (v1):
v1 (hard) >> v1 (soft)

HELMHOLTZ
ASSOCIATION

Survey of the reaction

$\Delta\rho_{SM\text{-}HM}$ at t_{pass}

The choice of the EoS influences the reaction scenario predicted by the model ⇨ reflected by the difference (SM-HM) of the proton densities projected onto the ij plane,

$$\Delta\rho_{ij} = \rho_{ij}^{SM} - \rho_{ij}^{HM}\ (\text{event}^{-1}\text{fm}^{-2})$$

Density of protons in the geometrical overlap region of projectile and target: higher for a soft EoS.
At larger distances from the reaction center: higher density for a hard EoS

At 0.6 AGeV: this surplus in the density for a hard EoS is larger in x-direction, but it becomes rather isotropic at 1.5 AGeV

The excess in x-direction has its origin in the in-plane flow of the spectator matter expressed by a finite directed flow (v1):
v1 (hard) >> v1 (soft)

In y-direction the surplus in density of the hard EoS is concentrated at around z=0, being less extended but stronger at higher energies. The emission of these particles is caused by a stronger density gradient (and hence a stronger force) in y-direction for a hard (HM) EoS as compared to a soft (SM) one.

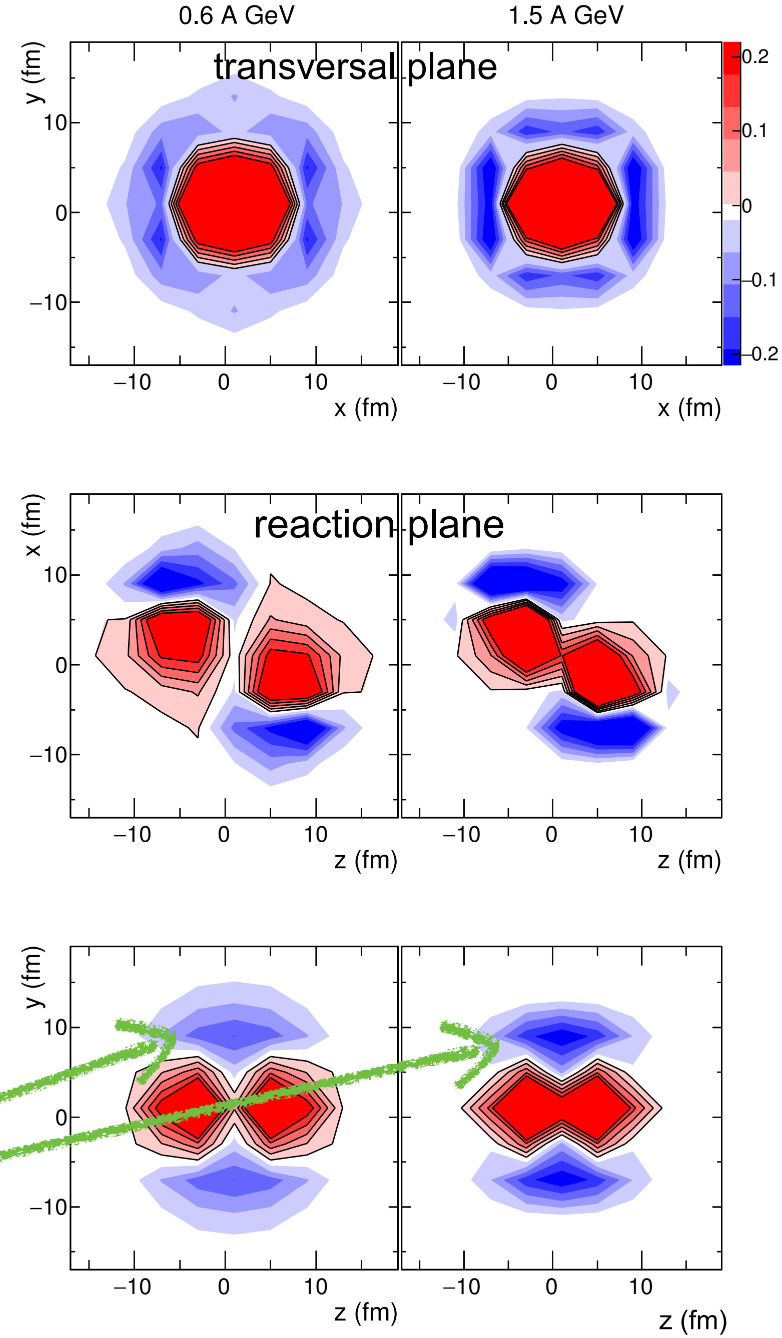

Survey of the reaction

$\Delta\varrho_{SM-HM}$

at t_{pass}

In velocity space we observe a complementary distribution.

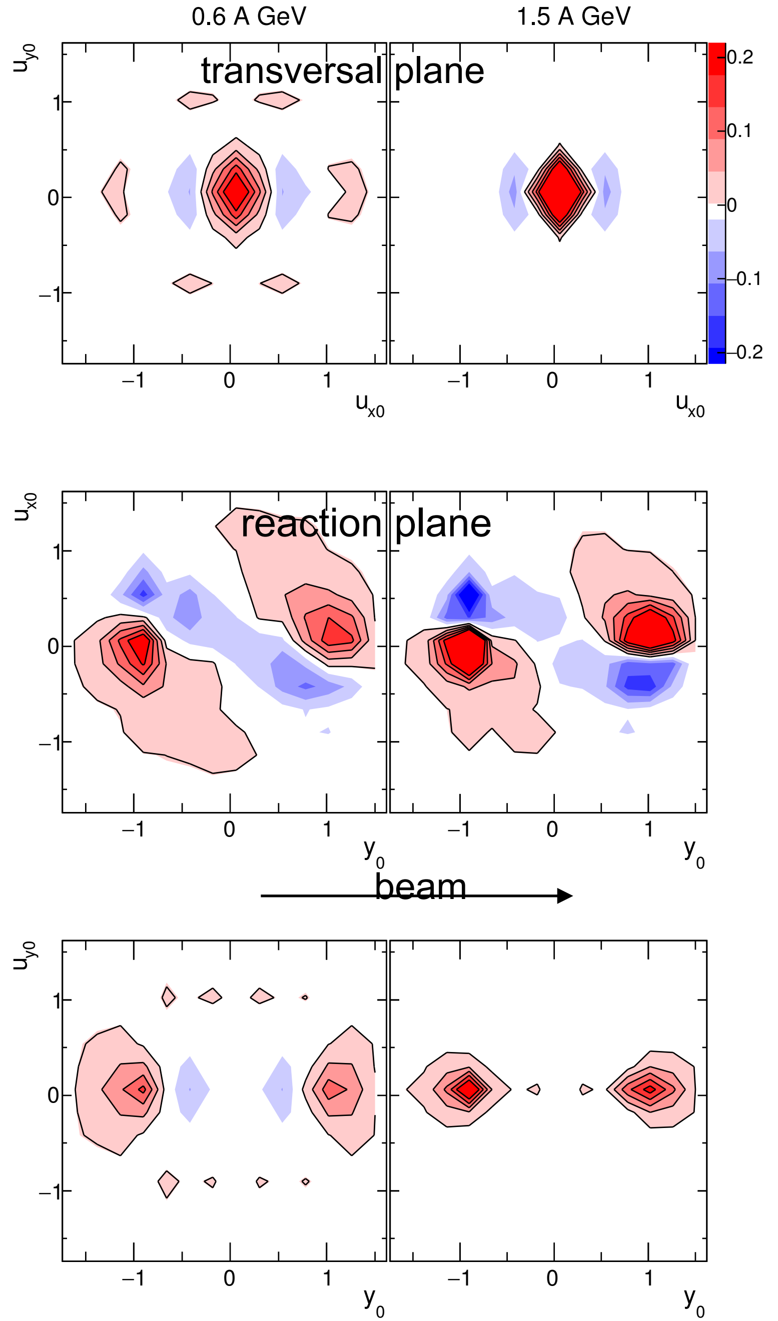

Survey of the reaction

$\Delta\rho_{SM\text{-}HM}$

at t_{pass}

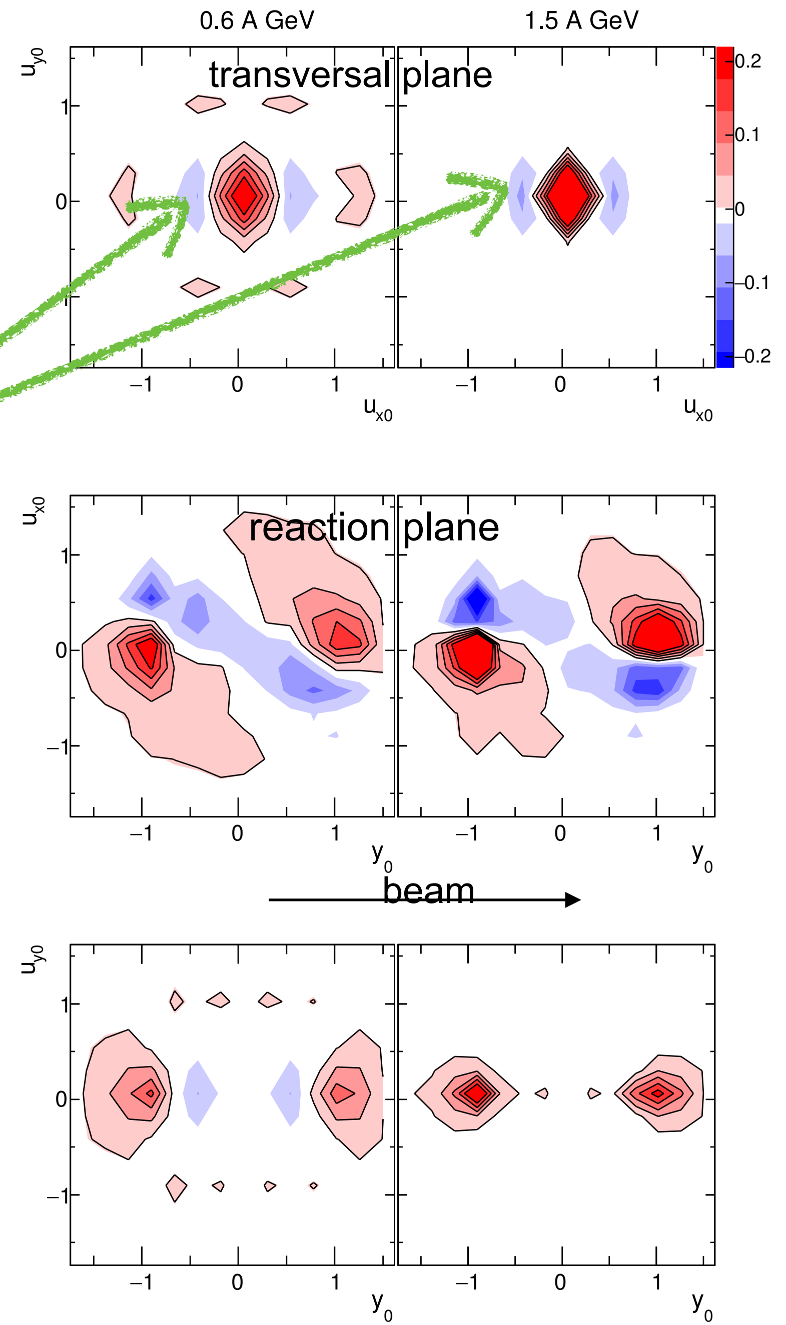

In velocity space we observe a complementary distribution.

In the xy plane, the shift of protons in x direction is smaller for a soft (SM) than for a hard (HM) EoS

Survey of the reaction

$\Delta\rho_{SM\text{-}HM}$

at t_{pass}

In velocity space we observe a complementary distribution.

In the xy plane, the shift of protons in x direction is smaller for a soft (SM) than for a hard (HM) EoS

This is due to a smaller acceleration yielding a weaker in-plane flow and hence a smaller velocity in x-direction

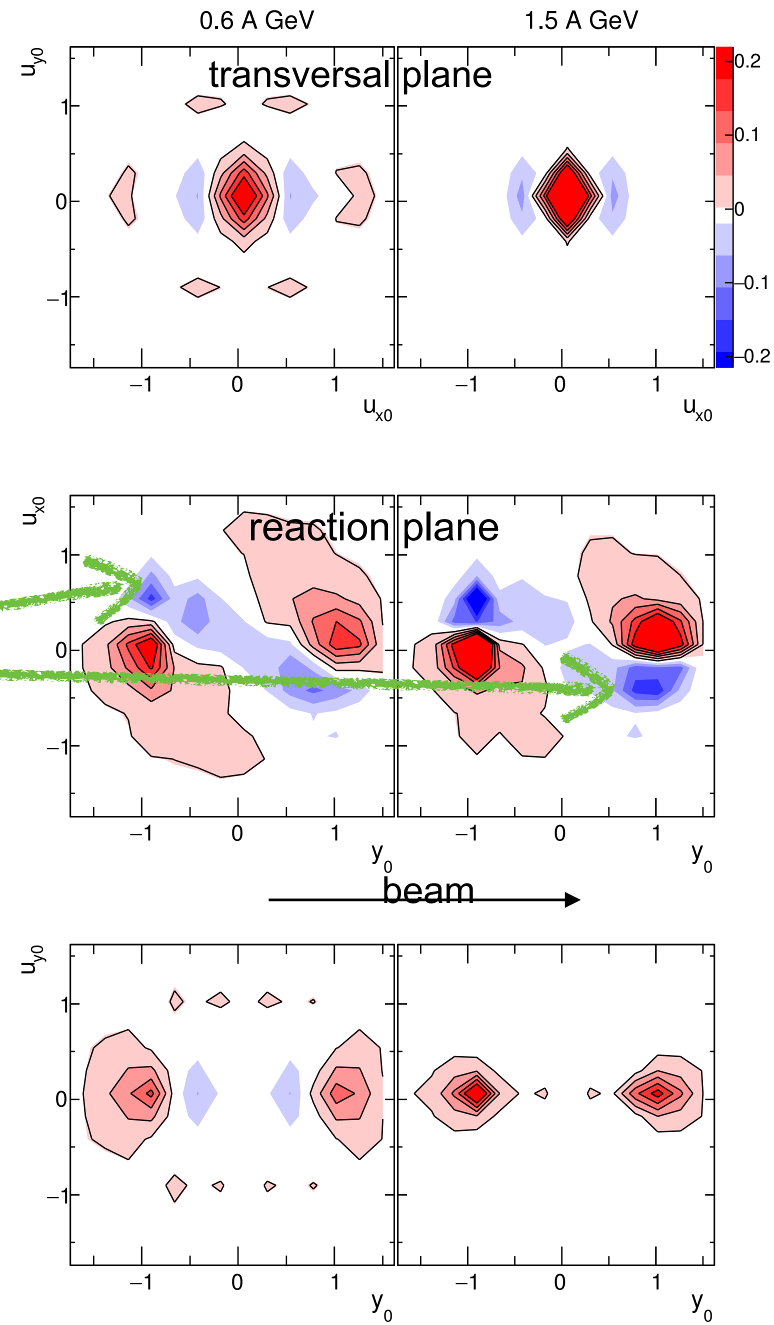

Survey of the reaction

$\Delta\varrho_{SM-HM}$

at t_{pass}

In velocity space we observe a complementary distribution.

In the xy plane, the shift of protons in x direction is smaller for a soft (SM) than for a hard (HM) EoS

This is due to a smaller acceleration yielding a weaker in-plane flow and hence a smaller velocity in x-direction

The soft EoS leads also to less stopping

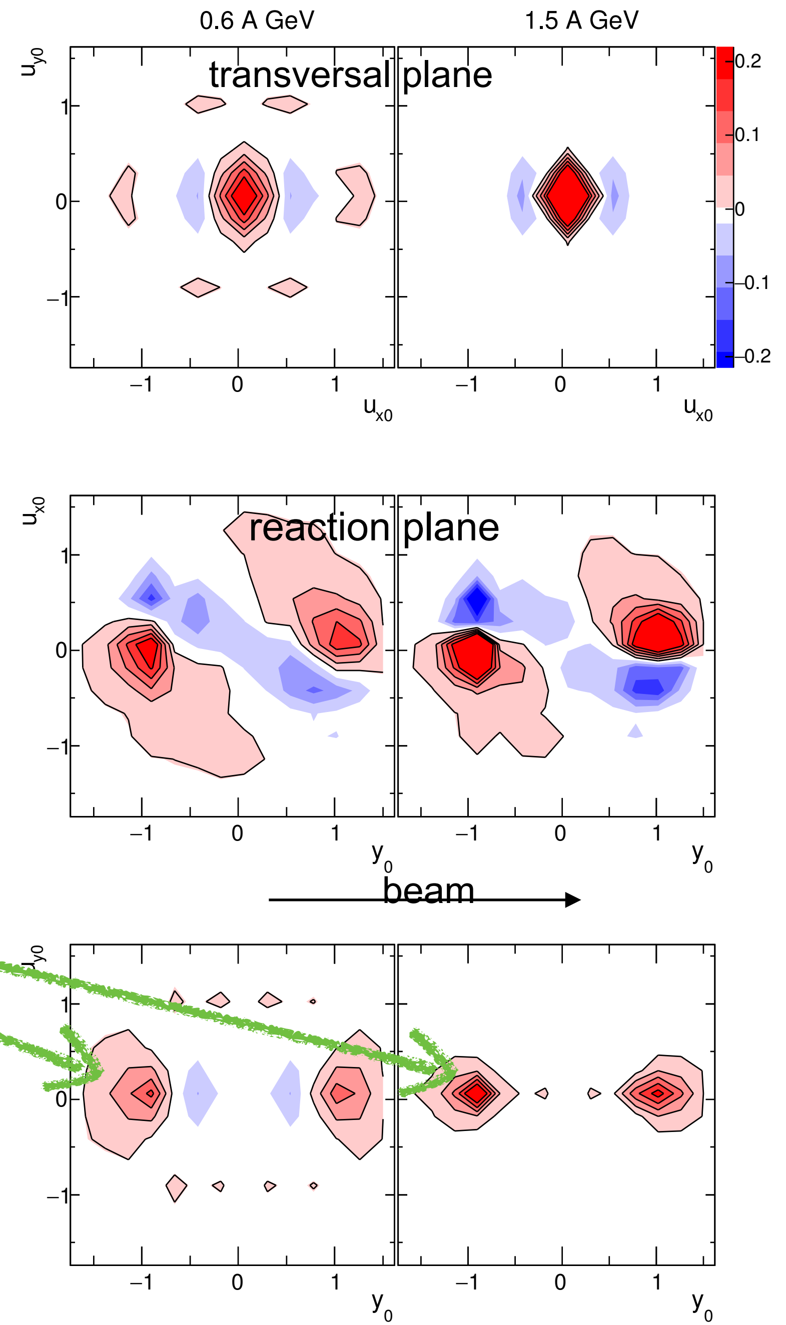

Survey of the reaction

We select now fast moving particles in the transverse direction at mid-rapidity:

$|y0| < 0.2$, $ut0 > 0.4$ (used by the FOPI collaboration for the v2 investigation) in color. Compared to all (black contours).

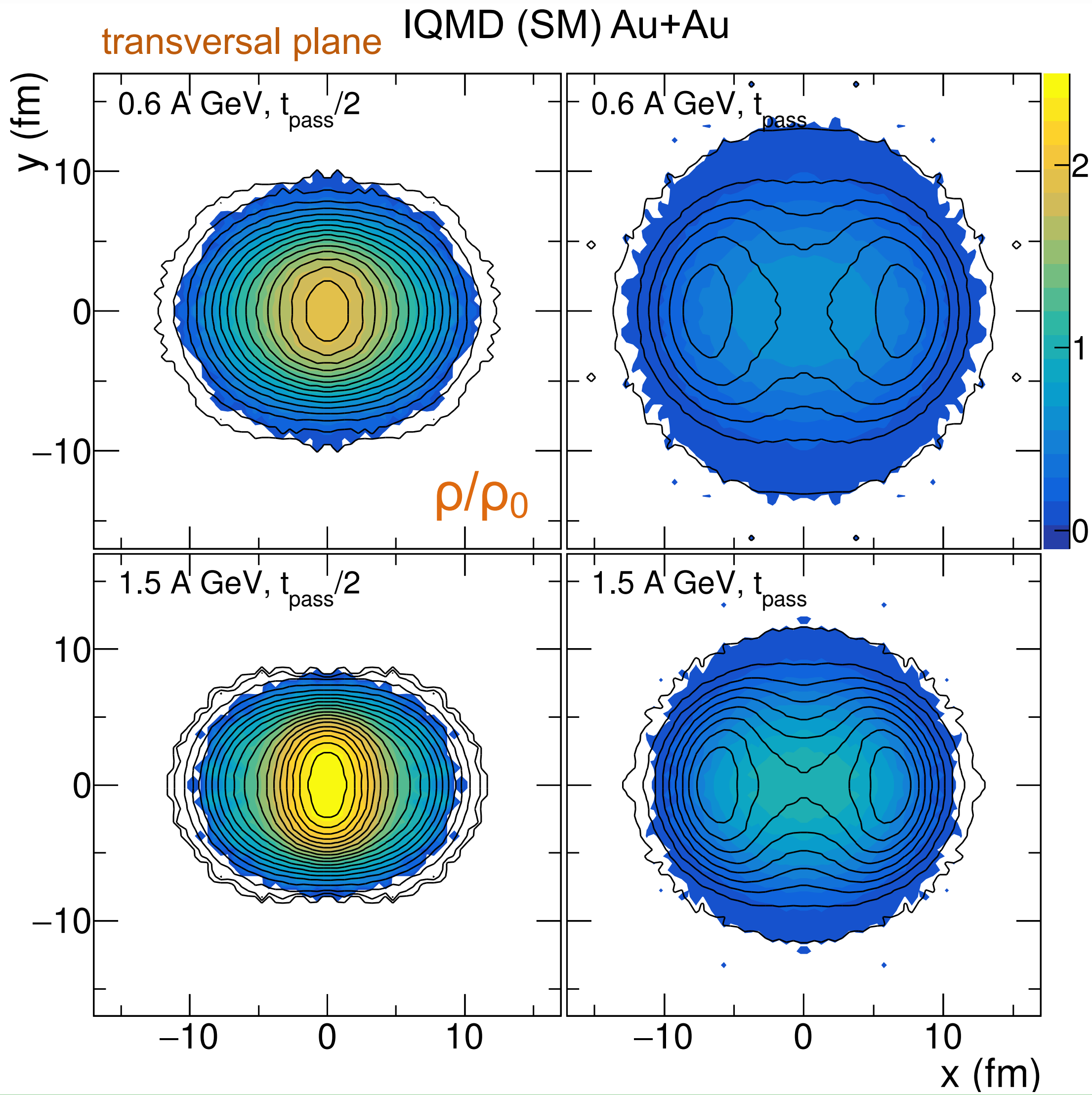

Survey of the reaction

We select now fast moving particles in the transverse direction at mid-rapidity:

$|y0| < 0.2$, $ut0 > 0.4$ (used by the FOPI collaboration for the v2 investigation) in color. Compared to all (black contours).

At full overlap:

- the innermost participants = a dense almond shaped core, <u>out-of-plane</u> elongated, compression is highest.

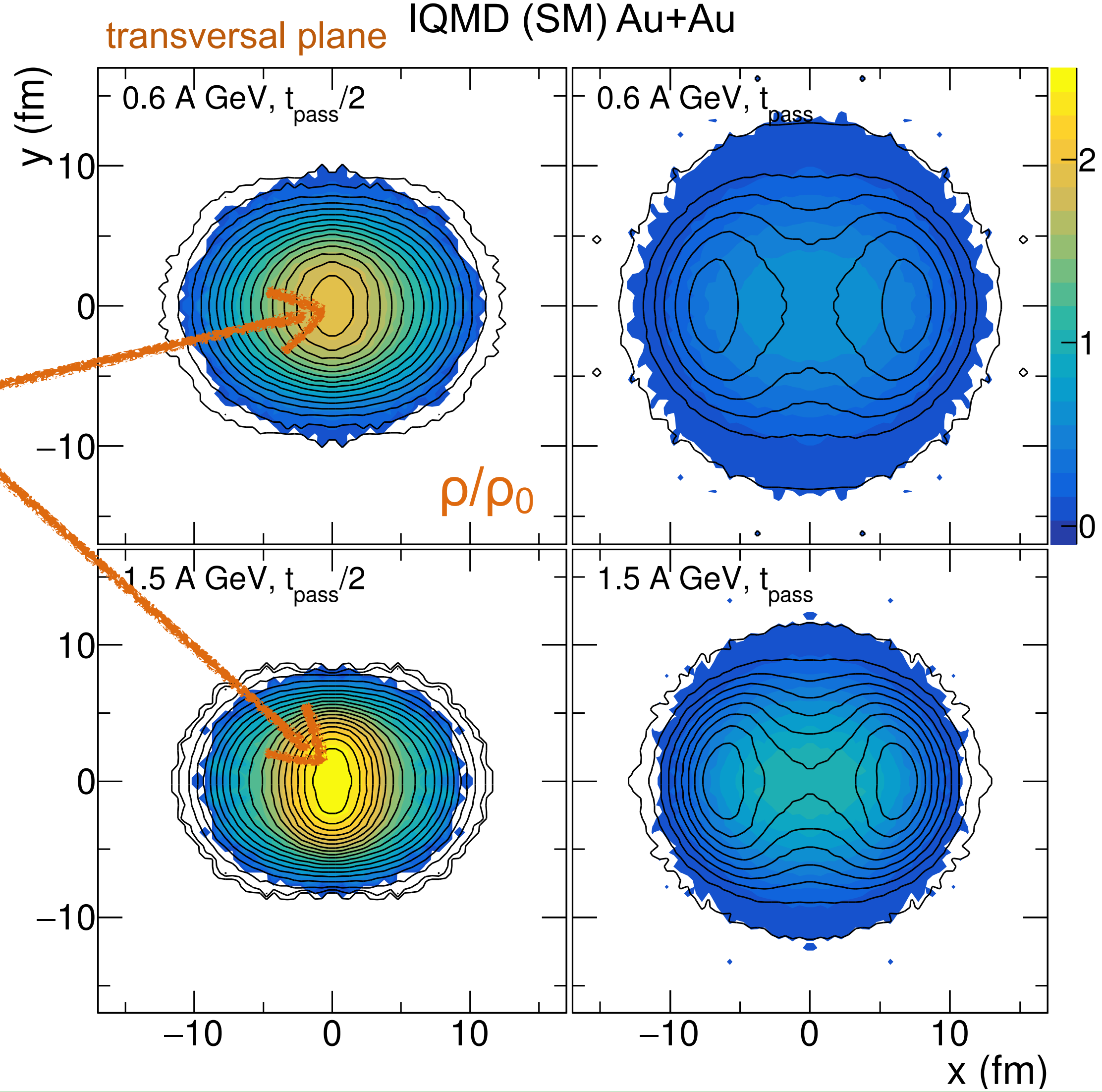

Survey of the reaction

We select now fast moving particles in the transverse direction at mid-rapidity:

$|y0| < 0.2$, $ut0 > 0.4$ (used by the FOPI collaboration for the v2 investigation) in color. Compared to all (black contours).

At full overlap:

- the innermost participants = a dense almond shaped core, out-of-plane elongated, compression is highest.
- the outermost participants = more dilute, extending in-plane, aligned with the spectator distribution.

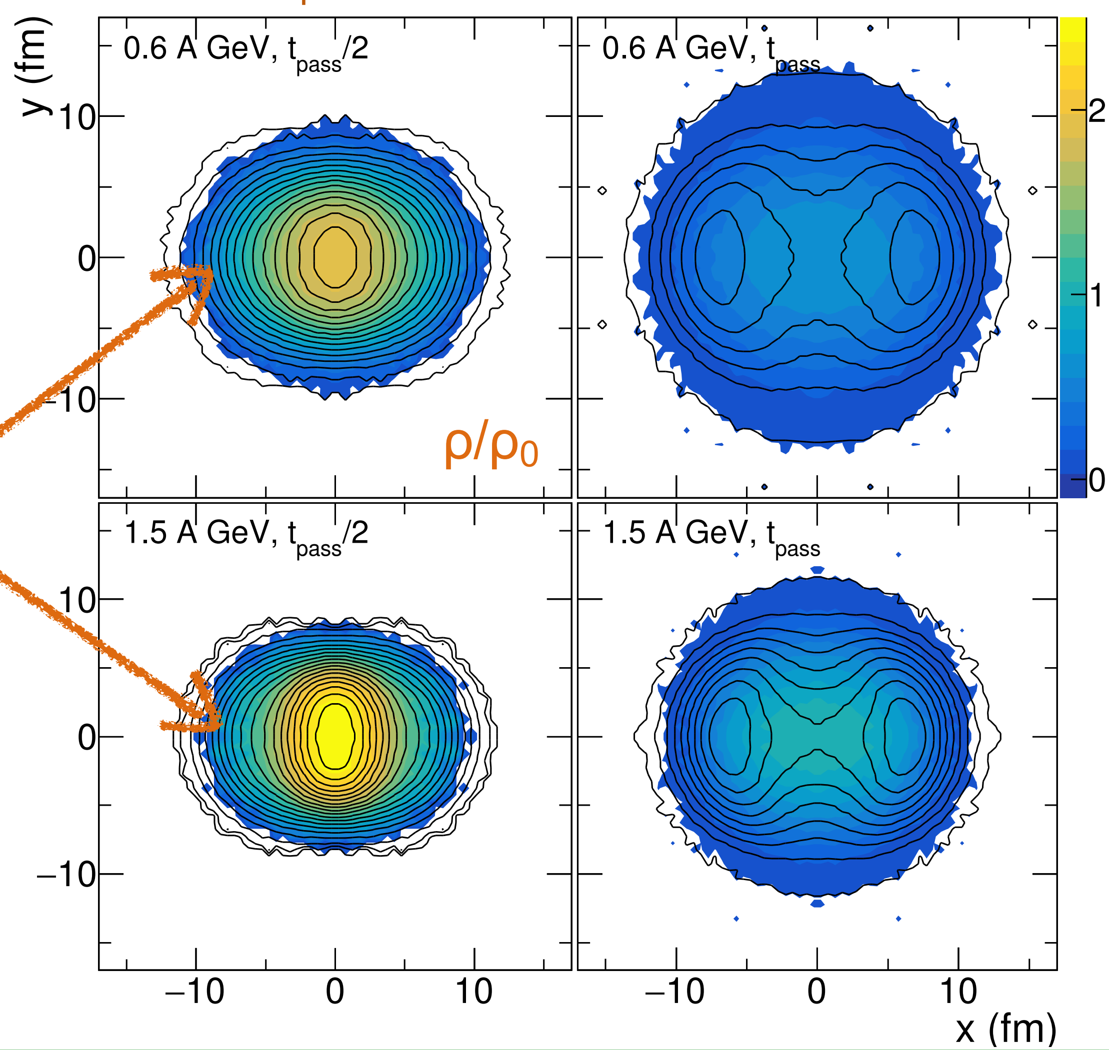

Survey of the reaction

We select now fast moving particles in the transverse direction at mid-rapidity:

$|y0| < 0.2$, $ut0 > 0.4$ (used by the FOPI collaboration for the v2 investigation) in color. Compared to all (black contours).

At full overlap:

- the innermost participants = a dense almond shaped core, out-of-plane elongated, compression is highest.
- the outermost participants = more dilute, extending in-plane, aligned with the spectator distribution.

At passing time, the innermost (compressed) participants expand in-plane, but not with enough pressure to produce a positive elliptic flow v2 (seen later), in contrast to higher bombarding energies

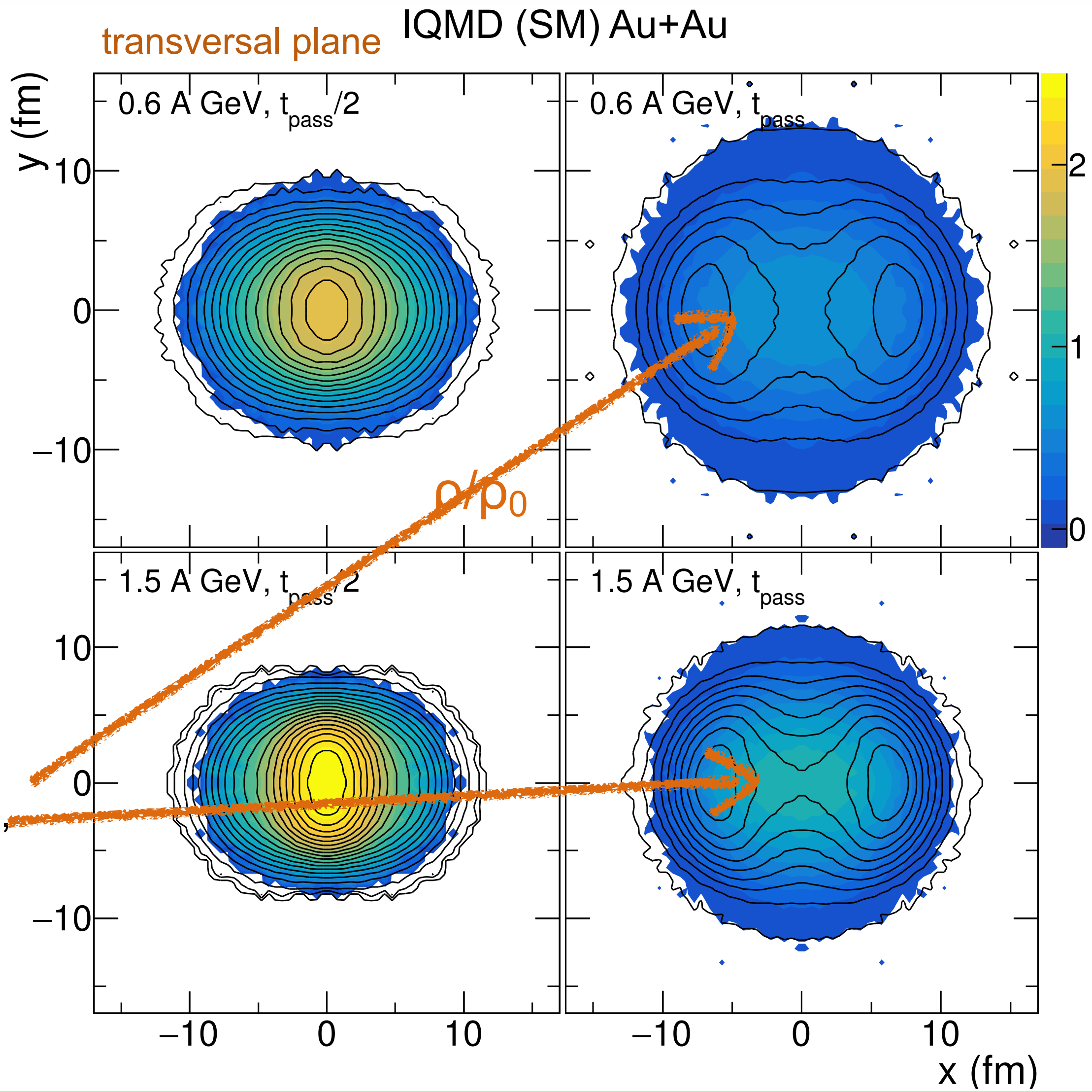

Survey of the reaction

Formation of an in-plane ridge between the bulk of the spectators.

Incident energy ↗ ⇒ ridge & initial almond core density ↗

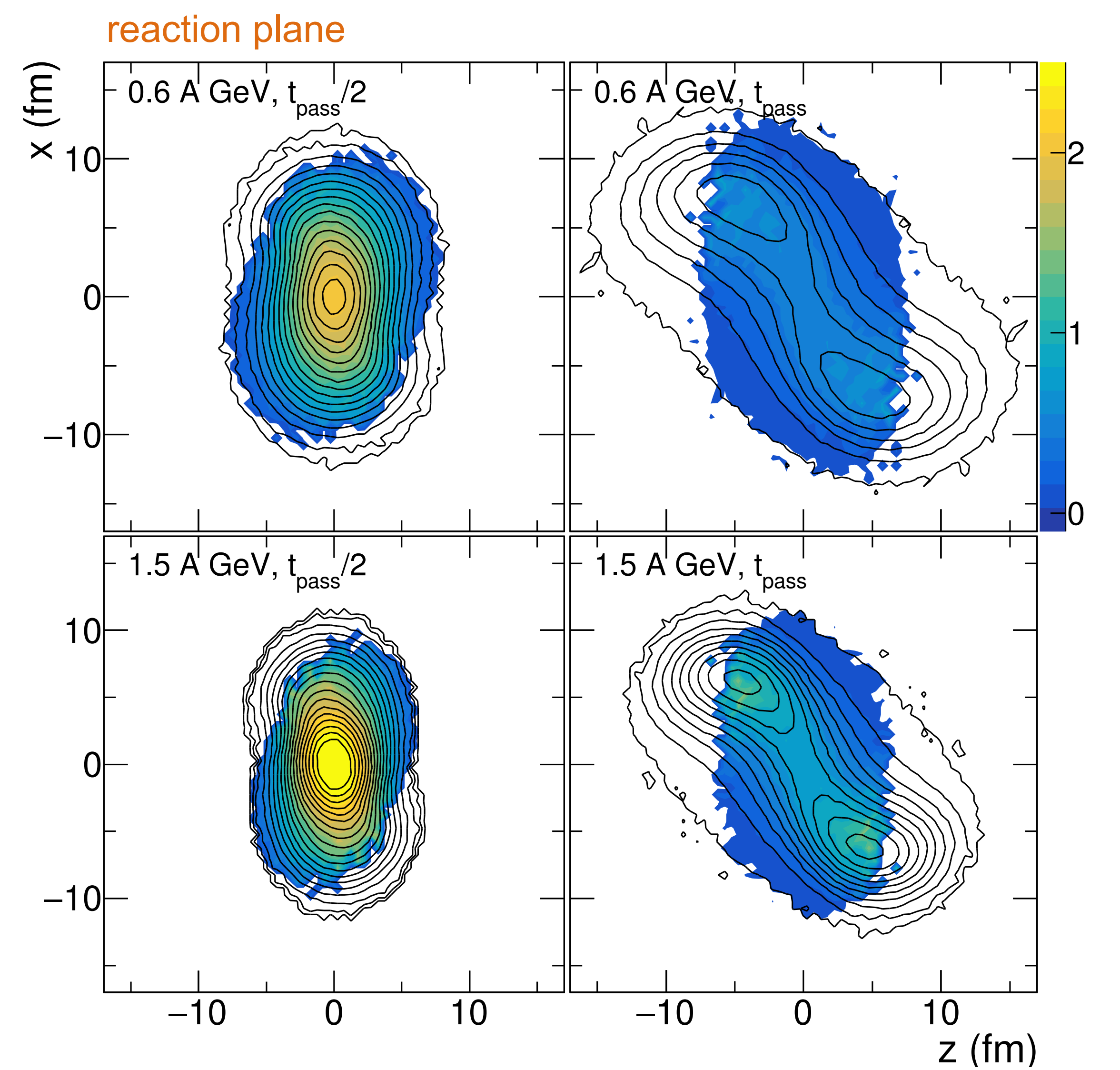

The elliptic flow time evolution

$$v_2(t) = \frac{p_x^2(t) - p_y^2(t)}{p_x^2(t) + p_y^2(t)}$$

at mid-rapidity

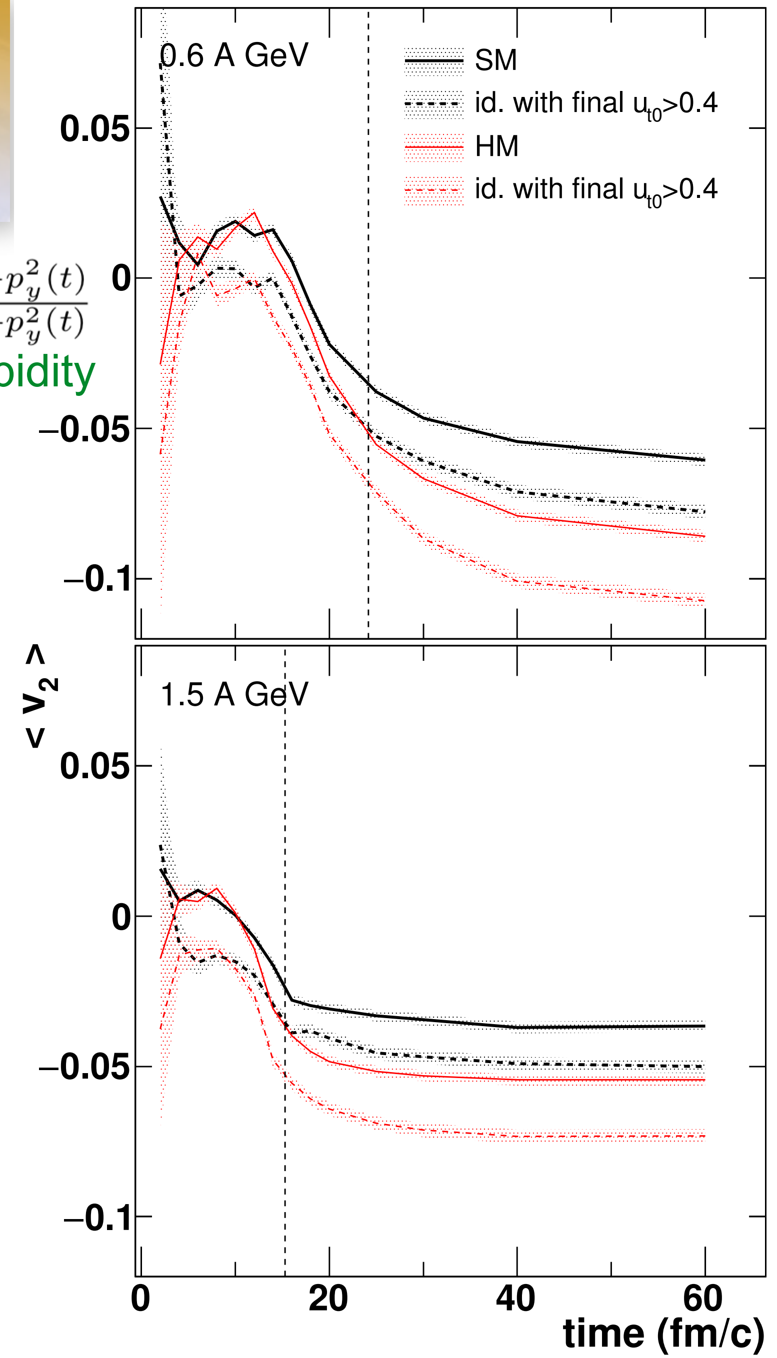

The elliptic flow time evolution

$$v_2(t) = \frac{p_x^2(t) - p_y^2(t)}{p_x^2(t) + p_y^2(t)}$$

at mid-rapidity

- v_2 starts to develop after approximately max. overlap and evolves rapidly.

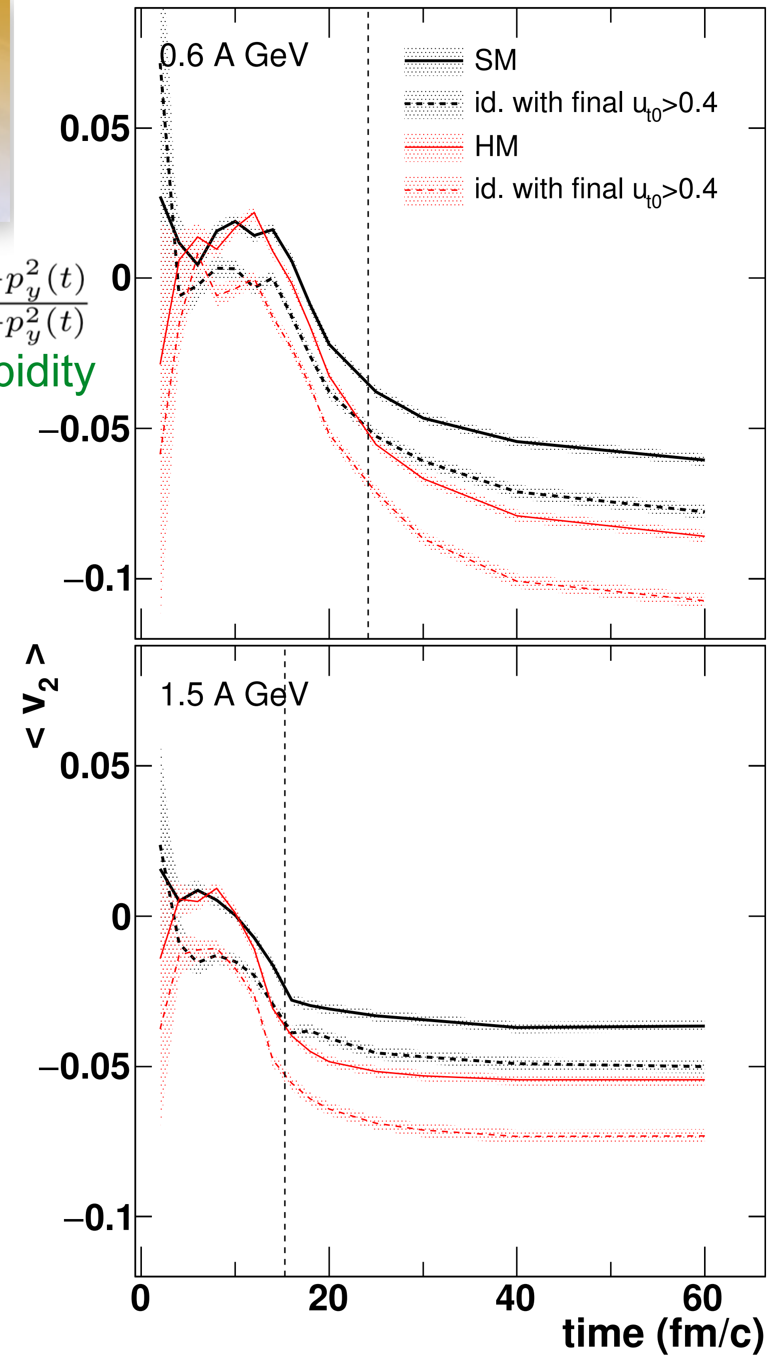

The elliptic flow time evolution

$$v_2(t) = \frac{p_x^2(t) - p_y^2(t)}{p_x^2(t) + p_y^2(t)}$$

at mid-rapidity

- v_2 starts to develop after approximately max. overlap and evolves rapidly.
- After twice the passing time, v_2 reaches its final value.

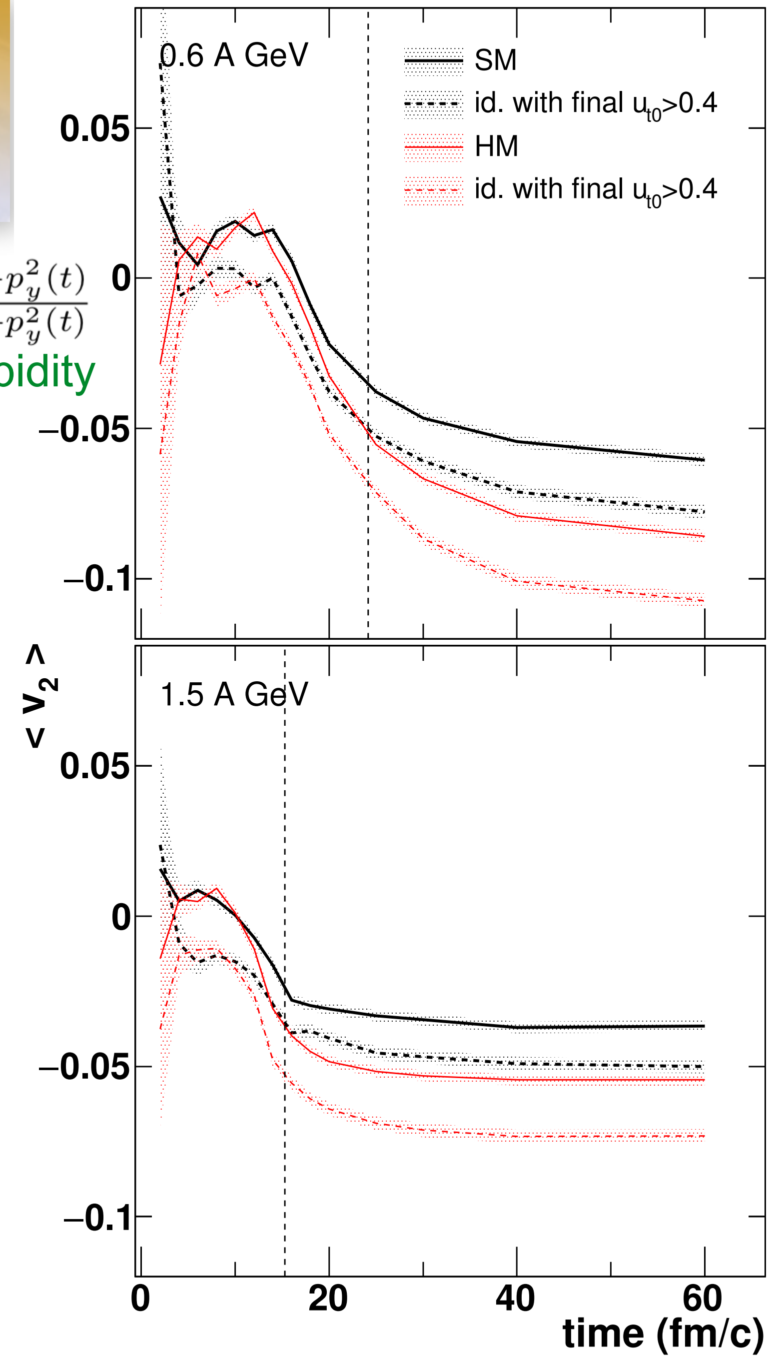

The elliptic flow time evolution

$$v_2(t) = \frac{p_x^2(t) - p_y^2(t)}{p_x^2(t) + p_y^2(t)}$$

at mid-rapidity

- v_2 starts to develop after approximately max. overlap and evolves rapidly.
- After twice the passing time, v_2 reaches its final value.
- Negative for most of the collision times and for both energies.

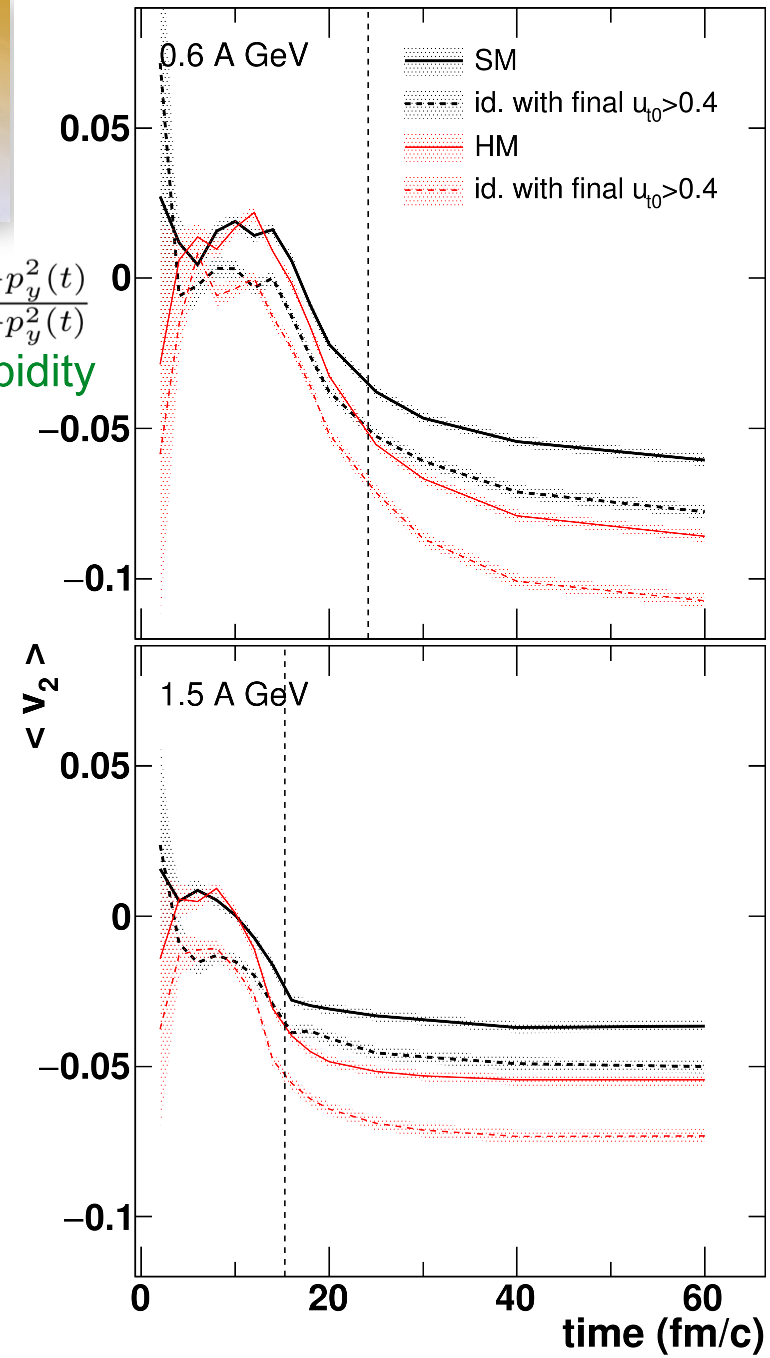

The elliptic flow time evolution

$$v_2(t) = \frac{p_x^2(t) - p_y^2(t)}{p_x^2(t) + p_y^2(t)}$$

at mid-rapidity

- v_2 starts to develop after approximately max. overlap and evolves rapidly.
- After twice the passing time, v_2 reaches its final value.
- Negative for most of the collision times and for both energies.
- But a tendency to be positive in the early stage of the collision.

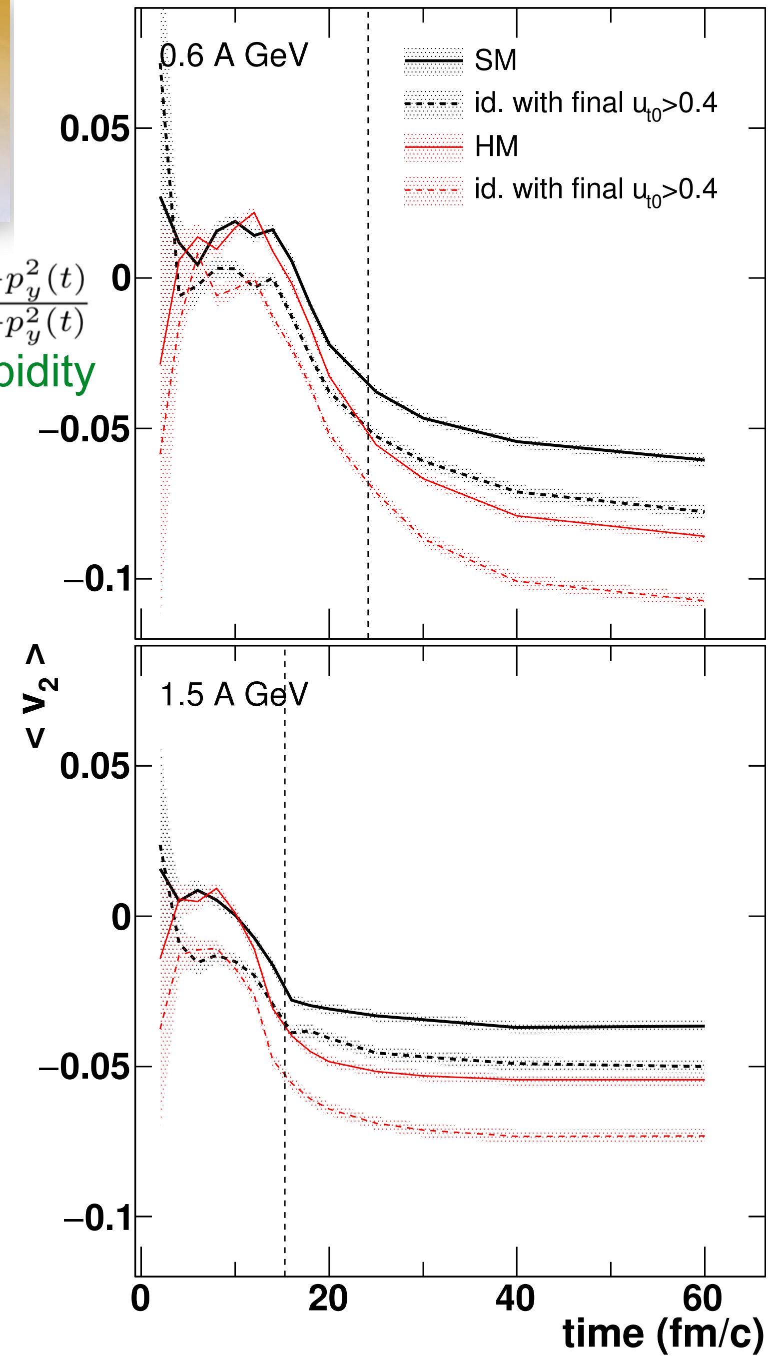

The elliptic flow time evolution

$$v_2(t) = \frac{p_x^2(t) - p_y^2(t)}{p_x^2(t) + p_y^2(t)}$$

at mid-rapidity

- v_2 starts to develop after approximately max. overlap and evolves rapidly.
- After twice the passing time, v_2 reaches its final value.
- Negative for most of the collision times and for both energies.
- But a tendency to be positive in the early stage of the collision.
- With fastest protons ($u_{t0} > 0.4$) v_2 is higher and always negative

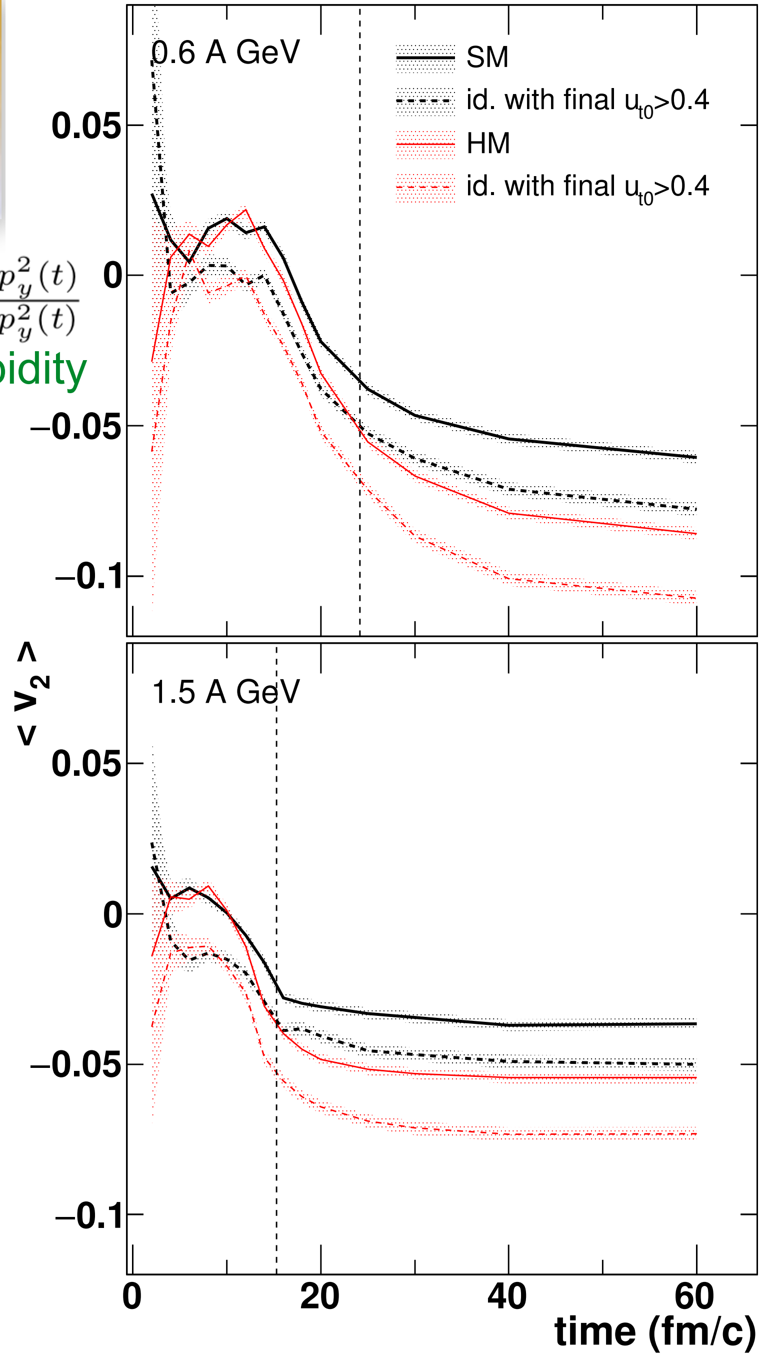

The elliptic flow time evolution

$$v_2(t) = \frac{p_x^2(t) - p_y^2(t)}{p_x^2(t) + p_y^2(t)}$$

at mid-rapidity

- v_2 starts to develop after approximately max. overlap and evolves rapidly.
- After twice the passing time, v_2 reaches its final value.
- Negative for most of the collision times and for both energies.
- But a tendency to be positive in the early stage of the collision.
- With fastest protons ($u_{t0} > 0.4$) v_2 is higher and always negative
- SM vs HM: v_2 at mid-rapidity depends strongly on the EoS; effect enhanced for fastest protons.

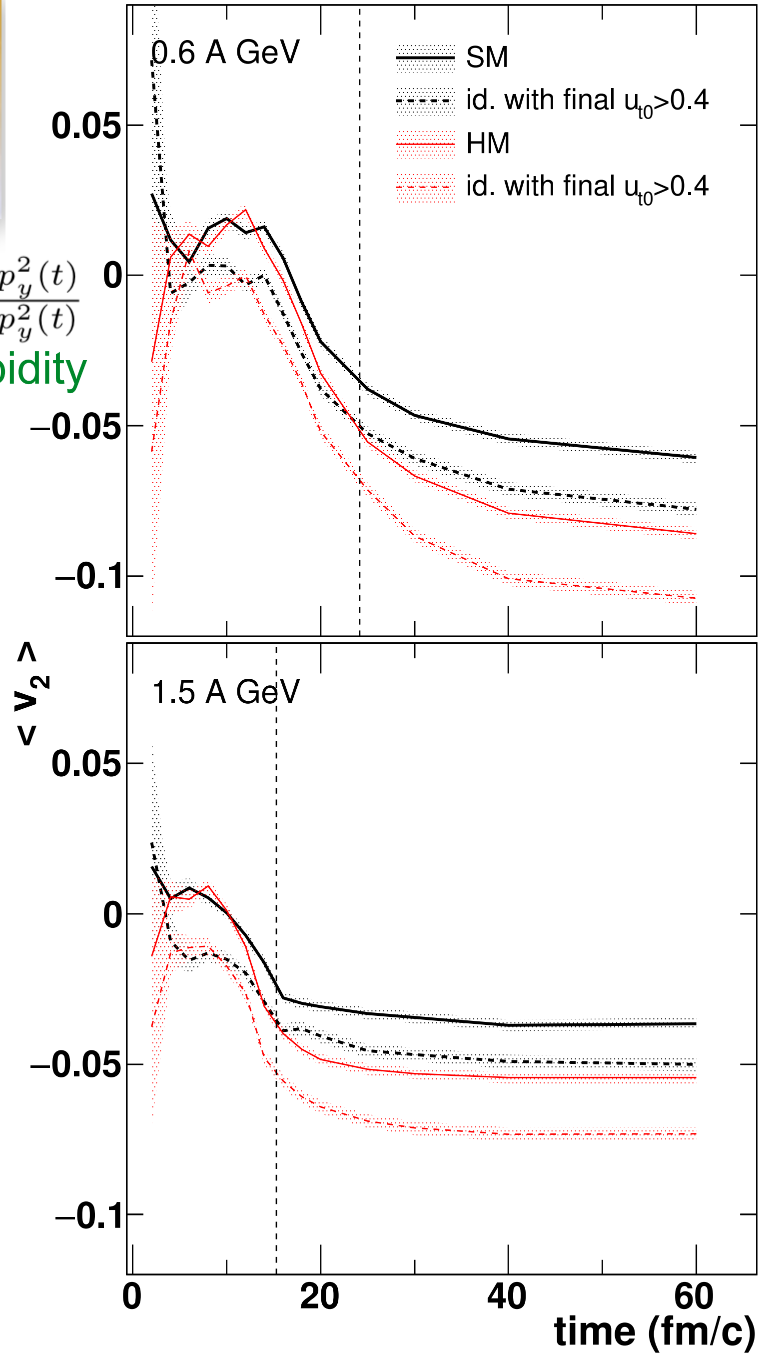

The elliptic flow: collisions versus mean field

An observable to quantify their respective contribution to it: transverse momentum modification induced projected on the direction of the final momentum:

$$\langle \Delta P_t^o(t) \rangle = \langle \boldsymbol{\Delta P_t}(t) \cdot \frac{\boldsymbol{p}_{final}}{|\boldsymbol{p}_{final}|} \rangle$$

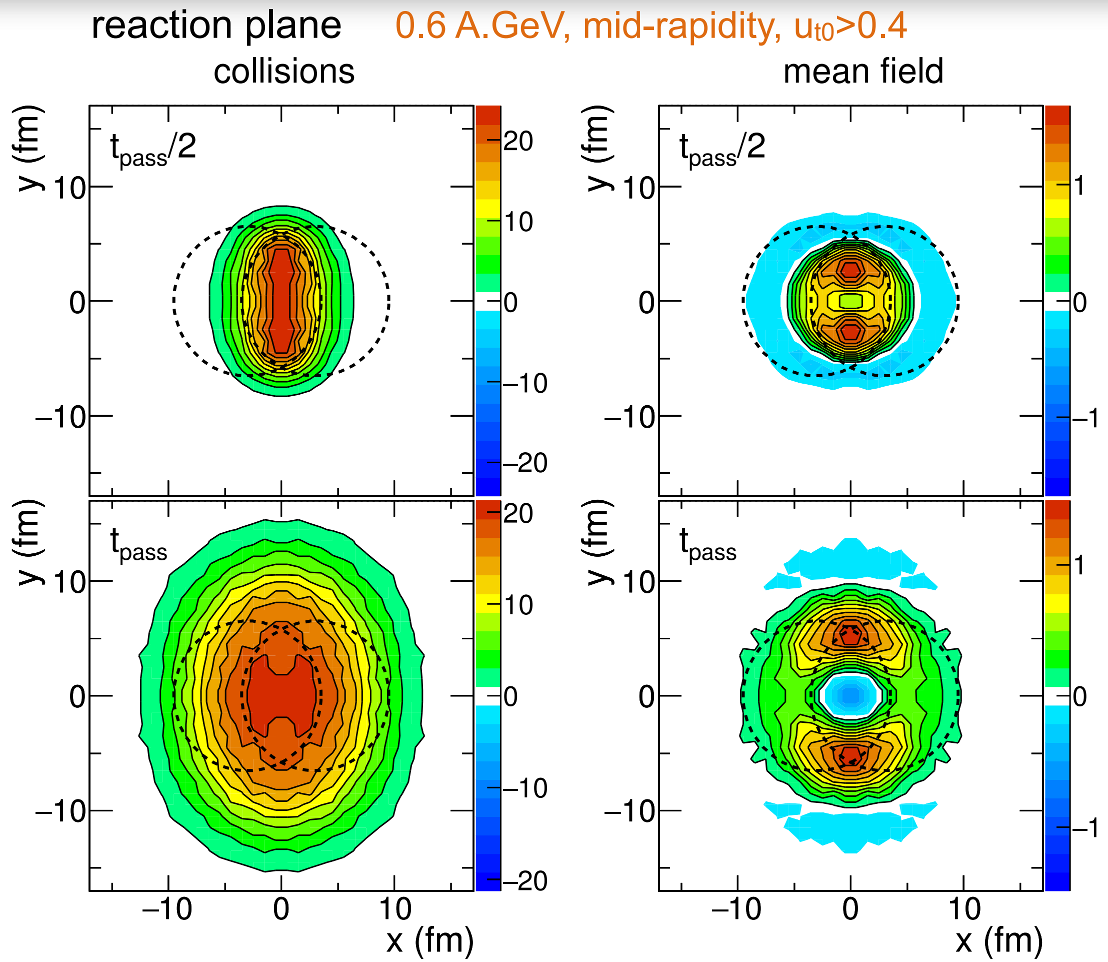

The elliptic flow: collisions versus mean field

An observable to quantify their respective contribution to it: transverse momentum modification induced projected on the direction of the final momentum:

$$\langle \Delta P_t^o(t) \rangle = \langle \boldsymbol{\Delta P_t}(t) \cdot \frac{\boldsymbol{p}_{final}}{|\boldsymbol{p}_{final}|} \rangle$$

From collisions: about an order of magnitude larger than from mean field, set fast in the overlap zone ⇨ this zone of violent collisions expands rapidly keeping its almond shape.

reaction plane 0.6 A.GeV, mid-rapidity, u_{t0}>0.4

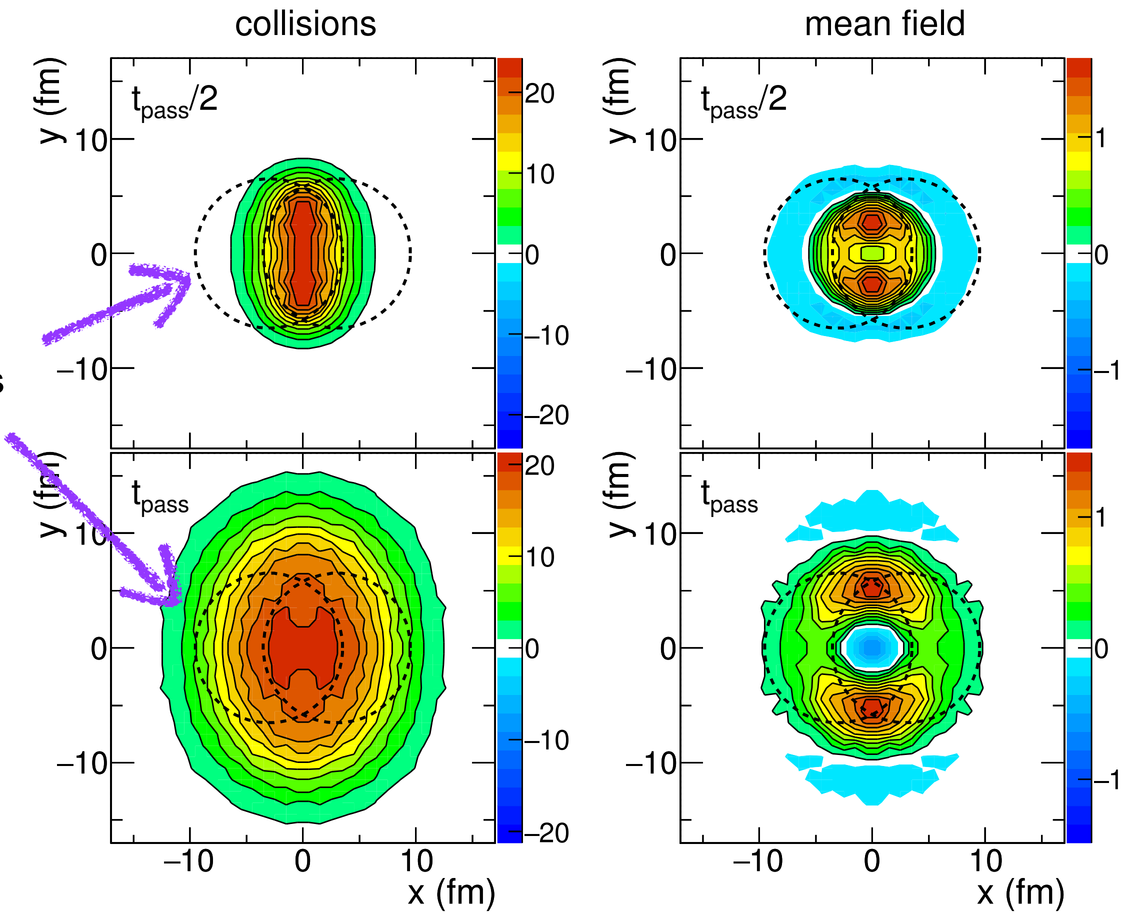

The elliptic flow: collisions versus mean field

An observable to quantify their respective contribution to it: transverse momentum modification induced projected on the direction of the final momentum:

$$\langle \Delta P_t^o(t) \rangle = \langle \boldsymbol{\Delta P_t}(t) \cdot \frac{\boldsymbol{p}_{final}}{|\boldsymbol{p}_{final}|} \rangle$$

From collisions: about an order of magnitude larger than from mean field, set fast in the overlap zone ⇨ this zone of violent collisions expands rapidly keeping its almond shape.

From mean field: large out-of plane momentum transfer at the tips of the almond shape because here nucleons are between vacuum and the central densest zone ⇨ highest density gradient, largest force ⇨ move in y-direction out of the overlap zone.

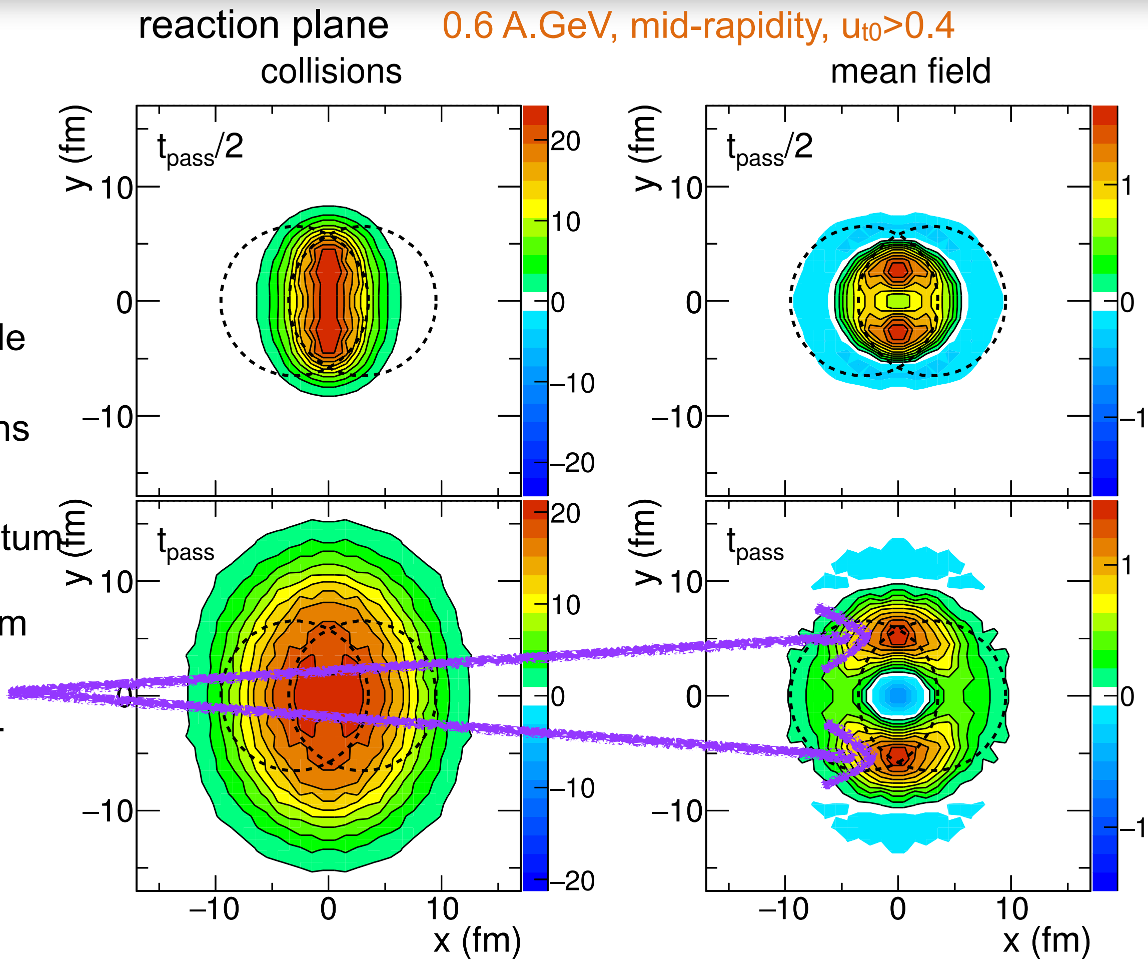

The elliptic flow: collisions versus mean field

An observable to quantify their respective contribution to it: transverse momentum modification induced projected on the direction of the final momentum:

$$\langle \Delta P_t^o(t) \rangle = \langle \boldsymbol{\Delta P_t}(t) \cdot \frac{\boldsymbol{p}_{final}}{|\boldsymbol{p}_{final}|} \rangle$$

From collisions: about an order of magnitude larger than from mean field, set fast in the overlap zone ⇨ this zone of violent collisions expands rapidly keeping its almond shape.

From mean field: large out-of plane momentum transfer at the tips of the almond shape because here nucleons are between vacuum and the central densest zone ⇨ highest density gradient, largest force ⇨ move in y-direction out of the overlap zone.

Outer blue areas ⇦ attractive potential of the remnant, deceleration.

Inner blue area: inner density decreases and attraction by the moving spectators ⇨ transverse velocity decreases

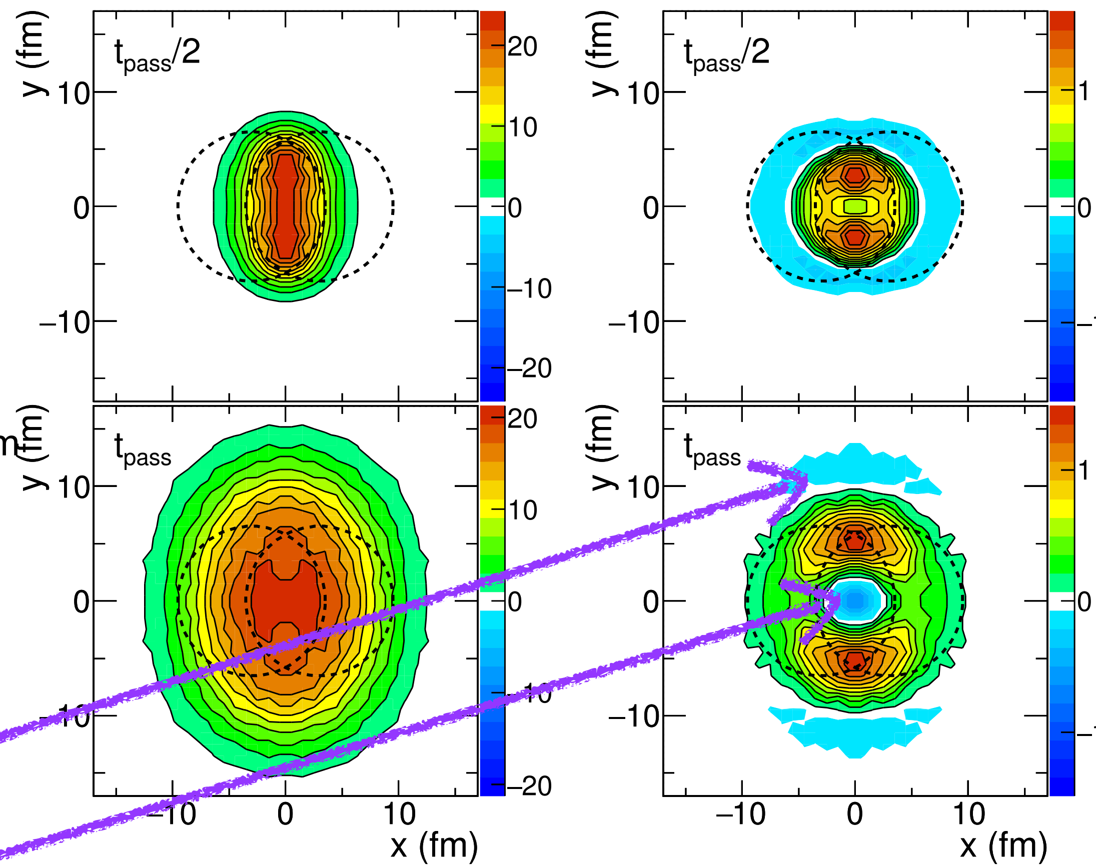

The elliptic flow: collisions versus mean field

Little difference between 0.6 AGeV and at 1.5 AGeV.

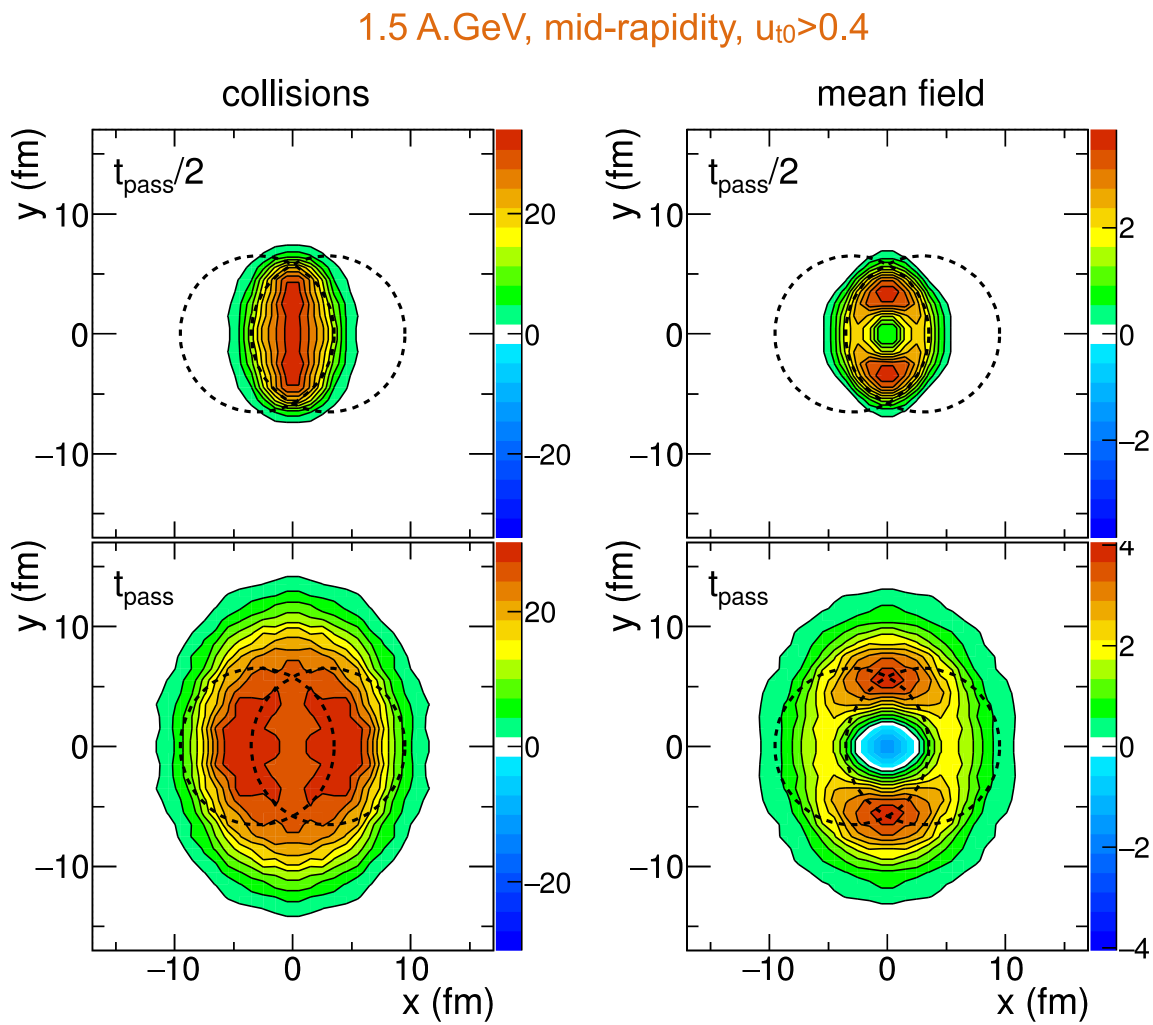

The elliptic flow: collisions versus mean field

v2 directly related to its anisotropy in x and y.

$$\langle \Delta P_i^o(t) \rangle = \langle \Delta P_i(t) \cdot \frac{p_{i,final}}{|p_{i,final}|} \rangle$$

Collision contribution: always much larger than that of mean field.

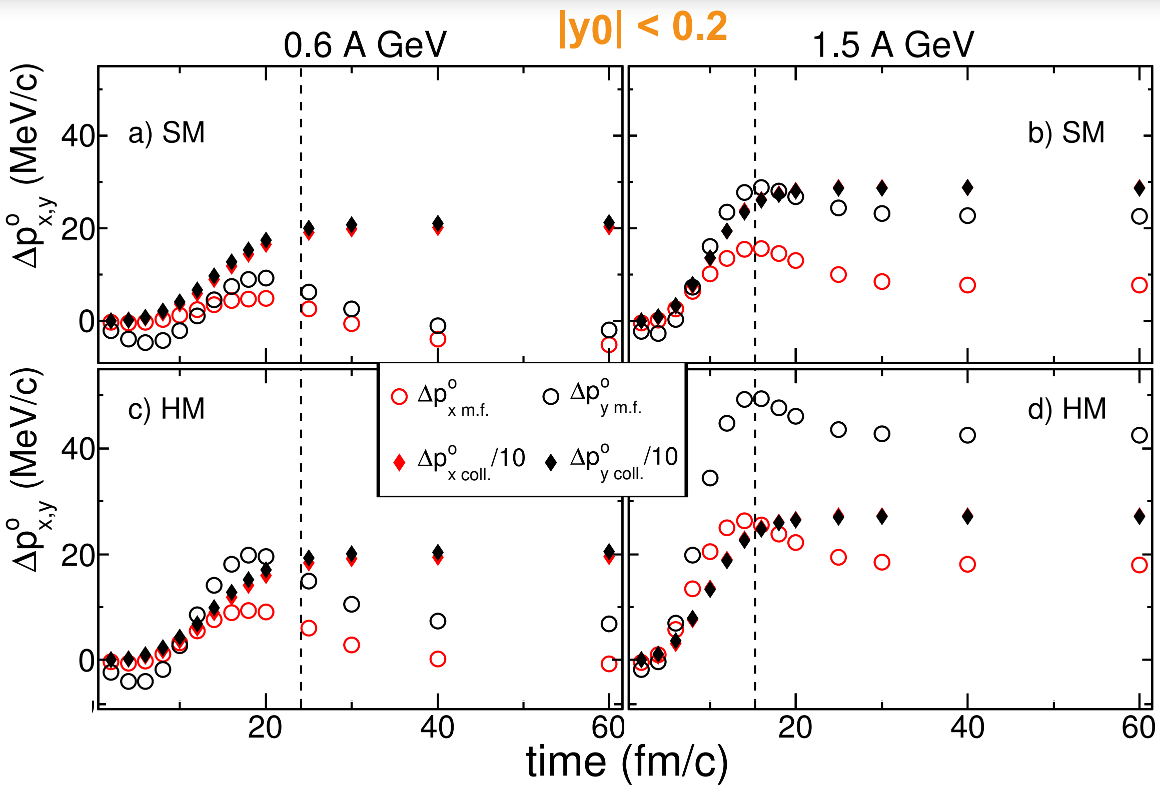

The elliptic flow: collisions versus mean field

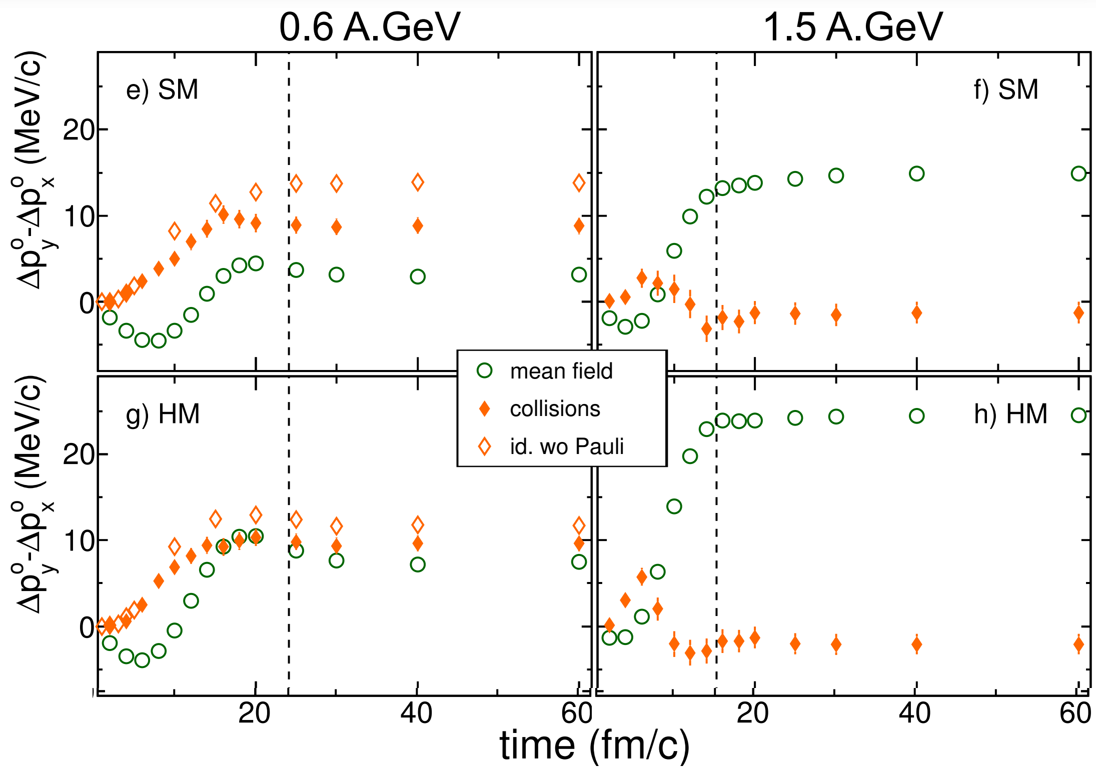

The elliptic flow: collisions versus mean field

Excess in the y- direction: clearly visible for the mean field AND the collisions. For the collisions: becomes smaller with higher projectile velocity until it vanishes at 1.5 AGeV incident energy.

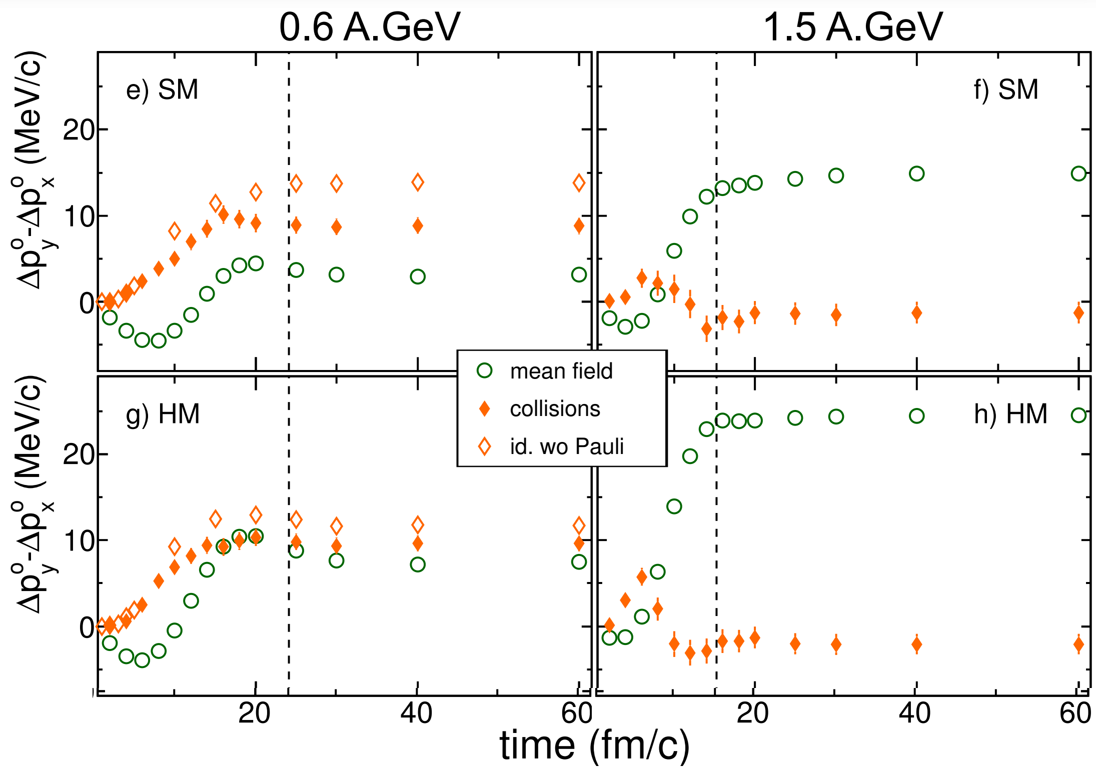

The elliptic flow: collisions versus mean field

Excess in the y- direction: clearly visible for the mean field AND the collisions. For the collisions: becomes smaller with higher projectile velocity until it vanishes at 1.5 AGeV incident energy.

K_0 has no visible influence on the amplitude of the collisional out-of-plane momentum excess because the number of collisions is almost unchanged by the choice of the EoS.

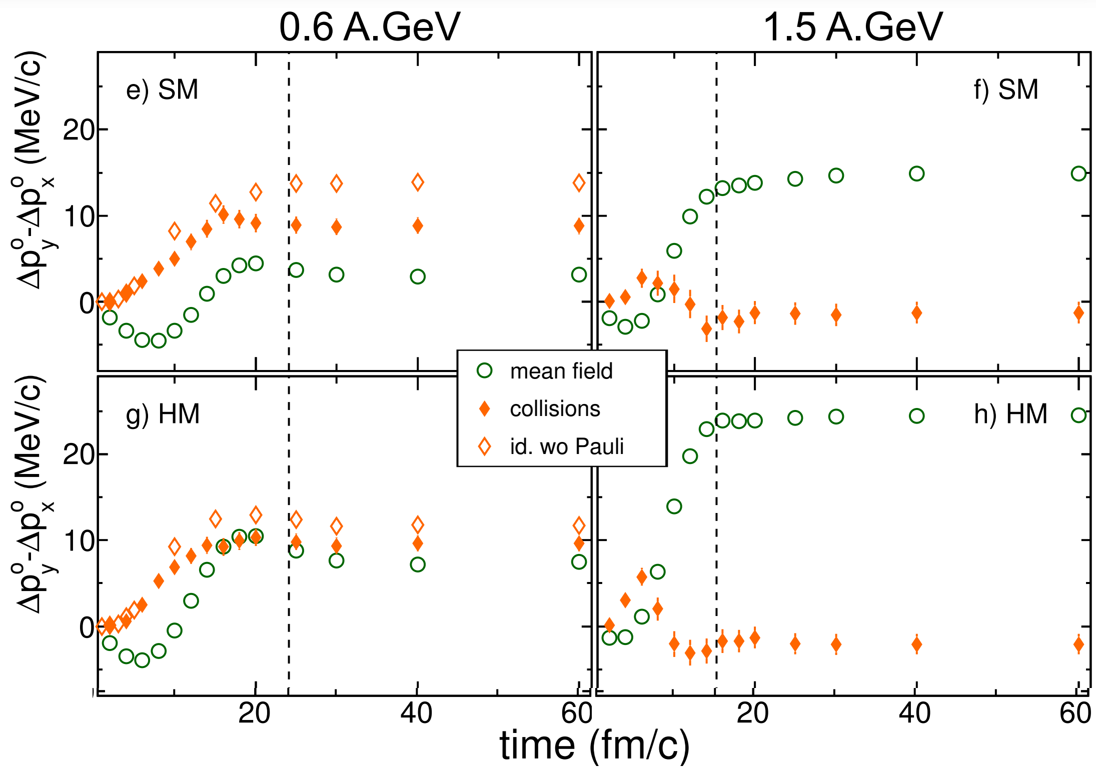

The elliptic flow: collisions versus mean field

Excess in the y- direction: clearly visible for the mean field AND the collisions. For the collisions: becomes smaller with higher projectile velocity until it vanishes at 1.5 AGeV incident energy.

K_0 has no visible influence on the amplitude of the collisional out-of-plane momentum excess because the number of collisions is almost unchanged by the choice of the EoS.

Pauli blocking: quenches $v_2<0$ due to collisions, from the densest phase of the collisions, stronger for SM because larger densities are reached.

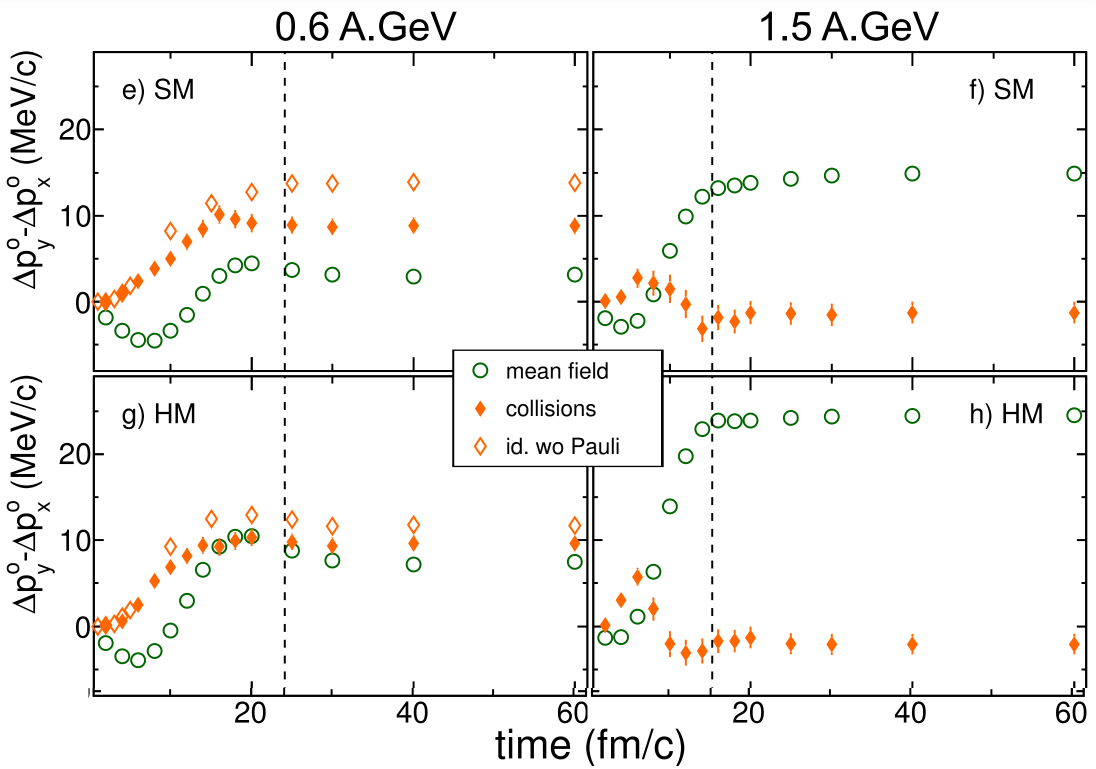

The elliptic flow: collisions versus mean field

Excess in the y- direction: clearly visible for the mean field AND the collisions. For the collisions: becomes smaller with higher projectile velocity until it vanishes at 1.5 AGeV incident energy.

K_0 has no visible influence on the amplitude of the collisional out-of-plane momentum excess because the number of collisions is almost unchanged by the choice of the EoS.

Pauli blocking: quenches $v_2<0$ due to collisions, from the densest phase of the collisions, stronger for SM because larger densities are reached.

⇨ Without Pauli blocking, there would be a collisional contribution to the EoS dependence of v_2.

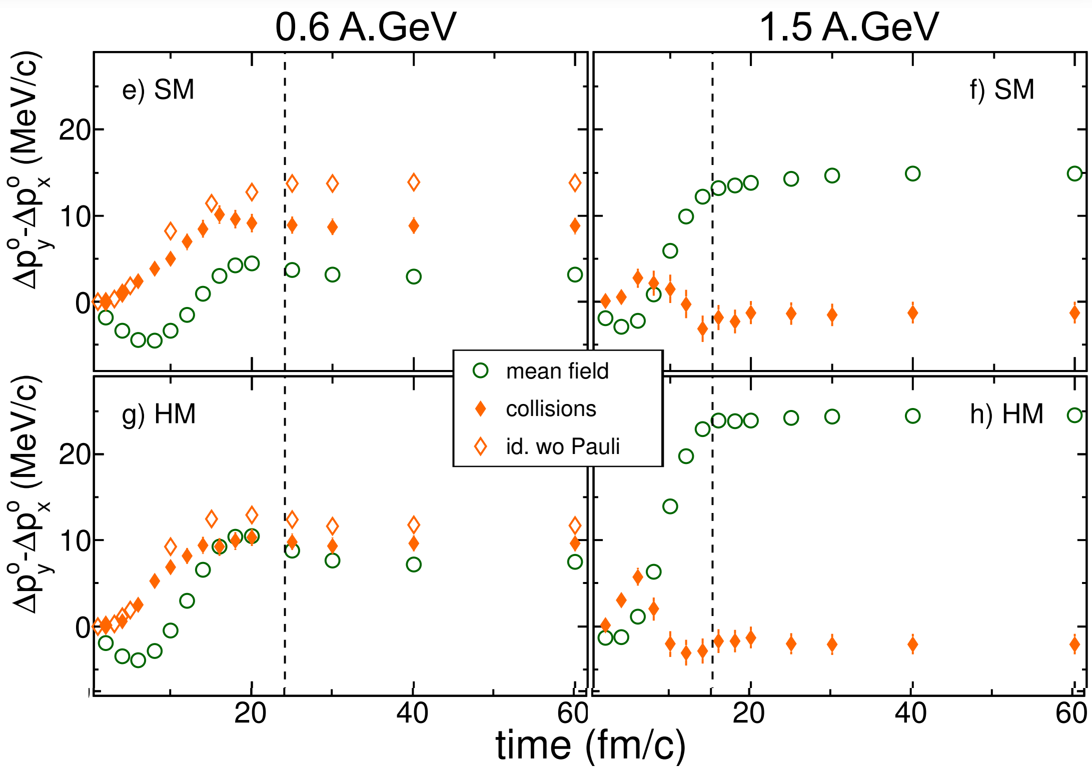

The elliptic flow: collisions versus mean field

Excess in the y- direction: clearly visible for the mean field AND the collisions. For the collisions: becomes smaller with higher projectile velocity until it vanishes at 1.5 AGeV incident energy.

K_0 has no visible influence on the amplitude of the collisional out-of-plane momentum excess because the number of collisions is almost unchanged by the choice of the EoS.

Pauli blocking: quenches $v_2<0$ due to collisions, from the densest phase of the collisions, stronger for SM because larger densities are reached.

⇨ Without Pauli blocking, there would be a collisional contribution to the EoS dependence of v_2.

Mean field contribution to $v_2<0$: dependent on incident energy and K_0: moderate at 0.6 AGeV with the soft EoS, contributing to only 30% of the total $\Delta P_y^o - \Delta P_x^o$, very strong and dominating at 1.5 AGeV with the stiffer EoS.

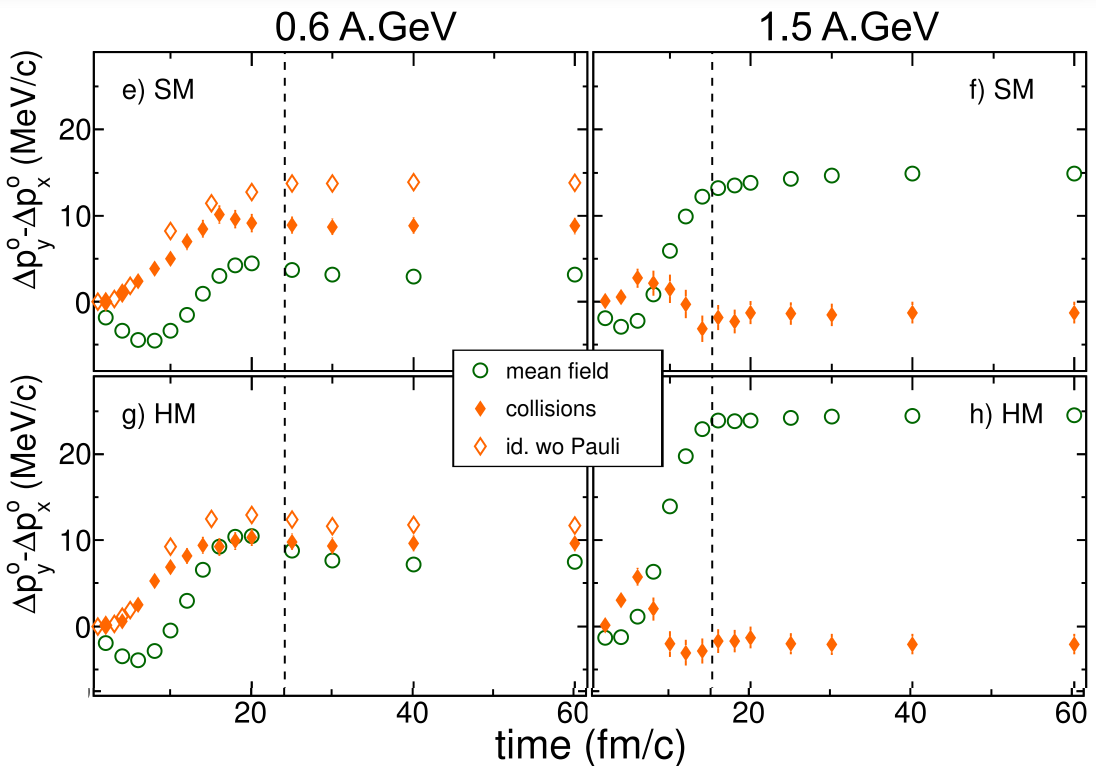

The elliptic flow: collisions vs mean field

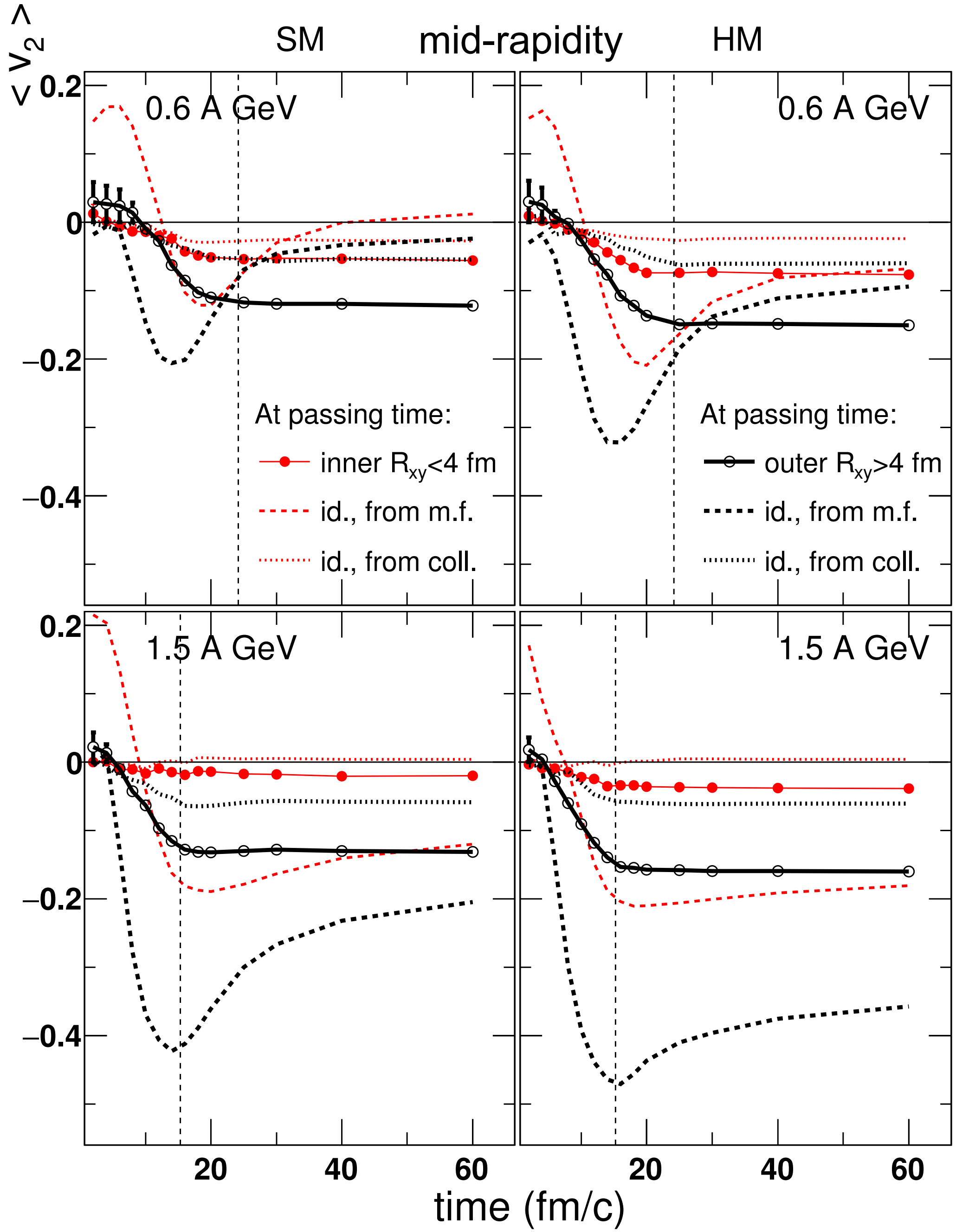

The elliptic flow: collisions vs mean field

Outermost nucleons (R_{xy} > 4 fm) = the main source of the overall negative v_2 :

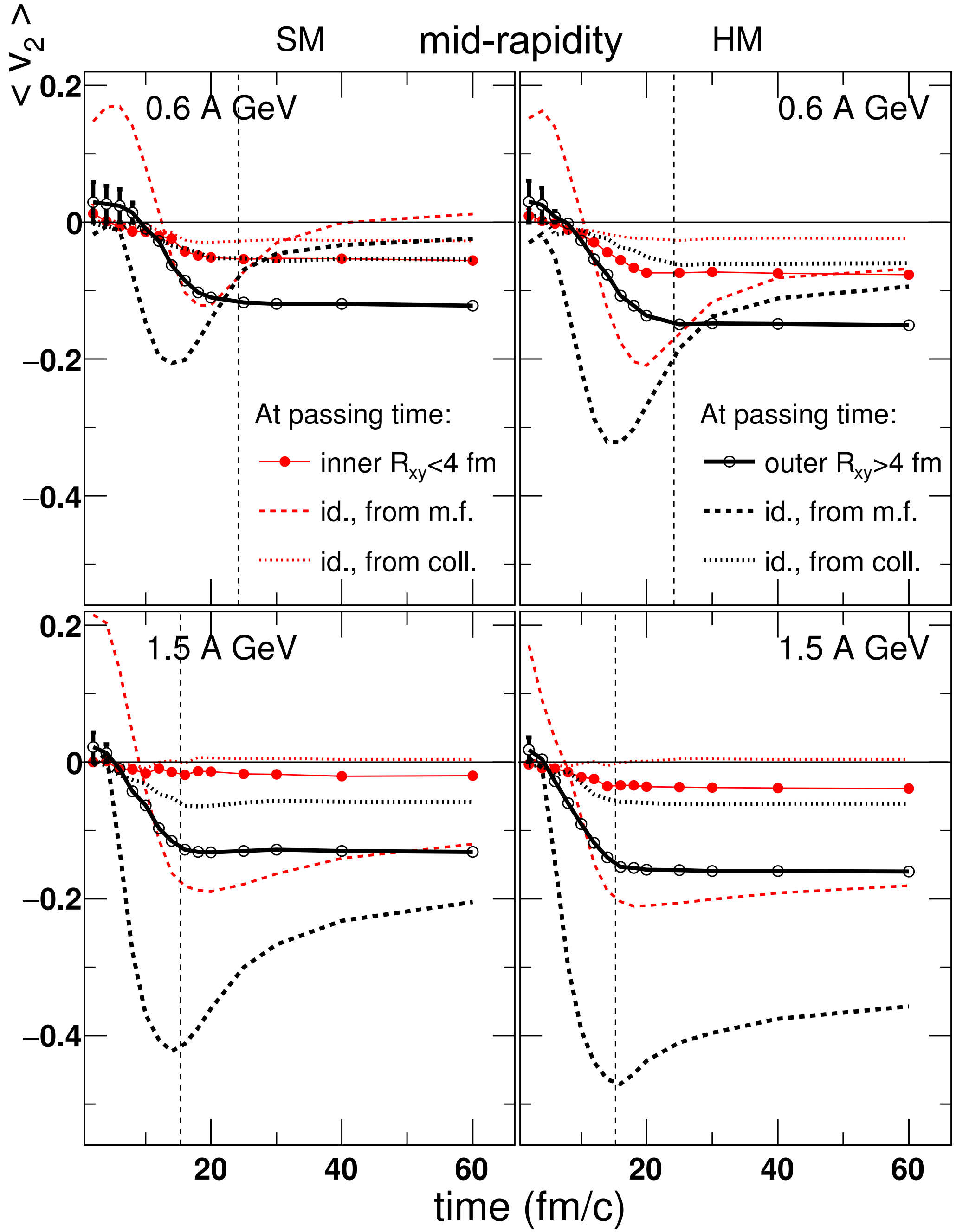

The elliptic flow: collisions vs mean field

Outermost nucleons (R_{xy} > 4 fm) = the main source of the overall negative v_2 :

* From collisions: the early in-plane screening by the spectators ($\rightarrow v_2<0$) affects only the outermost nucleons, whereas the collisions of the inner nucleons create a nearly azimuthally isotropic distribution ($v_2 \approx 0$).

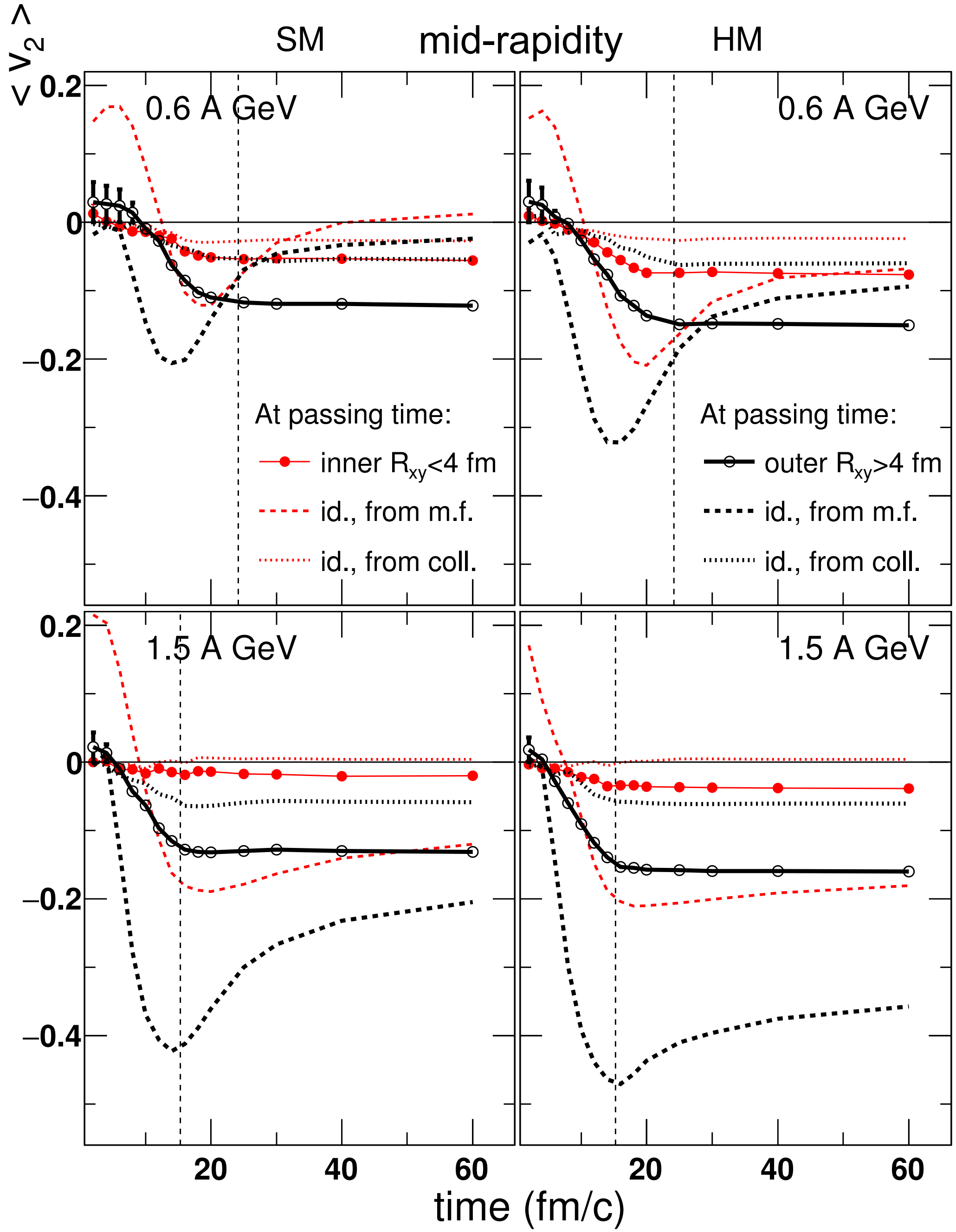

The elliptic flow: collisions vs mean field

Outermost nucleons (R_{xy} > 4 fm) = the main source of the overall negative v_2 :

* From collisions: the early in-plane screening by the spectators (→v_2<0) affects only the outermost nucleons, whereas the collisions of the inner nucleons create a nearly azimuthally isotropic distribution ($v_2 \approx 0$).

* From the mean field: density gradient larger at the tips of the overlapping zone (outermost nucleons); decreases later due to the formation of the in-plane ridge

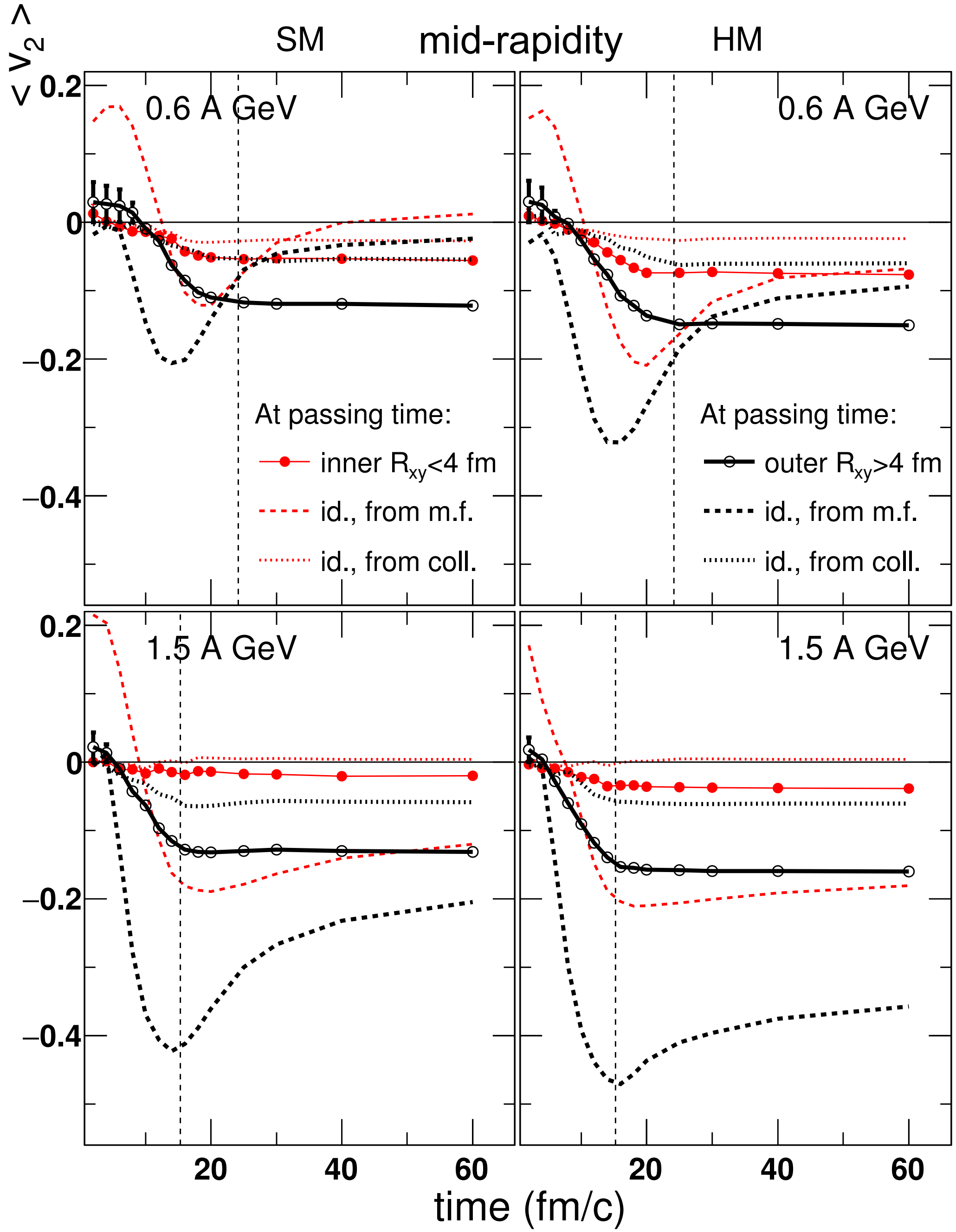

GSI HELMHOLTZ ASSOCIATION

The elliptic flow: collisions vs mean field

Outermost nucleons (R_{xy} > 4 fm) = the main source of the overall negative v_2 :

* From collisions: the early in-plane screening by the spectators ($\rightarrow v_2<0$) affects only the outermost nucleons, whereas the collisions of the inner nucleons create a nearly azimuthally isotropic distribution ($v_2 \approx 0$).

* From the mean field: density gradient larger at the tips of the overlapping zone (outermost nucleons); decreases later due to the formation of the in-plane ridge

* Asymptotically, the mean field = the main origin of the overall out-of-plane v_2, apart from reactions at energies below 1 AGeV where the collisions contribute equally when the nuclear matter EoS is soft, i.e. the number of collisions is large.

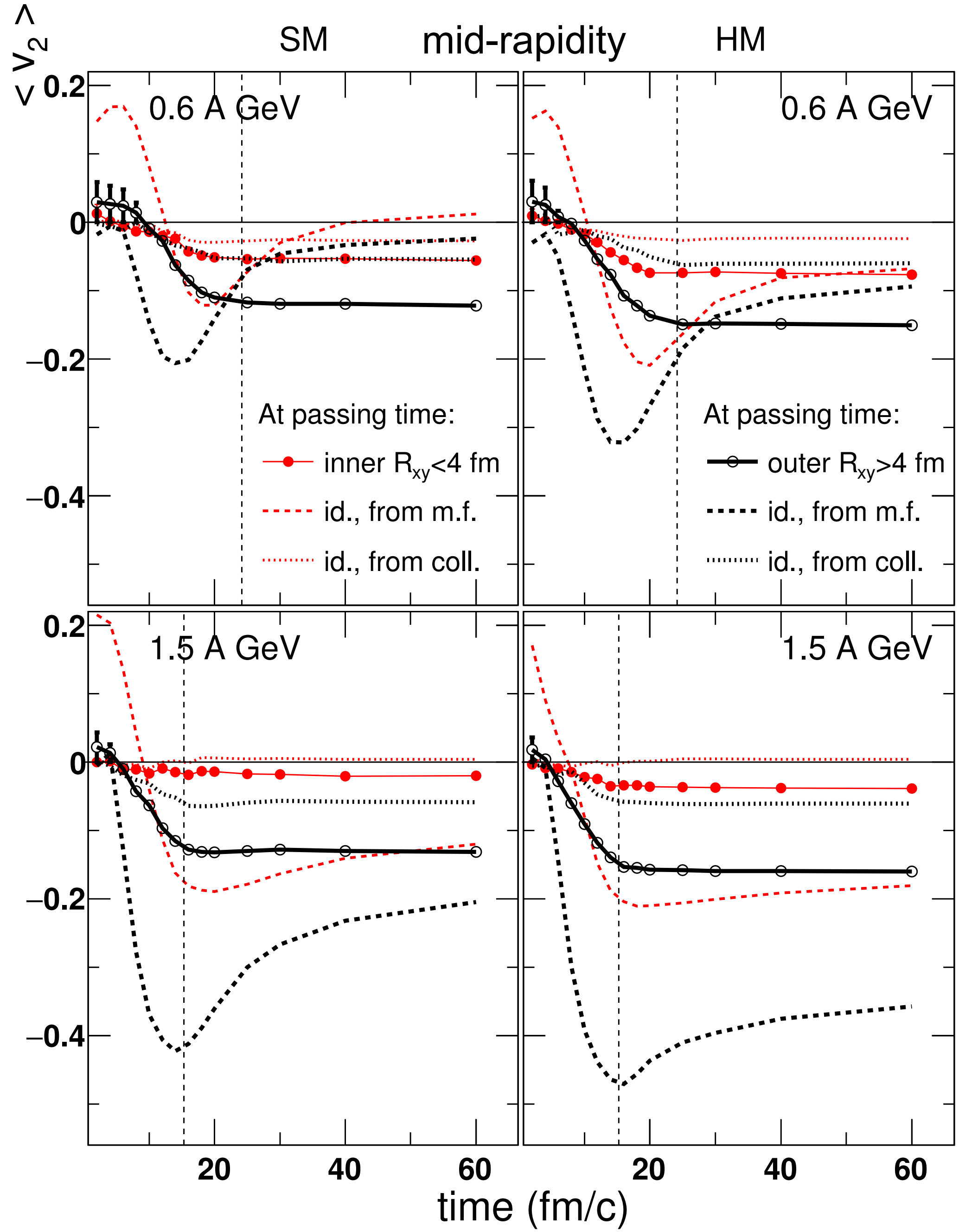

The elliptic flow: incident energy dependance

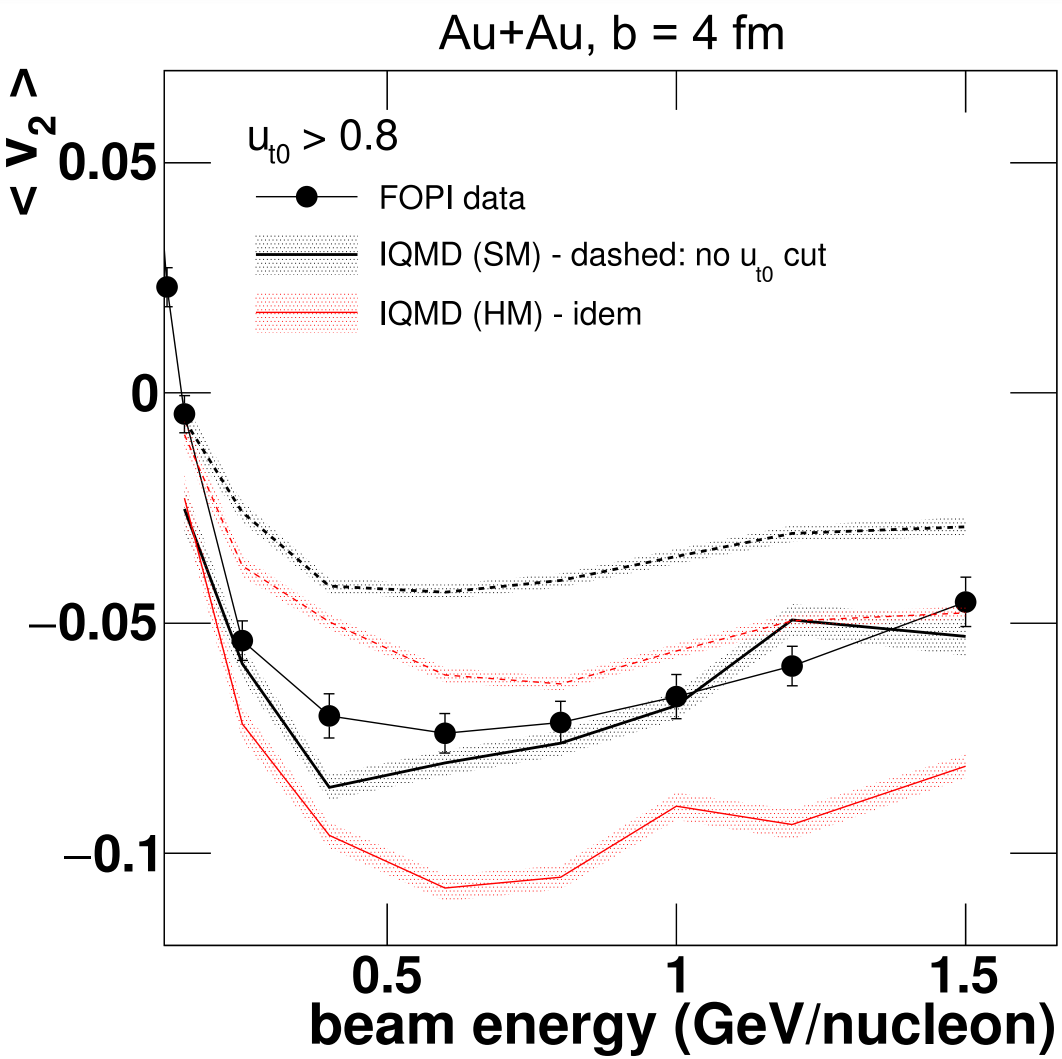

The elliptic flow: incident energy dependance

- Strong beam energy dependence for $E_{inc} > 0.4$ AGeV

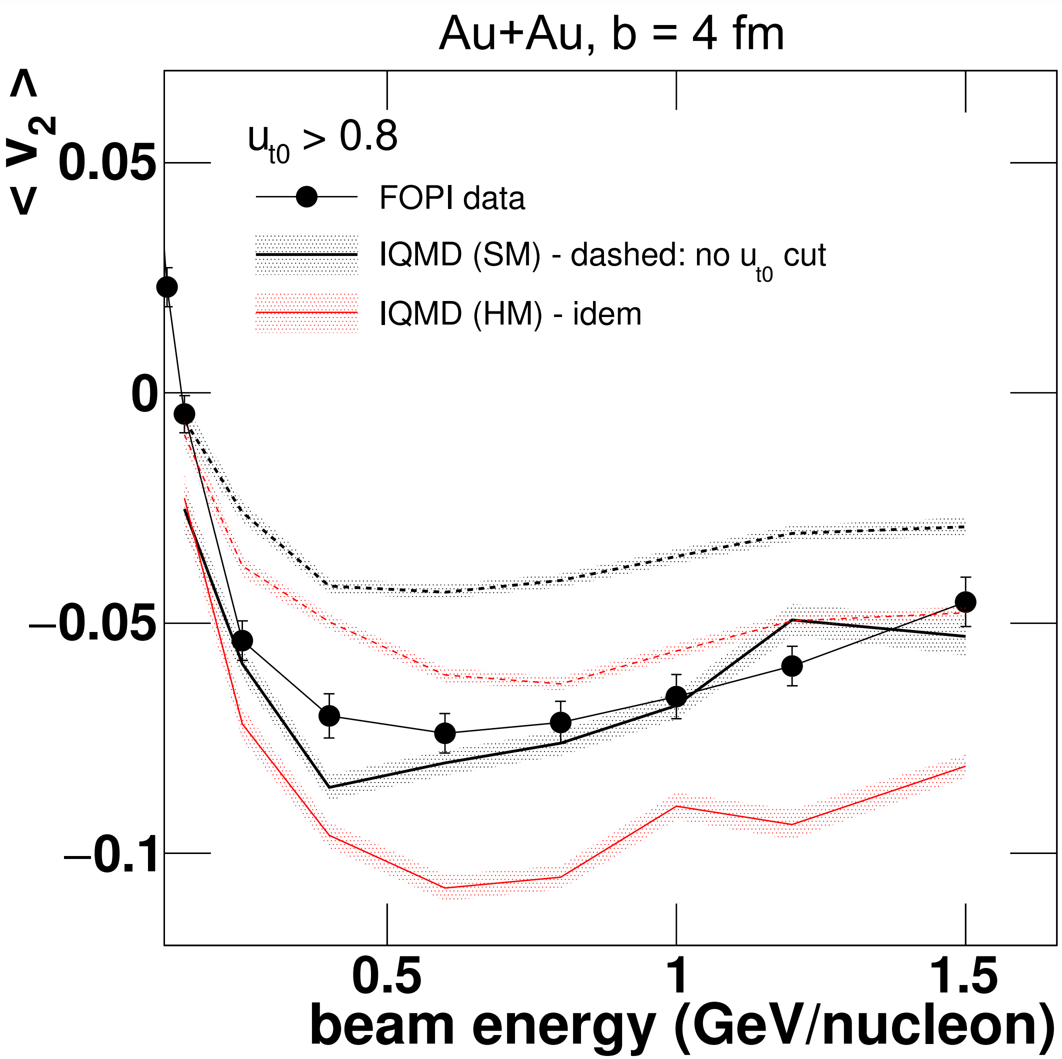

The elliptic flow: incident energy dependance

- Strong beam energy dependence for E_{inc} > 0.4 AGeV
- Maximum of amplitude at around 0.6 AGeV.

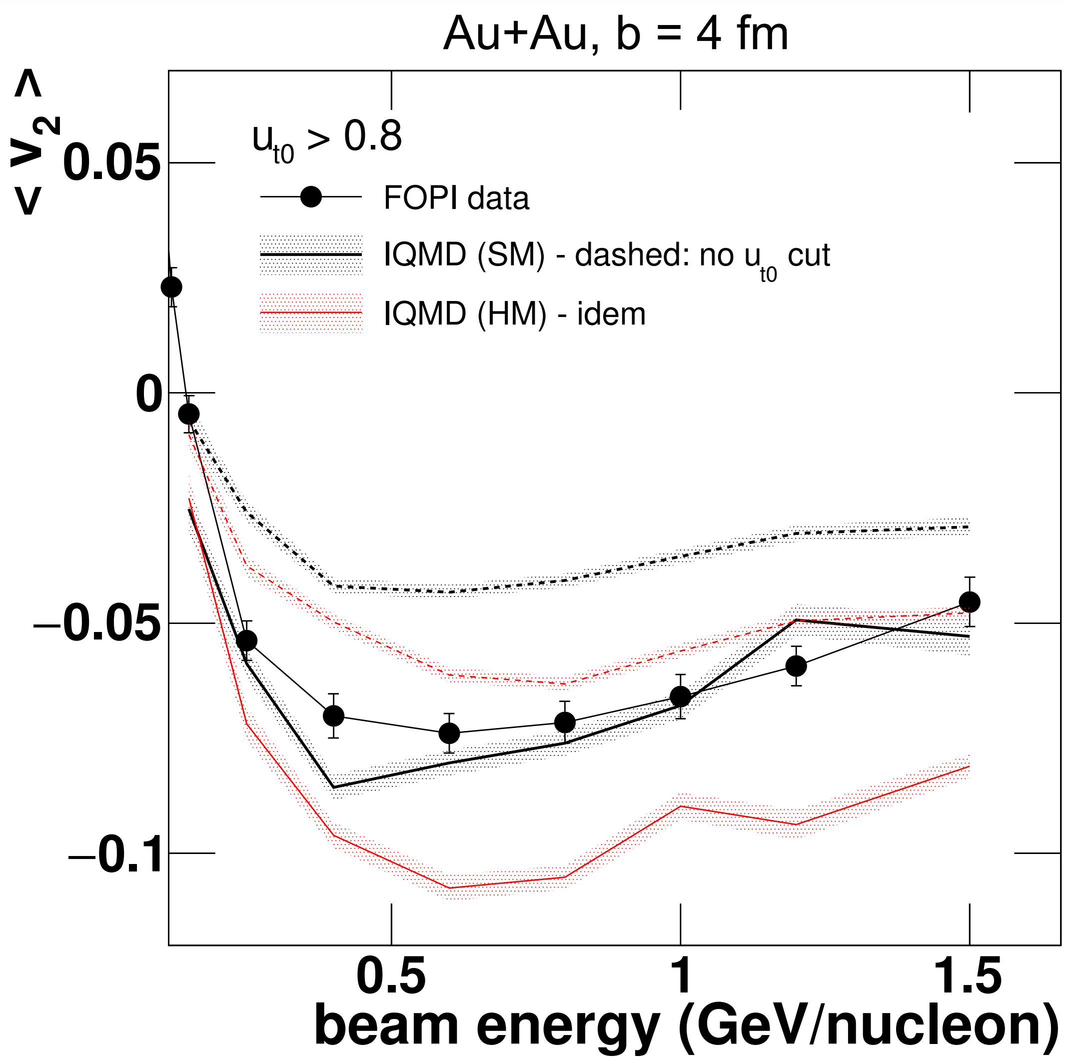

The elliptic flow: incident energy dependance

- Strong beam energy dependence for E_{inc} > 0.4 AGeV
- Maximum of amplitude at around 0.6 AGeV.
- Strength enhanced with protons with a large transverse velocity.

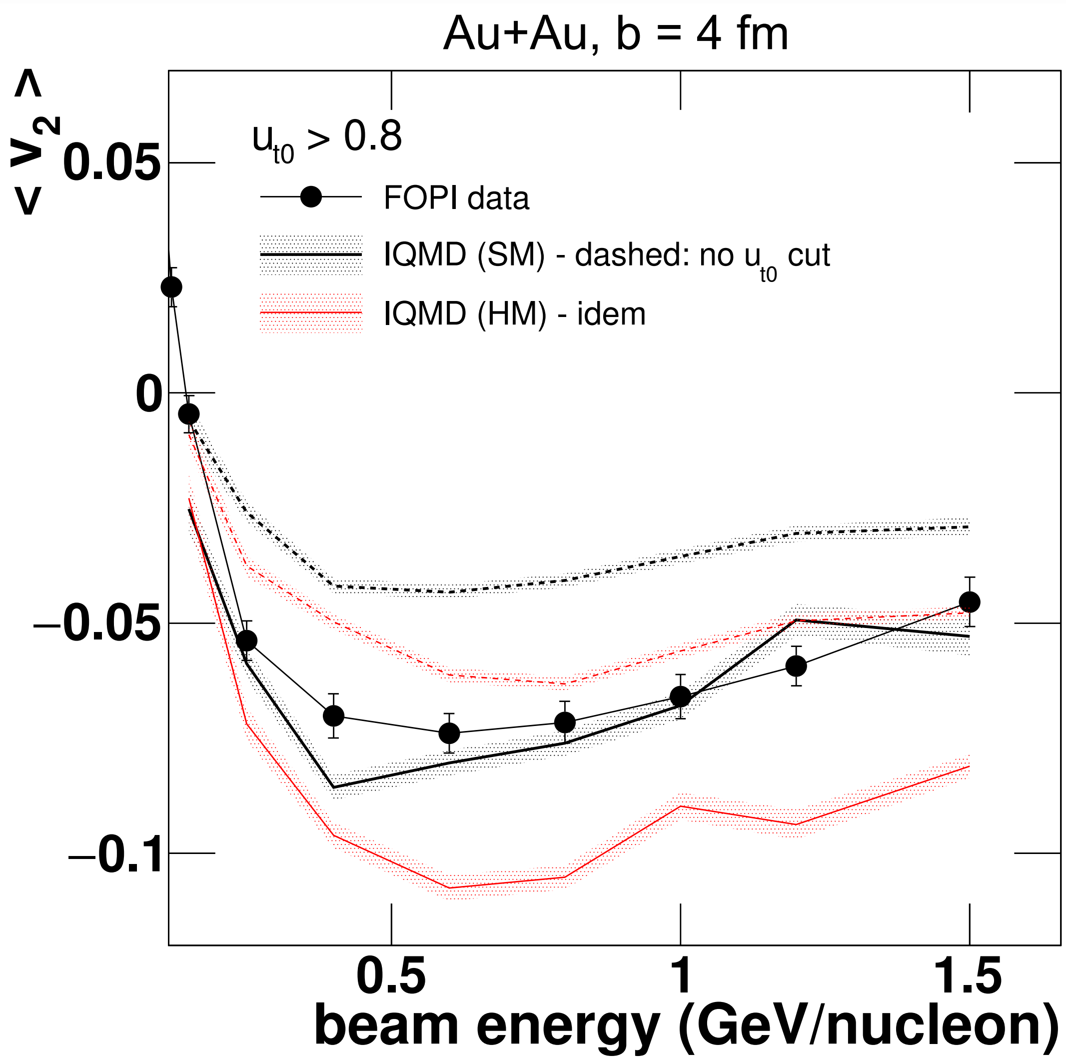

The elliptic flow: incident energy dependance

- Strong beam energy dependence for E_{inc} > 0.4 AGeV
- Maximum of amplitude at around 0.6 AGeV.
- Strength enhanced with protons with a large transverse velocity.
- Comparison with FOPI observations (protons with u_{t0} > 0.8, same impact parameter) ⇨ good agreement (amplitude and evolution) using the soft (SM) EoS.

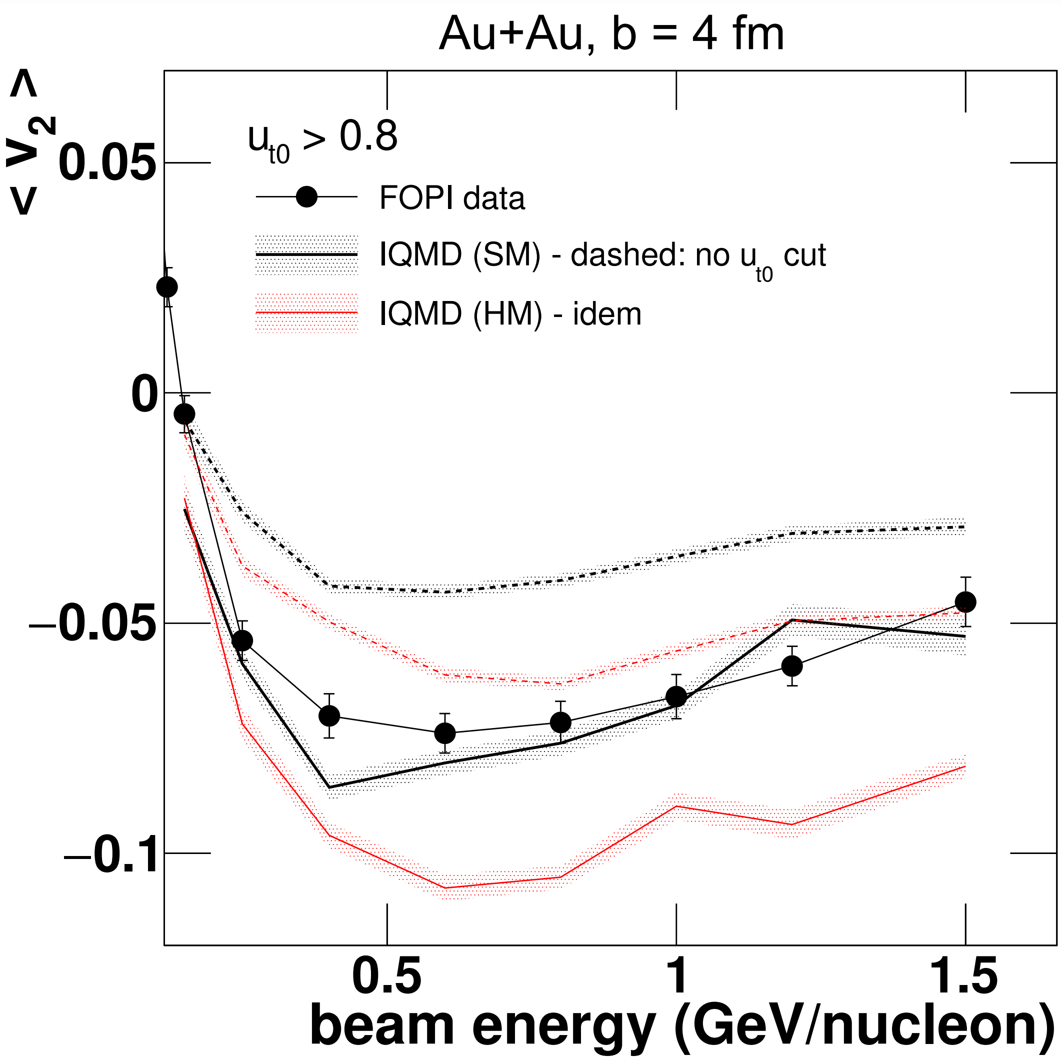

Summary

Summary

Summary:

Summary

Summary:

❖ The elliptic flow observed in the reactions around $E_{kin} \approx 1$ AGeV for protons at mid-rapidity ($|y_0| < 0.2$) has two origins:

Summary

Summary:

❖ The elliptic flow observed in the reactions around $E_{kin} \approx 1$ AGeV for protons at mid-rapidity ($|y_0| < 0.2$) has two origins:

- ❖ the collisions of participant nucleons with the spectator matter

HELMHOLTZ ASSOCIATION

Summary

Summary:

- The elliptic flow observed in the reactions around $E_{kin} \approx 1$ AGeV for protons at mid-rapidity ($|y_0| < 0.2$) has two origins:
    - the collisions of participant nucleons with the spectator matter
    - the acceleration of participants in the mean field.

Summary

Summary:

- The elliptic flow observed in the reactions around $E_{kin} \approx 1$ AGeV for protons at mid-rapidity ($|y_0| < 0.2$) has two origins:
    - the collisions of participant nucleons with the spectator matter
    - the acceleration of participants in the mean field.
- The collisional component of v_2 is almost independent of the EoS (due to Pauli blocking),

Summary

Summary:

- The elliptic flow observed in the reactions around $E_{kin} \approx 1$ AGeV for protons at mid-rapidity ($|y_0| < 0.2$) has two origins:
  - the collisions of participant nucleons with the spectator matter
  - the acceleration of participants in the mean field.
- The collisional component of v_2 is almost independent of the EoS (due to Pauli blocking),
- The mean field contribution is for a hard EoS (HM) roughly twice as large as that for a soft EoS (SM).

Summary

Summary:

- The elliptic flow observed in the reactions around $E_{kin} \approx 1$ AGeV for protons at mid-rapidity ($|y_0| < 0.2$) has two origins:
  - the collisions of participant nucleons with the spectator matter
  - the acceleration of participants in the mean field.
- The collisional component of v_2 is almost independent of the EoS (due to Pauli blocking),
- The mean field contribution is for a hard EoS (HM) roughly twice as large as that for a soft EoS (SM).
- At largest out-of-plane emission (0.6 AGeV$\leftrightarrow$ max. stopping), for a soft EoS, collisional and mean field contributions are about equal,

Summary

Summary:

- The elliptic flow observed in the reactions around $E_{kin} \approx 1$ AGeV for protons at mid-rapidity ($|y_0| < 0.2$) has two origins:
  - the collisions of participant nucleons with the spectator matter
  - the acceleration of participants in the mean field.
- The collisional component of v_2 is almost independent of the EoS (due to Pauli blocking),
- The mean field contribution is for a hard EoS (HM) roughly twice as large as that for a soft EoS (SM).
- At largest out-of-plane emission (0.6 AGeV$\leftrightarrow$ max. stopping), for a soft EoS, collisional and mean field contributions are about equal,
- In all other cases the contribution of the mean field dominates.

Summary

Summary:

- The elliptic flow observed in the reactions around $E_{kin} \approx 1$ AGeV for protons at mid-rapidity ($|y_0| < 0.2$) has two origins:
  - the collisions of participant nucleons with the spectator matter
  - the acceleration of participants in the mean field.
- The collisional component of v_2 is almost independent of the EoS (due to Pauli blocking),
- The mean field contribution is for a hard EoS (HM) roughly twice as large as that for a soft EoS (SM).
- At largest out-of-plane emission (0.6 AGeV$\leftrightarrow$ max. stopping), for a soft EoS, collisional and mean field contributions are about equal,
- In all other cases the contribution of the mean field dominates.
- Mean field out-of-plane flow comes from nucleons close to the tips of fireball: strongest density gradient in y-direction

Summary

Summary:

- The elliptic flow observed in the reactions around $E_{kin} \approx 1$ AGeV for protons at mid-rapidity ($|y_0| < 0.2$) has two origins:
  - the collisions of participant nucleons with the spectator matter
  - the acceleration of participants in the mean field.
- The collisional component of v_2 is almost independent of the EoS (due to Pauli blocking),
- The mean field contribution is for a hard EoS (HM) roughly twice as large as that for a soft EoS (SM).
- At largest out-of-plane emission (0.6 AGeV$\leftrightarrow$ max. stopping), for a soft EoS, collisional and mean field contributions are about equal,
- In all other cases the contribution of the mean field dominates.
- Mean field out-of-plane flow comes from nucleons close to the tips of fireball: strongest density gradient in y-direction
- This effect is amplified if one selects particles with a high transverse velocity.

Summary

Summary:

- The elliptic flow observed in the reactions around $E_{kin} \approx 1$ AGeV for protons at mid-rapidity ($|y_0| < 0.2$) has two origins:
  - the collisions of participant nucleons with the spectator matter
  - the acceleration of participants in the mean field.
- The collisional component of v_2 is almost independent of the EoS (due to Pauli blocking),
- The mean field contribution is for a hard EoS (HM) roughly twice as large as that for a soft EoS (SM).
- At largest out-of-plane emission (0.6 AGeV$\leftrightarrow$ max. stopping), for a soft EoS, collisional and mean field contributions are about equal,
- In all other cases the contribution of the mean field dominates.
- Mean field out-of-plane flow comes from nucleons close to the tips of fireball: strongest density gradient in y-direction
- This effect is amplified if one selects particles with a high transverse velocity.
- The calculations with a soft EoS (SM) are in better agreement with the experimental data than that with a hard equation of state (HM).

Thank you for your attention!

Introduction

- Alternative method: in earth laboratories, heavy ion collisions over a wide range of incident energies, system sizes and compositions.
  - limited to E_{beam}<10 A.GeV ⬅ some kind of a clock is available (sound velocity versus participant-spectator interaction).
  - KaoS (1990's), C+C, Au+Au, K^+ yields -> 'soft' EOS. But:
    - kaons rare at E_{beam}=0.8 A.GeV (max. sensitivity to the EOS).
    - all 'bulk' observables (multiplicities, clusterisation, stopping, flow) under control in the transport model ?
  - EoS (1996), Au+Au @ 0.25 to 1.15 A.GeV, radial & sideward flow, squeeze-out versus QMD -> no strong sensitivity on the nuclear incompressibility K_0.
  - FOPI (2005), Au+Au @ 0.09-1.5 A.GeV, Z=1 elliptic flow, versus 4 different transport codes -> 'no strong constraint on the EOS can be derived at this stage'.
  - BEVALAC & AGS accelerators, proton flows versus transport theories -> K_0 = 167-200 MeV (soft) from V_1, K_0 = 300 MeV (semi-stiff) from V_2 -> contradictions.

Introduction

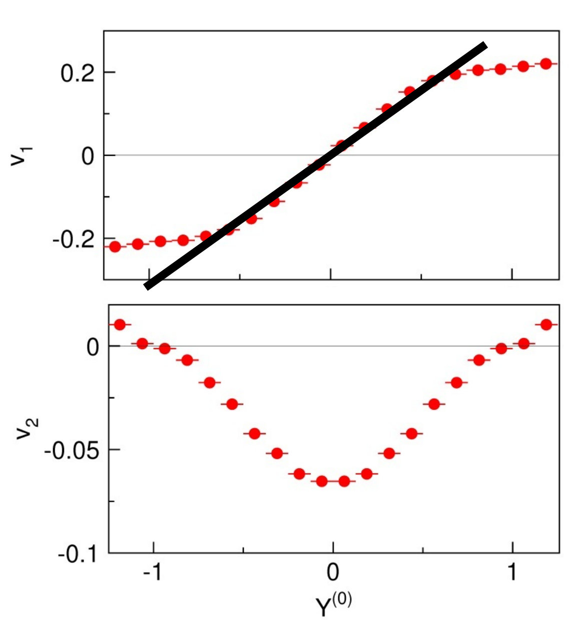

th laboratories, heavy ion collisions over a wide range of incident compositions.

GeV ⬅ some kind of a clock is available (sound velocity versus interaction).

+Au, K^+ yields -> 'soft' EOS. But:

$_{am}$=0.8 A.GeV (max. sensitivity to the EOS).

ples (multiplicities, clusterisation, stopping, flow) under control in del ?

0.25 to 1.15 A.GeV, radial & sideward flow, squeeze-out versus sitivity on the nuclear incompressibility K_0.

- FOPI (2005), Au+Au @ 0.09-1.5 A.GeV, Z=1 elliptic flow, versus 4 different transport codes -> 'no strong constraint on the EOS can be derived at this stage'.
- BEVALAC & AGS accelerators, proton flows versus transport theories -> K_0 = 167-200 MeV (soft) from V_1, K_0 = 300 MeV (semi-stiff) from V_2 -> contradictions.

The elliptic flow